WNT SIGNALING REGULATES ACETYLCHOLINE RECEPTOR TRANSLOCATION AND SYNAPTIC PLASTICITY IN THE ADULT NERVOUS SYSTEM

by

Michael Jensen

A dissertation submitted to the faculty of
The University of Utah
in partial fulfillment of the requirements for the degree of

Doctor of Philosophy

Department of Biology

The University of Utah

December 2012

Copyright © Michael Jensen 2012

All Rights Reserved

The University of Utah Graduate School

STATEMENT OF DISSERTATION APPROVAL

The dissertation of **Michael Jensen**

has been approved by the following supervisory committee members:

Andres V Maricq	, Chair	**08/07/12** Date Approved
Markus Babst	, Member	**08/07/12** Date Approved
Julie Hollien	, Member	**08/07/12** Date Approved
Richard Dorsky	, Member	**08/07/12** Date Approved
Erik Jorgensen	, Member	Date Approved

and by **Neil Vickers**, Chair of the Department of **Biology**

and by Charles A. Wight, Dean of The Graduate School.

ABSTRACT

The adult nervous system is plastic and undergoes activity dependent alterations, which are essential for behaviors such as learning and memory. Paramount to plasticity is the expeditious insertion and removal of synaptic receptors; however, the molecular mechanism(s) that regulate the abundance of receptors at synapses are poorly understood. Recently, we identified a Wnt signaling pathway that increases neurotransmitter receptor levels by specifically augmenting the translocation of one class of acetylcholine receptors (AChRs) at adult synapses. We found that mutations in CWN-2 (Wnt ligand), LIN-17 (Frizzled), CAM-1 (Ror receptor tyrosine kinase), or DSH-1 (disheveled) result in similar subsynaptic accumulations of the α7 AChR homolog ACR-16 in *C. elegans.* Secondary to accumulation of ACR-16 receptors in subsynaptic membranes is a consequent reduction in synaptic current, and anticipated behavioral defects. Interestingly, perturbation of Wnt signaling results in decreased surface expression and mobility of ACR-16/α7 at synapses. Transient expression and genetic experiments revealed that novel LIN-17/CAM-1 heteromeric receptors regulate ACR-16/α7 translocation to synapses. Using an optogenetic nerve stimulation paradigm, we demonstrate that increased neural activity induces plastic changes in ACR-16/α7 receptor localization and current,

and that plasticity is dependent on Wnt signaling. We are currently assessing which subsynaptic membrane pools contribute to ACR-16/α7 translocation in response to increased synaptic activity, and if SNARE complexes regulate this process. We hypothesize that our findings will have direct relevance to ongoing studies of activity mediated receptor translocation in the vertebrate nervous system.

TABLE OF CONTENTS

LIST OF FIGURES

ACKNOWLEDGMENTS

First, I would like to thank my advisor, Dr. A. Villu Maricq, for all his encouragement, input, and support throughout my graduate career. His intense ardor and commitment to science pushed me to seek answers to difficult questions, and allowed me to obtain a broad understating of the scientific process. Also, I would like to thank my committee members, Dr. Markus Babst, Dr. Julie Hollien, Dr. Erik Jorgensen, and Dr. Rich Dorsky, for all of their helpful comments and enthusiasm.

I have a great appreciation for many members in the Maricq laboratory, whose helpful suggestions and encouragement were invaluable for the completion of my dissertation. I would like to thank Michael Francis, Jerry Mellem, Penny Brockie, Fred Hörndli, Dave Madsen, Dane Maxfield, Craig Walker, Colin Thacker, and Rui Wang. I am very grateful to the American Heart Association for awarding me a predoctoral research fellowship.

Finally, I would like to thank my parents Russell and Shanna, my wife Erica, my siblings Corbin, Whitney, and Stori, for always being there for me when I needed them.

CHAPTER 1

INTRODUCTION

The synapse

The elemental role of the nervous system is to process sensory input from the surrounding environment and engender an appropriate behavioral response. This function is performed by a complex network of billions of neurons that send and receive information through trillions of connections. For neural communication to occur efficiently, neural circuits must form the appropriate connections to process sensory input and generate the desired behavioral response in a timely manner. Therefore, In order to understand how neurons process information and generate behavior, it is essential to elucidate the molecular and cellular mechanisms that regulate neurotransmission.

Neurons send and receive information through specialized points of contact called synapses (Sudhof, 2004). At the synapse, small signaling molecules called neurotransmitters are released from the membrane of presynaptic neurons, where they diffuse through the synaptic cleft (the space between synapses), and then bind to and activate neurotransmitter receptors on the postsynaptic membrane (Figure 1.1). At presynaptic release sites,

neurotransmitters are packaged into membrane-bound vesicles (synaptic vesicles) that are docked and primed for release (exocytosis) at the active zone of the release terminal. Exocytosis of vesicles is performed by SNARE (soluble NSF attachment protein receptor) complexes that release neurotransmitter by facilitating fusion of synaptic vesicles with the presynaptic membrane of the active zone (Söllner et al., 1993; Broadie et al., 1995; Risselada and Grubmüller, 2012). Vesicle fusion is initiated upon Ca^{2+} influx into the release terminal, which occurs when voltage-gated Ca^{2+} channels are activated following depolarization of the presynaptic neuron via invasion of an action potential (AP). An AP is a fast, transient rise in the membrane potential (voltage) of a neuron caused by the activation of voltage-gated ion channels in the axon initial segment. APs propagate in a unidirectional manner down the length of the axon where they terminate at the presynaptic release terminal facilitating neurotransmitter release (Figure 1.1). Binding of neurotransmitter to its respective receptor initiates a downstream signaling cascade that is specific to the type of neurotransmitter released (Sudhof, 2004).

There are two distinct classes of neurotransmitter receptors in the membrane of postsynaptic cells – metabotropic and ionotropic (Kew and Kemp, 2005). Metabotropic receptors are seven-pass G-protein-coupled receptors that signal through diverse second messenger pathways in cells. Ionotropic receptors are composed of several protein subunits that combine to form either a homomeric or heteromeric channel that contains an ion pore. Binding of the cognate ligand to the ionotropic receptor gates open the pore allowing ions to

traverse the cell membrane, causing a change in the membrane potential of the cell. Ion channels permeable to cations (Na^+, K^+, Ca^{2+}) depolarize the cell membrane causing excitation, and channels permeable to anions (Cl^-) hyperpolarize the cell and are inhibitory. Acetylcholine (ACh) is an excitatory neurotransmitter that controls a broad range of neuronal functions by activating a diverse set of ionotropic and metabotropic acetylcholine receptors (Gotti and Clementi, 2004; Gotti et al., 2006).

Acetylcholine receptors

Ionotropic nicotinic acetylcholine receptors (nAChRs) are pentameric ligand-gated cation channels that belong to the superfamily family of Cys-loop receptors. The individual receptor subunits have several conserved domains: a large extracellular loop; four transmembrane domains: M1, M2, M3, M4; a large intracellular loop between domains M3 and M4; and an extracellular C-terminus. The M2 domain of the five subunits contains a hydrophobic leucine residue that forms the pore of the ion channel (Gotti and Clementi, 2004; Gotti et al., 2006) (Figure 1.2).

nAChRs have three functional states: resting, active and desensitized. In the resting state, nAChRs are not bound to ACh and the diameter of the ion pore is 6 Å, making it impermeable to all hydrated mono- and divalent cations. When ACh binds to the nAChR, the receptor becomes active and the size of the ion pore increases to 9Å, allowing the cations Na^+, K^+, and Ca^{2+} to readily move through the open pore. In the desensitized state, the receptor is still bound to

ACh but the ion pore is closed and impermeable to cations. The duration and recovery from desensitization is dependent on the concentration of ACh to which the receptor is exposed to and the combination of subunits that make up the nAChR (Gotti and Clementi, 2004; Jensen et al., 2005; Gotti et al., 2006).

In vertebrates, there are 17 nAChR subunits composed of ten α (α1-α10), four β (β1-4), and one γ, δ, and ε. nAChR subunits form both homomeric and heteromeric channels depending on subunit type. Homomeric channels are composed of five α subunits, and ACh binds at the N-terminal interface between two adjacent α subunits (Figure 1.2). α7-α9 subunits form homomeric channels; however, only α7 is expressed in the central nervous system (CNS). Heteromeric channels have at least two α subunits in combination with various non-α subunits (β, γ, δ, and ε). ACh usually binds at the N-terminal interface between α and β, except in muscle nAChRs where ACh binds at the interface between α1-γ and α1-δ (Figure 1.2). Of these receptor subunits, α2-α6, α10, and β2-β4 are expressed in neurons and various tissue types, while α1, β1, γ, δ, and ε are expressed in muscle. In brain, the most abundant nAChR subunits are α4, α7, and β2 (Gotti and Clementi, 2004; Jensen et al., 2005; Gotti et al., 2006).

Heteromeric α4β2 nAChRs are the major nAChR found in brain. α4β2 nAChRs are characterized by insensitivity to α-bungarotoxin and have high affinity for ACh. In brain, α4β2 nAChRs are localized to presynaptic terminals where they modulate the strength of synaptic signaling by altering the release of multiple classes of neurotransmitters – dopamine, γ-aminobutyric acid (GABA), noradrenalin (NA) and ACh (Jensen et al., 2005; Gotti et al., 2006). α7-α9

nAChR subunits form homomeric nAChRs and are characterized by α-bungarotoxin sensitivity, low affinity for ACh, and high permeability to Ca^{2+}. The α7 nAChR is the main homomeric channel in brain, and is present in the hippocampus, cortex and subcortical limbic regions – areas important for learning and memory. α7 receptors are enriched in presynaptic terminals where they augment synaptic transmission via increasing Ca^{2+} influx into presynaptic release sites. Interestingly, α7 nAChRs have an essential role in augmenting synaptic transmission of glutamatergic synapses (Gotti and Clementi, 2004; Jensen et al., 2005; Gotti et al., 2006).

Glutamate (Glu) is the major excitatory neurotransmitter in brain (Brockie and Maricq, 2010). Ionotropic glutamate receptors (iGluR) are expressed throughout the nervous system and are concentrated in the hippocampus. iGluRs are required for the cellular models of synaptic plasticity known as long-term potentiation (LTP) and long-term depression (LTD) (Song and Huganir, 2002). Perturbations in hippocampal glutamatergic signaling prevent induction of LTP and LTD, leading to defects in learning and memory. Interestingly, α7 nAChRs are present in hippocampal neurons and cluster at presynaptic release sites where they augment the strength of glutamatergic neurotransmission (Gotti et al., 2006). Recent studies in mouse hippocampus have shown that presynaptic α7 nAChRs are required for synaptic plasticity in hippocampal Schaffer Collateral (SC) to CA1 synapses (Gu and Yakel, 2011). SC/CA1 synaptic plasticity was obviated when α7 nAChRs were pharmacologically blocked, and neural stimulation of α7 knockout mice fails to induce plasticity in SC/CA1 synapses.

Also, soluble oligomeric β-amyloid (Aβ) blocked α7-dependent SC/CA1 plasticity, suggesting that α7 nAChRs have a role in Alzheimer's disease pathology.

Dysfunction of nAChR signaling is implicated in numerous neurological disorders and diseases (Gotti et al., 2006). Nicotine is a selective agonist for nAChRs and chronic exposure to nicotine results in addiction. Binding of nicotine to nAChRs results in receptor desensitization and augmented levels of nAChRs at synapses. In behavioral studies, wild-type mice readily self-administer nicotine, and α4β2 nAChRs are increased in many brain regions following chronic nicotine exposure (Gotti and Clementi, 2004; Gotti et al., 2006). The role that α4β2 nAChRs have in nicotine addiction is further demonstrated by studies showing that β2 knockout mice fail to self-administer nicotine (Picciotto et al. 1998). These results support a model where functional alterations in synaptic α4β2 nAChRs leads to addiction. Recent studies demonstrate that synaptic levels of nAChRs are tightly regulated in brain and that deviations in nAChR surface expression may contribute to disease pathology. For example, individuals afflicted with schizophrenia were found to have decreased levels of synaptic α7 nAChRs in hippocampus, thalamus and prefrontal cortex. Loss of synaptic α7 nAChRs has also been associated with Alzheimer's and Parkinson disease (Gotti et al., 2006).

Despite the extensive role nAChRs have in neuronal function and disease pathology, little is known about the genetic pathway(s) that localize and maintain nAChRs at synapses. How are nAChRs trafficked and targeted to synapses and what signaling mechanisms regulate synaptic levels of nAChRs? Unfortunately, limitations in synaptic accessibility and neuronal complexity have hindered

studies aimed at elucidating the signaling mechanism(s) that regulate nAChRs in neurons. To address these questions, extensive studies were undertaken to elucidate signaling mechanisms that regulate nAChRs at the neuromuscular junction (NMJ).

The neuromuscular junction

The NMJ is a model synapse that is used to elucidate the cellular mechanisms that regulate nAChRs at synapses. At the NMJ, cholinergic motor neurons (MNs) , that emanate from the ventral horn or medulla of the spinal cord, innervate postsynaptic muscle cells and regulate muscle contraction (Ruff, 2003). Depolarization of MNs elicits ACh release, which then diffuses through the synaptic cleft and binds to nAChRs on the surface of postsynaptic muscle cells. The surface of the postsynaptic muscle – which is juxtaposed to the MN release terminal – contains deep membrane invaginations that have a high concentration of nAChRs at the shoulders of the invaginations. Within the folds of the invaginations are high concentrations of voltage-gated Na^+ channels. Cation influx through nAChRs, following release of ACh from the MN, activates voltage-gated Na^+ channels resulting in muscle contraction. nAChRs in muscle are composed of α1, β1, γ, δ, and ε subunits that form a heteromeric ionotropic receptor (Gotti and Clementi, 2004; Jensen et al., 2005) (Figure 1.2). In fetal muscle, the ε subunit is a component in the nAChR until innervation occurs resulting in the ε subunit being replaced by γ. Mature nAChRs are clustered at

the NMJ by a vast postsynaptic scaffolding complex that is organized by nerve-derived signaling molecules.

At nascent NMJs, invading MNs release two essential nerve-derived factors – neuregulin and agrin – that regulate formation and maintenance of the NMJ. Neuregulin activates ErbB (receptor tyrosine kinase) receptors that are localized to the postsynaptic muscle membrane (III and Burden, 1995; Moscoso et al., 1995). Activated ErbB receptors induce expression of nAChRs and other postsynaptic components in muscle. Agrin is a heparin-sulphate proteoglycan that initiates clustering of nAChRs at the NMJ (Gautam et al., 1996). Both MNs and muscle express various splice variants of agrin; however, the nerve-derived z-agrin isoform is far more efficacious in clustering nAChRs than muscle-derived agrin (Ferns et al., 1993). Application of z-agrin induces robust clustering of nAChRs in myotubes, and agrin mutant mice have defects in nAChRs clustering and localization of scaffolding proteins (Ferns et al., 1993; Gesemann et al., 1995; Gautam et al., 1996). Agrin regulates nAChRs clustering by inducing tyrosine phosphorylation of muscle-specific tyrosine kinase (MuSK).

MuSK is required for nAChRs surface expression and clustering, and recruits various scaffold and signaling proteins that are necessary for stabilizing and maintaining nAChRs at the NMJ (DeChiara et al., 1996; Glass et al., 1996). Dystroglycan is a dimer of α and β subunits that links the extracellular matrix with the cytoskeleton. The α subunit binds the extracellular matrix protein, laminin, and the β subunit binds the scaffolding protein, utrophin. Utrophin binds to F-actin and this association stabilizes the dystroglycan complex with the

cytoskeleton. In muscle, MuSK activates Src and Abl kinases that promote phosphorylation of the nAChR β-subunit (Mittaud et al., 2004; Ghazanfari et al., 2011). Rapsyn – an adaptor protein – binds the phosphorylated nAChR β-subunit and the β subunit of dystroglycan (Apel et al., 1995; Korkut and Budnik, 2009). The rapsyn-dystroglycan association anchors nAChRs to the cytoskeleton in muscle. This model is supported by studies in MuSK and rapsyn mutant mice where nAChRs fail to cluster and scaffolding proteins do not localize to the NMJ (Gautam et al., 1995; DeChiara et al., 1996).

Clustering of nAChRs at the NMJ is dependent on the small GTPases, Rac and Rho(Cdc42). Application of agrin onto muscle stimulates Rac and Cdc42 GTPase activity, and dominant negative forms of Rac and Cdc42 inhibit nAChRs aggregation (Weston et al., 2000). Agrin activation of MuSK actuates p21-activated kinase (PAK1) in muscle. PAK1-dependent clustering of nAChRs is dependent on Rac and Cdc42 signaling, which suggests that PAK1 functions downstream to of MuSK to localize nAChRs at the NMJ (Luo et al., 2002). The signaling mechanisms that regulate Rac and Cdc42 function are not well known.

Agrin induces tyrosine phosphorylation of MuSK; however, agrin does not directly bind to MuSK, suggesting that MuSK interacts with a co-receptor(s) at the NMJ (Glass et al., 1996). Recent studies in mice identified low-density lipoprotein receptor related protein 4 (LRP4) as the target of agrin at the NMJ (Zhang et al., 2008, 2009). Activated LRP4 binds to MuSK and induces tyrosine phosphorylation of the LRP4/MuSK complex. Suppression of LRP4 expression in muscle diminishes nAChRs clustering, NMJ maturation, and agrin-induced

phosphorylation of MuSK. The ligand for MuSK remained unknown until it was recently discovered that members of the Wnt signaling family interact with MuSK.

Wnt signaling

Wnts (an acronym from *Drosophila wingless* and *Mus* Int1) are small-secreted glycoproteins that control a broad range of cellular and developmental processes such as cell polarity, cellular differentiation and migration, and synaptogenesis (Speese and Budnik, 2007; Zhang et al., 2009; van Amerongen and Nusse, 2009). The mechanisms whereby Wnts regulate these cellular processes are incredibly diverse and are complicated by the large number of Wnt genes – seven in flies, five in worms, and 19 in both mice and humans. Wnt signaling is further convoluted by the presence of multiple classes of Wnt receptors (Speese and Budnik, 2007). Typical Wnt receptors are seven-pass transmembrane proteins known as Frizzled (Fzd), and can form receptor complexes with members of the LRP family. The hallmark of Fzd receptors is the presence of a Wnt-binding cysteine-rich domain (CRD) in the extracellular region of the protein. Atypical receptors consist of Ror receptor tyrosine kinases (RTK) and related to receptor tyrosine kinase (RYK), both of which can associate with other receptor types to regulate Wnt signaling (Green et al., 2008; van Amerongen and Nusse, 2009; Park and Shen, 2012).

In canonical Wnt signaling, Wnt binds to a receptor complex consisting of Fzd and LRP5/6. The Wnt-bound receptor complex activates the phosphoprotein disheveled (Dvl), which inhibits the β-catenin (cadherin-associated protein β)

destruction complex. This complex consists of adenomatous polyposis coil (APC), Axin, and GSK3β. In the absence of Wnt signaling, β-catenin is phosphorylated by the destruction complex and targeted for destruction by the proteasome. When Wnt signaling is active, the destruction complex is inhibited by Dvl leading to β-catenin's translocation to the nucleus where it interacts with the LEF/TCF transcription factor and augments transcription of target gene products (Speese and Budnik, 2007).

Many cells form polarized structures – epithelia tissue and sterocilia – in order to perform their necessary functions. Wnts regulate cell polarity through a pathway known as planar cell polarity (PCP). In the PCP pathway, Wnt binds to its respective Fzd receptor and actuates Dvl. Dvl activates Rho and Rac, which interact with JUN N-terminal kinase (JNK) to alter the cytoskeletal structure and cell polarity (Speese and Budnik, 2007; Korkut and Budnik, 2009).

Ca^{2+} is essential for numerous second messenger signaling pathways in cells, and Wnts regulate Ca^{2+} signaling to control cell fate and migration. In the Wnt Ca^{2+} pathway, Wnts bind to Fzd receptors, which activate Dvl leading to augmented levels of intracellular Ca^{2+}. A rise in intracellular Ca^{2+} prevents autoinhibition of calcium/camodulin-dependent protein kinase II (CaMKII), resulting in nuclear import of the transcription factor nuclear-factor of activated T cells (NFAT). Regulation of gene transcription via the Wnt Ca^{2+} pathway is also controlled through protein kinase C (PKC) signaling (Speese and Budnik, 2007; Korkut and Budnik, 2009).

Atypical Wnt signaling pathways mediated by Ror RTKs and Ryk are less characterized than the classic Wnt signaling pathways described above. Ror RTKs are highly conserved throughout the animal kingdom and are identified based on the presence of several conserved protein domains: an extracellular immunoglobulin domain (IG), CRD, Kringle domain (KR), intracellular tyrosine kinase domain (TK), serine/threonine-rich domain (S/TRD) and a proline-rich domain (PRD) (Green et al., 2008; Park and Shen, 2012). Several studies have demonstrated that Rors have a conserved role in mediating Wnt signaling in order to regulate a diverse number of cellular processes. Ror RTKs are expressed in many tissue types and are required for normal brain development, cellular proliferation and differentiation, angiogenesis and synaptogenesis (Green et al., 2008; Minami et al., 2010; Paganoni et al., 2010). Ror RTKs direct these cellular processes by regulating cell migration and polarity. Studies in *Xenopus* observed that loss of Ror signaling resulted in mediolateral orientation defects in polarized mesodermal cells. Instability of polarized cell structures were also observed in cells from Keller open face explants when Ror signaling was disrupted (Schambony and Wedlich, 2007). In *C. elegans,* Ror signaling regulates neural cell migration and cellular proliferation (Green et al., 2008; Park and Shen, 2012). In mice, loss of *Ror1* or *Ror2* results in dwarfism, facial abnormalities, limb growth defects and death (Oishi et al., 2003; Minami et al., 2010). Interestingly, the expression pattern of *Ror2* is similar to that of *Wnt5a* in mice, and *Ror2* mutant defects are similar to those observed in *Wnt5a* mutants. The presence of the CRD in Rors indicates that Ror RTKs interact with Wnts.

This is further supported by studies showing that WNT5a initiates polarized cell migration in mouse embryonic fibroblasts (MEFs) (Nishita et al., 2006). Inhibition of Ror2 function prevents MEFs from undergoing polarized cell migration in response to Wnt5a. Further studies revealed that the CRD present in Ror2 is required for binding to Wnt5a. Also, it was discovered that the CRD in Ror2 interacts with the putative Wnt5a receptor Fzd2 (frizzled-2) (Oishi et al., 2003). Experiments showing that Wnts associate with the CRD in Ror RTKs, suggest that other classes of CRD containing tyrosine kinases might also interact with Wnts. MuSK contains a CRD and recent experiments in zebrafish, mice, and *C. elegans* indicate that Wnts regulate the development and function of the NMJ (Kim et al., 2003; Francis et al., 2005; Henriquez et al., 2008; Jing et al., 2009).

Wnt signaling regulates development and function of the NMJ

At the NMJ, Wnt signaling molecules have fundamental roles in promoting surface expression and clustering of nAChRs. Studies in mice demonstrate that Dvl is required for localization of nAChRs in muscle. Dvl was found to bind MuSK and PAK1, and perturbations in this association inhibited Agrin-induced clustering of nAChRs. Coupling of MuSK to PAK1 by Dvl, suggests that PCP signaling may be involved in clustering nAChRs via activation of Rac and Cdc42 (Luo et al., 2002). At the NMJ, APC co-localizes with nAChRs and Agrin fails to cluster nAChRs in muscle where ACP function is inhibited. APC has been shown to bind to the β-subunit of nAChRs, β-catenin, and the microtubule end binding protein EB1 (Wang et al., 2003; Korkut and Budnik, 2009). Thus, APC is

predicted to serve as an anchoring protein linking nAChRs to scaffolding proteins and the cytoskeleton. Also, β-catenin interacts with rapsyn and nAChRs, suggesting a model where intracellular Wnt signaling molecules aid in coupling nAChRs to the cytoskeleton via a noncanonical signaling pathway (Zhang et al., 2007).

Wnts have also been show to regulate the formation and function of the NMJ. Application of Wnt1 in cultured myotubes does not affect nAChR clustering in muscle, but does augment expression of MuSK (Kim et al., 2003). In cultured muscle cells, Wnt3 increases the size and number of nAChR clusters when in the presence of agrin (Henriquez et al., 2008). Recent studies in zebrafish demonstrated that Wnts signal through MuSK to regulate MN axon guidance and patterning of nAChRs at the NMJ (Jing et al., 2009). In MuSK mutants, nAChRs fail to localize properly and MN growth cones do not migrate to their intended targets. Knockdown of *wnt11r* results in synaptic defects similar to those found in zebrafish MuSK mutants. *In vitro* experiments showed that *wnt11r* directly binds to the CRD in MuSK, and attenuation of Dvl signaling in zebrafish lead to nAChRs patterning defects homologous to those observed in *wnt11r* knockdown. These experiments support a model where Wnt binds to MuSK and directs MN growth cones and nAChRs in a Dvl dependent manner.

Elegant experiments in *D. melanogaster* have demonstrated that Wnts have essential roles in regulating synaptic function and plasticity. The *Drosophila* NMJ is glutamatergic, and MNs organize into presynaptic boutons that innervate postsynaptic muscle cells (Korkut and Budnik, 2009). At the *Drosophila* NMJ, the

Wnt ligand *Wingless (Wg)* is secreted from MNs and accumulates at both pre- and post-synaptic terminals (Packard et al., 2002). *Wg* binds to the *Frizzled-2* receptor in postsynaptic muscle resulting in cleavage of the *Frizzled-2* intracellular region (Mathew et al., 2005; Ataman et al., 2008; Mosca and Schwarz, 2010). Cleaved *Frizzled-2* then associates with GRIP (7-PDZ-domain glutamate-receptor interacting protein) and is imported into the nucleus. In the nucleus, cleaved *Frizzled-2* localizes to chromatin where it likely alters target gene transcription (Korkut et al., 2009; Speese et al., 2012). The frizzled nuclear import pathway promotes synaptic formation, growth, and recruitment of iGluRs to the NMJ. In *Drosophila,* increased synaptic activity augments bouton formation and leads to an increase in neurotransmitter release and *Wg* secretion (Ataman et al., 2008). Nuclear levels of cleaved *Frizzled-2* also increase after synaptic stimulation. Synaptic plasticity at the NMJ is dependent on *Wg* signaling, based on observations that bouton size and number do not increase following synaptic stimulation in heterozygous *Wg* mutants (Ataman et al., 2008). Thus, Wnt signaling has a conserved role in regulating formation, function, and plasticity of the NMJ.

Wnts regulate synaptic function in neurons

Wnt signaling has an extensive role in regulating NMJ development and function, but the capacity of Wnts to mediate transmission at neuronal synapses is just beginning to emerge. In rat hippocampal neurons, application of Wnt7a induces clustering of the presynaptic proteins synaptophysin, SV2, and

synaptotagmin. Electrophysiological studies in hippocampal slices showed that Wnt7a decreased paired-pulse facilitation and increased the frequency of miniature excitatory postsynaptic currents (Cerpa et al., 2008). Following studies revealed that inhibition of frizzled-5 (Fzd5) blocks Wnt7a dependent increases in synaptic transmission (Sahores et al., 2010), further supporting Wnt7a's role in promoting synaptic transmission. Recent studies have shown that Wnt7a regulates hippocampal synaptic transmission in a bidirectional manner via the Wnt Ca^{2+} signaling pathway. Wnt7a augments excitatory synaptic transmission by increasing dendritic spine growth, the density of both pre- and postsynaptic markers, and the frequency and size of mEPSC at hippocampal synapses. Overexpression of Dvl augmented dendritic spine size and inhibition of Dvl precluded all Wnt7a-dependent changes in hippocampal transmission. Application of Wnt7a leads to a concomitant activation of CaMKII in dendritic spines, and inhibition of CaMKII signaling prevents Wnt7a-dependent changes in spine morphology (Ciani et al., 2011). Thus, Wnt7a has an essential role in regulating excitatory synaptic transmission in hippocampal neurons.

Recent experiments observed that Wnt5a, along with Wnt7a, regulates excitatory synaptic transmission in hippocampal neurons. Application of Wnt5a to hippocampal neurons induced rapid insertion of N-methyl-D-aspartate receptors (NMDAR, a subclass of iGluRs) at synapses. Augmentation of NMDAR-mediated current is dependent on Ca^{2+}, JNK, and PKC signaling in neurons (Cerpa et al., 2011). The role of Wnt5a in the hippocampus is not confined to regulating excitatory synaptic transmission. GABA is an inhibitory neurotransmitter that acts

on $GABA_A$ receptors ($GABA_AR$) – pentameric ligand gated Cl^- channels – to hyperpolarize neurons. Wnt5a engenders rapid translocation of $GABA_ARs$ from subsynaptic pools to synapses, leading to an increase in inhibitory postsynaptic currents in hippocampal slices. Inhibition of CaMKII blocked Wnt5a dependent $GABA_ARs$ insertion at synapses (Cuitino et al., 2010).

Previous studies demonstrated that Wnt7a induces the disassociation of APC from the β-catenin destruction complex in hippocampal neurons. APC then localizes to the membrane of presynaptic terminals where it co-localizes with presynaptic release proteins. Wnt7a instigates clustering of α7 nAChRs in hippocampal neurons, which co-localize with APC at synaptic terminals (Farias, 2007). Recently, α7 nAChRs were shown to be required for synaptic plasticity at SC to CA1 hippocampal synapses. Do Wnts regulate α7 nAChR surface expression and clustering at adult hippocampal synapses? If so, does Wnt signaling regulate α7 nAChRs mediated LTP? Also, what is the molecular mechanism(s) that control α7 nAChR synaptic expression? Elucidating the cellular and molecular pathways that modulate α7 nAChRs at synapses will give fundamental insight into how synaptic function and plasticity is regulated in brain, which will ultimately lead to new therapeutic and diagnostic modalities for many neurological diseases and disorders. However, addressing these fundamental questions in adult vertebrate animals is impeded by the fact that many loss-of-function Wnt signaling mutations are lethal. Thus, the role of Wnt signaling in regulating synaptic function in adult animals has remained illusive. Therefore, in order to elucidate the function of Wnt signaling at adult synapses we are using

the model organism *Caenorhabditis elegans.*

Caenorhabditis elegans

C. elegans is a soil nematode well suited for explicating the cellular and molecular mechanisms that regulate synaptic function in adult animals (Francis et al., 2003). It is a relatively small organism comprised of approximately 1000 cells for which the genome has been fully sequenced. Adult worms are transparent, allowing for fluorescently labeled proteins to be easily imaged in live animals (Jorgensen and Mango, 2002a; Duerr et al., 2008). The life cycle of *C. elegans* is approximately four days at 20°C, and the hermaphroditic worms self-fertilize and generate a typical brood size of 300 progeny. The ability of *C. elegans* to self-fertilize is an immense advantage in facilitating genetic studies because recessive homozygous mutations can be readily isolated, even if the mutant of interest cannot move or mate. Hermaphroditic worms also have the ability to mate with males allowing for genetic mapping experiments to be conducted to isolate informative mutants (Jorgensen and Mango, 2002a). Most importantly, *C. elegans* can survive the elimination of genes fundamental to the function of the nervous system, which are invariably fatal in vertebrate model organisms (Francis et al., 2005; Park and Shen, 2012).

There are many powerful genetic tools that are used in *C. elegans* to generate transgenic strains and mutant alleles to study gene function. Transgenic strains are obtained by injecting DNA into the syncytial gonad of the worm. Mutant alleles are generated by exposing worms to chemical mutagens,

X-rays, or activated transposon and then screening for mutations in a desired gene product (Jorgensen and Mango, 2002b). Also, reagents for generating single-copy gene insertions and targeted gene deletions are readily available (Frøkjaer-Jensen et al., 2008; Frøkjær-jensen et al., 2010). Small interfering RNA (RNAi) is a powerful genetic tool to knockdown transcription of target gene products. For the worm, RNAi is targeted to a gene of interest by feeding worms bacteria that express a fragment of double stranded RNA (dsRNA) homologous to a given gene. When dsRNA enters the cell it is cleaved into small interfering RNAs (siRNAs). These siRNAs bind to their respective mRNA targets causing the mRNA to be degraded (Kamath et al., 2001; Mello and Conte, 2004). dsRNA is also used for tissue specific knockdown of a target gene of interest. This technique is achieved by generating transgenic worms that co-express a sense and antisense coding sequence driven under a tissue specific promoter (Esposito et al., 2007).

The *C. elegans* nervous system has many attributes that make it amenable for neurobiological studies. The circuitry of the hermaphroditic nervous system is well characterized, and is composed of 302 neurons for which the neuronal connectivity has been reconstructed from electron microscopic analysis (White et al., 1986). The nervous system consists of several identifiable head and tail ganglia that send out axons that run longitudinally along the ventral nerve cord (VNC). Many motor neuron cell bodies are contained within the cord and control muscle contraction. The cholinergic and GABAergic nervous systems work synergistically with command interneurons to control body wall muscle

contraction and sinusoidal movement (White et al., 1986; McIntire et al., 1993; Duerr et al., 2008). Approximately 120 of the 302 neurons in *C. elegans* are cholinergic; furthermore, the majority of cholinergic nerve cells are MNs. In the worm, cholinergic MNs are categorized into the following classes – VNC MNs: AS, VA, VB, VC, AS, DA, DB; sublateral MNs: SMD, SAB, SIB, SIA, SMB, and SAA; and pharyngeal MNs: MC, M2, M1, M4, and M5 (White et al., 1986; Duerr et al., 2001, 2008). GABAergic neurons comprise 26 of the 302 neurons in worms, and are organized into the following classes – VNC MNs: 13 VD, 6 DD; MNs: 4 RME; MNs: AVL and DVB; and interneuron: RIS (White et al., 1986; McIntire et al., 1993). Cholinergic and GABAergic MNs innervate BWM cells at the NMJ to regulate muscle contraction.

We are interested in elucidating the molecular mechanism(s) that regulate synaptic transmission. Specifically, we want to explicate the molecular pathway(s) that localize and regulate nAChRs at adult synapses. To address these fundamental questions, we are taking advantage of powerful genetic and electrophysiological techniques in worms to study synaptic function at the *C. elegans* NMJ.

The *C. elegans* NMJ

The *C. elegans* NMJ has many advantages that make it a model synapse for the study of neural function. The NMJ is easily accessible for electrophysiological analysis, facilitating studies of ligand-gated currents in voltage- or current-clamped muscle cells (Francis et al., 2003). The *C. elegans*

NMJ shares many characteristics with neuronal synapses, including the presence of multiple classes of neurotransmitter receptors (Richmond and Jorgensen, 1999) (Figure 1.3). Also, worms are transparent, allowing for fluorescently labeled proteins, e.g., neurotransmitter receptors, to be imaged using standard microscopy techniques (Francis et al., 2005; Jensen et al., 2012).

At the *C. elegans* NMJ, cholinergic and GABAergic MNs innervate body wall muscle (BWM) cells to coordinate muscle contraction (McIntire et al., 1993; Duerr et al., 2008). In *C. elegans,* there are 95 BWM cells organized into four quadrants that are two cells wide and run longitudinally from head to tail (Francis et al., 2003; Meissner et al., 2011). Two muscle quadrants run along the ventral side of the animal and two quadrants run parallel along the dorsal side. The VA, VB, VC, and GABAergic VD MNs located in the VNC innervate ventral BWM cells. The VNC emanates from the nerve ring, and runs parallel in between the two ventral muscle quadrants terminating at the tail. The dorsal nerve cord (DNC) runs longitudinally along the dorsal side of the worm and innervates dorsal BWM cells. The AS, DA, DB and GABAergic DD MNs cell bodies lie in the VNC and send out commissural projections that migrate to the dorsal side of the worm and form the DNC. BWM cells typically send out three to four membrane extensions, called muscle arms (MA), which grow towards and form synapses (NMJ) with the VNC or DNC respectively (McIntire et al., 1993; Francis et al., 2003; Duerr et al., 2008).

GABA is an inhibitory neurotransmitter released from VD and DD MNs at the NMJ in worms. *unc-49* encodes a GABAR that is essential for GABA-gated

currents in muscle (Richmond and Jorgensen, 1999). A large cationic current gated by ACh is present in muscle and is further divided into two receptor subclasses based on ligand sensitivity. One class of receptor is activated by the drug levamisole (L-AChRs); the other class of receptor is activated by nicotine (nAChRs) (Richmond and Jorgensen, 1999) (Figure 1.3). L-AChRs are heteromeric receptors composed of two α (*unc-38* and *unc-63*) and three non-α (*unc-29, lev-1,* and *lev-8)* AChR subunits. *lev-1* and *lev-8* are non-essential subunits; null mutations in *unc-38, unc-63,* and *unc-29* render the L-AChR non-functional, and abolish all Lev-gated current in muscle (Fleming et al., 1997; Richmond and Jorgensen, 1999; Boulin et al., 2008).

At the NMJ, L-AChRs are clustered at presynaptic release sites via the CUB domain protein LEV-10. LEV-9 is a secreted sushi domain protein that works synergistically with LEV-10 to cluster L-AChRs juxtaposed presynaptic release sites in MAs. In *lev-10* and *lev-9* mutants, L-AChR surface expression is unaffected but L-AChRs fail to cluster juxtaposed presynaptic active zones (Gally et al., 2004; Gendrel et al., 2009). The function of L-AChRs and the signaling pathway that regulate L-AChR localization at the NMJ is well characterized; however, the molecular mechanisms that govern nAChRs localization at the NMJ are less understood.

In muscle, the majority of ACh-gated current is mediated by nAChRs. The nAChR is a homomeric receptor composed of five subunits encoded by the gene *acr-16* (Francis et al., 2005; Touroutine et al., 2005). Interestingly, *acr-16* is the homolog of the vertebrate α7 nAChR subunit. In *acr-16* mutants, ACh-gated

current is severely reduced and nicotine-gated currents are absent; however, Lev-gated currents are unaffected. We are interested in explicating the molecular mechanism(s) that are required to localize ACR-16/α7 nAChRs at synapses. Because many of the gene products important for synaptic transmission are conserved from invertebrates to vertebrates, we hypothesize that what we learn from our studies at the worm NMJ will have immediate relevance to ongoing studies in the vertebrate nervous system, and might ultimately lead to new insights pertaining to the molecular mechanism(s) that regulate α7 nAChRs at synapses.

The Ror RTK *cam-1* is required for nicotinic current at the NMJ

Previous studies in *C. elegans* found that the Ror RTK *cam*-1 is required for nicotinic current at the NMJ (Francis et al., 2005) (Figure 1.4). In *cam-1* mutants, both ACh- and nicotine-gated currents are reduced; however, the Lev- and GABA-gated currents are unaffected. CAM-1 fused to green fluorescent protein (CAM-1::GFP) localizes to the distal tips of MAs (NMJ), consistent with its role in regulating synaptic receptors. ACR-16::GFP typically localizes at the distal tips of MAs (NMJ) in wild type worms. In *cam-1* mutants, ACR-16::GFP accumulates in the proximal region of MAs, presumably cumulating in sub-synaptic membrane pools. UNC-29::GFP and UNC-49::GFP in *cam-1* mutants are indiscernible when compared to wild type controls, suggesting that CAM-1 specifically regulates ACR-16 at the NMJ.

CAM-1 is a single pass transmembrane protein that contains several conserved domains including an extracellular IG, CRD, KR and intracellular TK, and S/TRD (Francis et al., 2005; Green et al., 2008) (Figure 1.4). Surprisingly, ACh-gated current in muscle is rescued by expressing a truncated version of CAM-1 lacking the intracellular domain (CAM-1ΔID) in *cam-1* mutants. Based on the predicted CRD in CAM-1, and that expression of CAM-1ΔID in muscle rescues ACh-gated current defects in *cam-1* mutants, we hypothesize that CAM-1 interacts with Wnt-signaling molecules to regulate ACR-16/α7 nAChRs at the NMJ.

Previous experiments have shown that Ror RTKs interact with Fzd via their CRD to initiate various Wnt-controlled pathways. We hypothesize that CAM-1 localizes ACR-16 nAChRs by a kinase-independent mechanism, possibly by interacting with a Fzd receptor in the worm. Binding of Wnts to Fzd receptors is known to activate Dvl. Therefore, we predict that a CAM-1/Fzd complex binds Wnts and activates Dvl to regulate ACR-16 nAChRs at the NMJ. There are five Wnts in worms: *cwn-1, cwn-1, lin-44, egl-20* and *mom-2*; four Fzd receptors: *cfz-2, mig-1, lin-17,* and *mom-5*; and three Dvls: *dsh-1, dsh-2,* and *mig-5* (Hardin and King, 2008; Park and Shen, 2012). In our preliminary results, we have identified three Wnt-signaling molecules in *C. elegans* that are required for ACh-gated current at the NMJ: CWN-2, LIN-17, and DSH-1. We hypothesize that CWN-2 binds to and activates the CAM-1/LIN-17 co-receptor complex that signals through DSH-1 to translocate ACR-16 receptors from subsynaptic pools to the NMJ.

Despite these initial results, several questions remain pertaining to the pathway that Wnt signaling utilizes to regulate ACR-16 receptors at the NMJ. Where are LIN-17, CWN-2, and DSH-1 expressed? In what tissue types is expression of LIN-17, CWN-2, and DSH-1 required to regulate ACR-16 receptors at synapses? Is Wnt signaling required for the development of the NMJ, or does Wnt signaling have an ongoing role in regulating synapses in adult animals? At the NMJ, is the canonical Wnt pathway required for surface expression of ACR-16 receptors, or are noncanonical signaling molecules utilized to regulate this process? To address these questions, we will use a combination of genetic, electrophysiology, and cell biology techniques to elucidate the molecular mechanisms that regulate surface expression of ACR-16 receptors at the *C. elegans* NMJ.

Figure 1.1. The synapse. In presynaptic neurons, an invading AP (lighting bolt) depolarizes the presynaptic terminal, eliciting fusion of synaptic vesicle with the plasma membrane and subsequent release of neurotransmitter. Once released, neurotransmitter diffuse through the synaptic cleft, where it binds to and activates neurotransmitter receptors located in the postsynaptic membrane. Binding of neurotransmitter to its respective ionotropic neurotransmitter receptor, gates open the ion pore, allowing charged ions (cations or anions) to pass through the postsynaptic membrane (arrows).

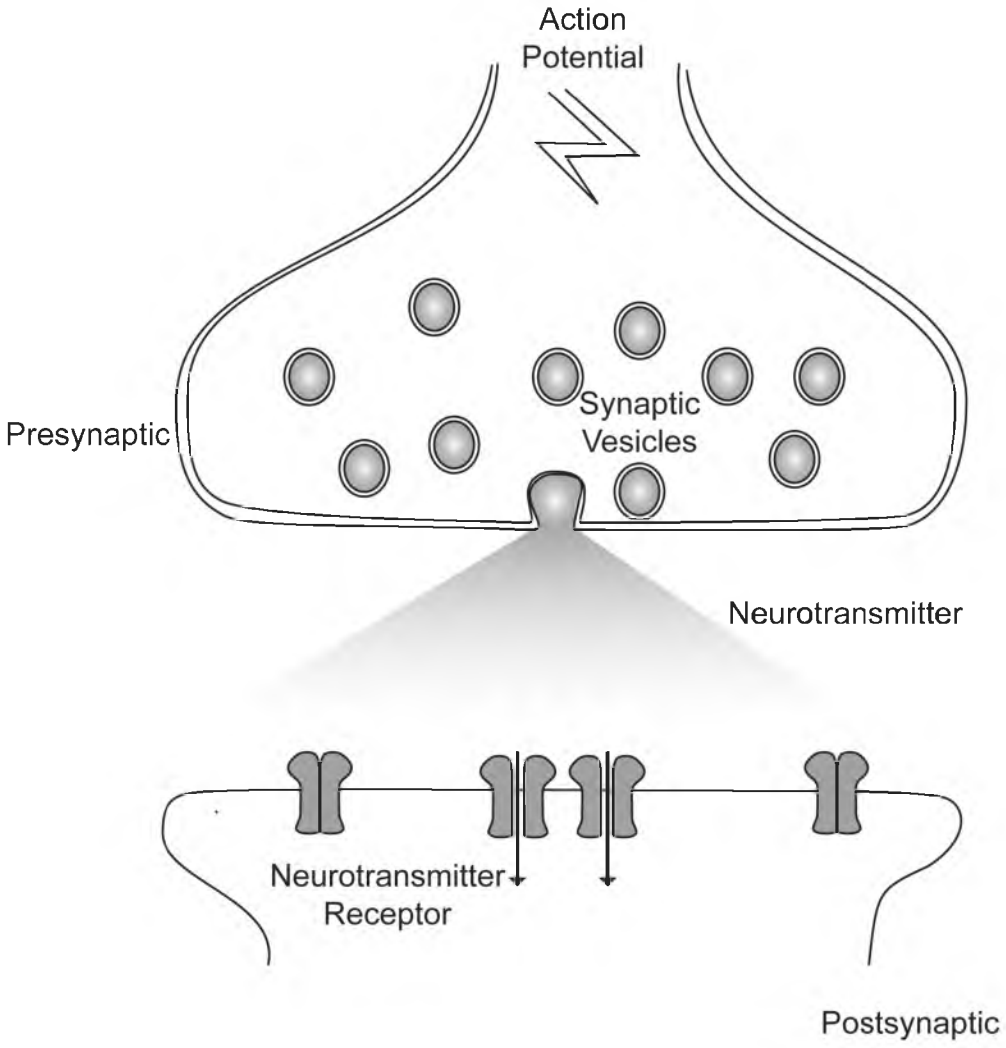
Action
Potential
Presynaptic
Synaptic
Vesicles
Neurotransmitter
Neurotransmitter
Receptor
Postsynaptic

Figure 1.2. Acetylcholine receptor stoichiometry and structure. (A) Various subunit combinations for nAChRs in muscle (top left) and neurons (top right and bottom). (B) Protein domain structure of a nAChR subunit. All receptors have a large extracellular N-terminus, four transmembrane domains (M1-M4), a large intracellular loop between M3 and M4, and an extracellular C-terminus.

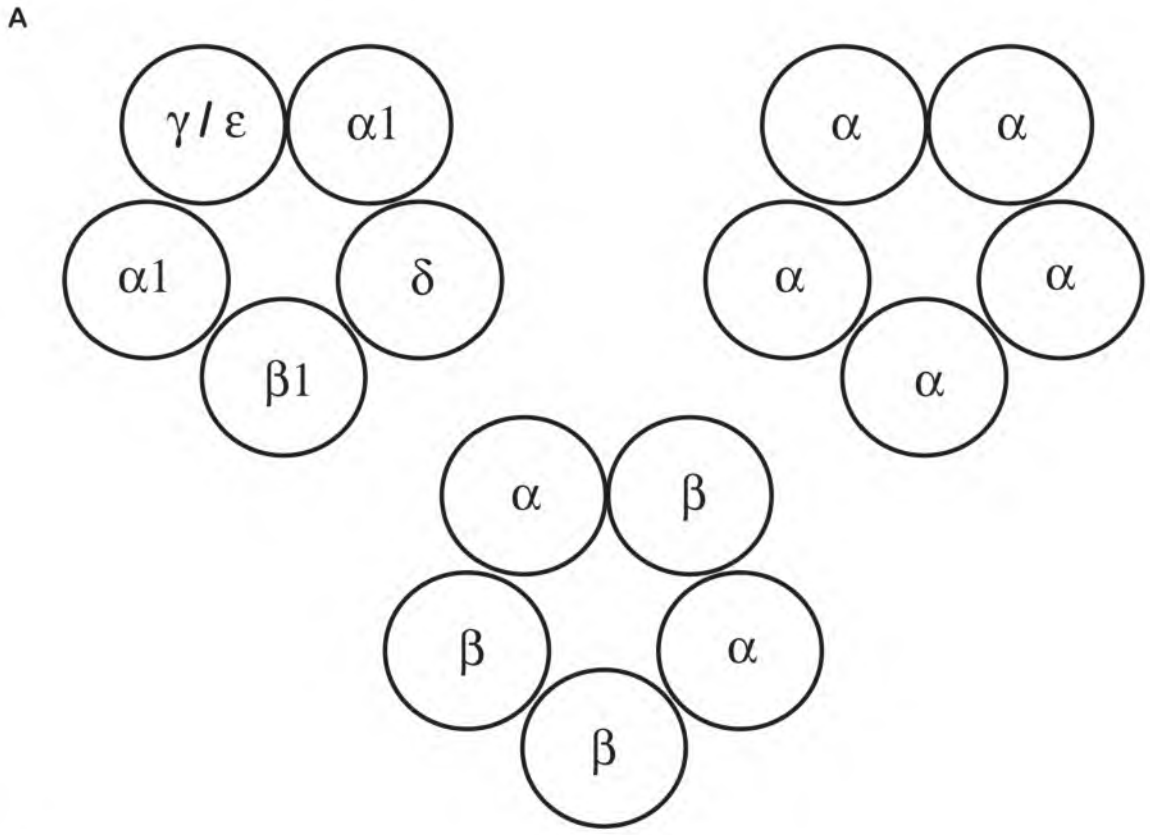
A
γ / ε
α1
α1
δ
β1
α
α
α
α
α
α
β
β
α
β
B
N-terminus
C-terminus
M1
M2
M3
M4
Extracellular
Intracellular

Figure 1.3. Neurotransmitter receptor classes at the *C. elegans* NMJ. (A) Cartoon schematic of a postsynaptic muscle arm containing L-AChRs (*unc-29, unc-38, unc-63, lev-1, lev-8*), nAChRs (*acr-16*), and GABARs (*unc-49*). (B) Electrophysiological recordings from voltage-clamped muscle cells in response to 100 µM ACh, 100 µM Lev, 100 µM nicotine, and 100 µM GABA. The combination of Lev- and nic- gated currents comprises the total ACh-gated current at the NMJ.

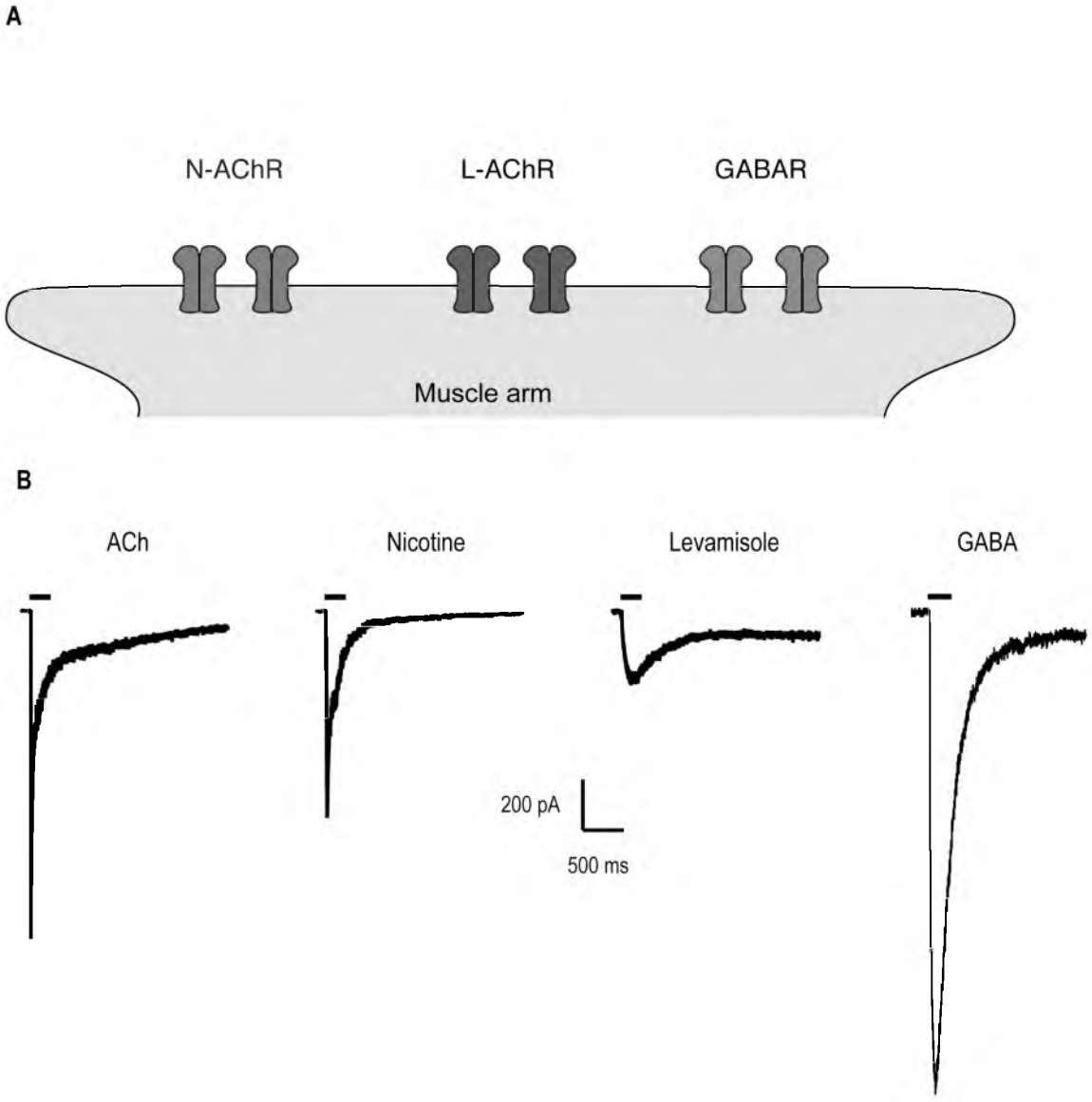
A
N-AChR
L-AChR
GABAR
Muscle arm
B
ACh
Nicotine
Levamisole
GABA
200 pA
500 ms

Figure 1.4. CAM-1 is required for nicotinic current at the NMJ. In *cam-1* mutants, ACh- and nicotine-gated currents are reduced and ACR-16 receptors accumulate in MAs, presumably in subsynaptic pools. Interestingly, the intracellular domain of CAM-1 is not required for ACR-16-mediated current, suggesting that CAM-1 forms a co-receptor with and unknown partner.

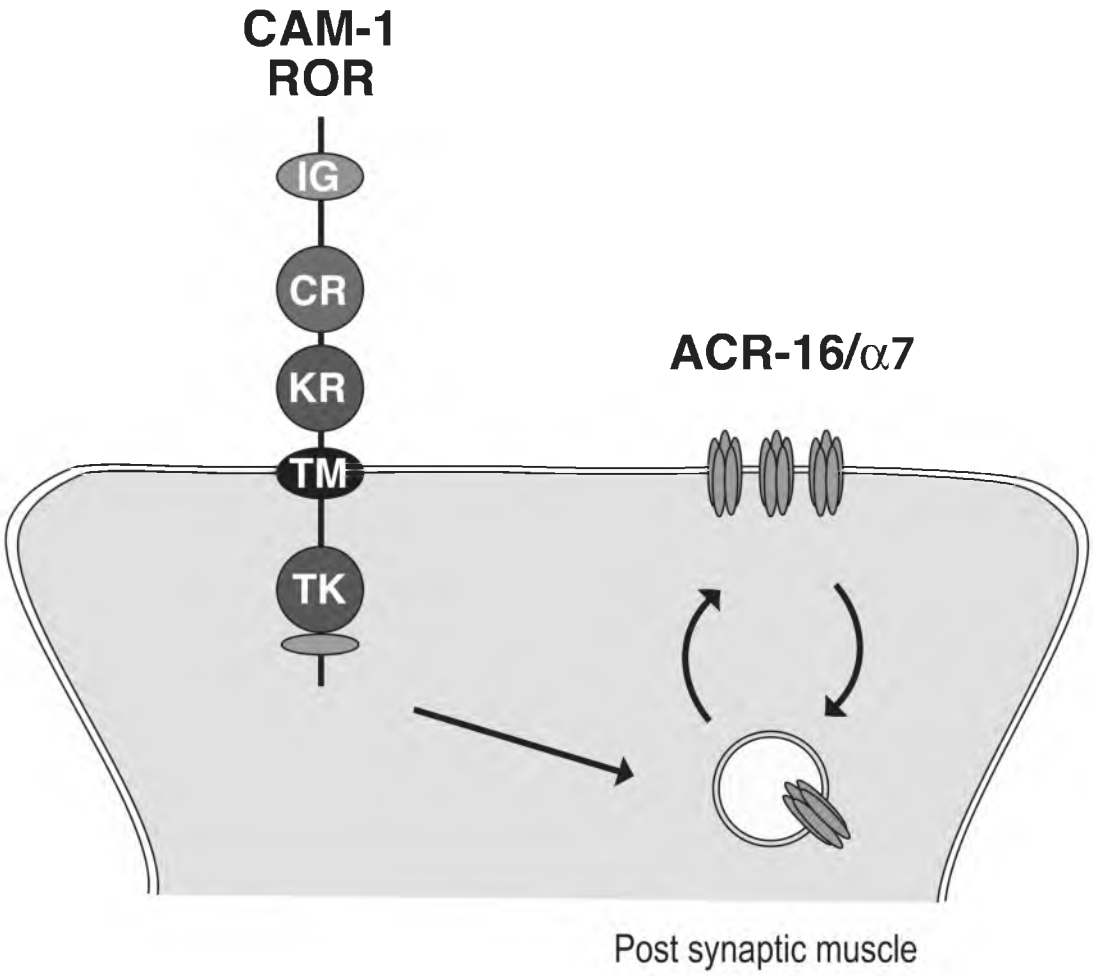
CAM-1
ROR
IG
CR
KR
TM
TK
ACR-16/α7
Post synaptic muscle

References

van Amerongen, R., and Nusse, R. (2009). Towards an integrated view of Wnt signaling in development. Development (Cambridge, England) *136*, 3205–3214.

Apel, E.D., Roberds, S.L., Campbell, K.P., and Merlie, J.P. (1995). Rapsyn may function as a link between the acetylcholine receptor and the agrin-binding dystrophin-associated glycoprotein complex. Neuron *15*, 115–126.

Ataman, B., Ashley, J., Gorczyca, M., Ramachandran, P., Fouquet, W., Sigrist, S.J., and Budnik, V. (2008). Rapid activity-dependent modifications in synaptic structure and function require bidirectional Wnt signaling. Neuron *57*, 705–718.

Boulin, T., Gielen, M., Richmond, J.E., Williams, D.C., Paoletti, P., and Bessereau, J.-L. (2008). Eight genes are required for functional reconstitution of the Caenorhabditis elegans levamisole-sensitive acetylcholine receptor. Proceedings of the National Academy of Sciences of the United States of America *105*, 18590–18595.

Broadie, K., Prokop, a, Bellen, H.J., O'Kane, C.J., Schulze, K.L., and Sweeney, S.T. (1995). Syntaxin and synaptobrevin function downstream of vesicle docking in Drosophila. Neuron *15*, 663–673.

Brockie, P.J., and Maricq, A.V. (2010). In a pickle: is cornichon just relish or part of the main dish? Neuron *68*, 1017–1019.

Cerpa, W., Gambrill, A., Inestrosa, N.C., and Barria, A. (2011). Regulation of NMDA-receptor synaptic transmission by Wnt signaling. The Journal of Neuroscience: The Official Journal of the Society for Neuroscience *31*, 9466–9471.

Cerpa, W., Godoy, J. a, Alfaro, I., Farías, G.G., Metcalfe, M.J., Fuentealba, R., Bonansco, C., and Inestrosa, N.C. (2008). Wnt-7a modulates the synaptic vesicle cycle and synaptic transmission in hippocampal neurons. The Journal of Biological Chemistry *283*, 5918–5927.

Ciani, L., Boyle, K.A., Dickins, E., Sahores, M., Anane, D., Lopes, D.M., Gibb, A.J., and Salinas, P.C. (2011). Wnt7a signaling promotes dendritic spine growth and synaptic strength through Ca^{2+}/Calmodulin-dependent protein kinase II. Proceedings of the National Academy of Sciences of the United States of America *108*, 10732–10737.

Cuitino, L., Godoy, J. a, Farías, G.G., Couve, A., Bonansco, C., Fuenzalida, M., and Inestrosa, N.C. (2010). Wnt-5a modulates recycling of functional GABAA receptors on hippocampal neurons. The Journal of Neuroscience: The Official Journal of the Society for Neuroscience *30*, 8411–8420.

DeChiara, T.M., Bowen, D.C., Valenzuela, D.M., Simmons, M.V., Poueymirou, W.T., Thomas, S., Kinetz, E., Compton, D.L., Rojas, E., Park, J.S., et al. (1996). The receptor tyrosine kinase MuSK is required for neuromuscular junction formation in vivo. Cell *85*, 501–512.

Duerr, J.S., Gaskin, J., and Rand, J.B. (2001). Identified neurons in C. elegans coexpress vesicular transporters for acetylcholine and monoamines. American Journal of Physiology. Cell Physiology *280*, C1616–22.

Duerr, J.S., Han, H.-P., Fields, S.D., and Rand, J.B. (2008). Identification of major classes of cholinergic neurons in the nematode Caenorhabditis elegans. The Journal of Comparative Neurology *506*, 398–408.

Esposito, G., Di Schiavi, E., Bergamasco, C., and Bazzicalupo, P. (2007). Efficient and cell specific knock-down of gene function in targeted C. elegans neurons. Gene *395*, 170–176.

Ferns, M.J., Campanelli, J.T., Hoch, W., Scheller, R.H., and Hall, Z. (1993). The ability of agrin to cluster AChRs depends on alternative splicing and on cell surface proteoglycans. Neuron *11*, 491–502.

Fleming, J.T., Squire, M.D., Barnes, T.M., Tornoe, C., Matsuda, K., Ahnn, J., Fire, a, Sulston, J.E., Barnard, E. a, Sattelle, D.B., et al. (1997). Caenorhabditis elegans levamisole resistance genes lev-1, unc-29, and unc-38 encode functional nicotinic acetylcholine receptor subunits. The Journal of Neuroscience : The Official Journal of the Society for Neuroscience *17*, 5843–5857.

Francis, M.M., Evans, S.P., Jensen, M., Madsen, D.M., Mancuso, J., Norman, K.R., and Maricq, A.V. (2005). The Ror receptor tyrosine kinase CAM-1 is required for ACR-16-mediated synaptic transmission at the C. elegans neuromuscular junction. Neuron *46*, 581–594.

Francis, M.M., Mellem, J.E., and Maricq, A.V. (2003). Bridging the gap between genes and behavior: recent advances in the electrophysiological analysis of neural function in Caenorhabditis elegans. Trends in Neurosciences *26*, 90–99.

Frøkjaer-Jensen, C., Davis, M.W., Hopkins, C.E., Newman, B.J., Thummel, J.M., Olesen, S.-P., Grunnet, M., and Jorgensen, E.M. (2008). Single-copy insertion of transgenes in Caenorhabditis elegans. Nature Genetics *40*, 1375–1383.

Frøkjær-jensen, C., Davis, M.W., Hollopeter, G., Taylor, J., Nix, P., Lofgren, R., Prestgard-duke, M., Bastiani, M., Moerman, G., and Jorgensen, E.M. (2010). NIH Public Access. *7*, 451–453.

Gally, C., Eimer, S., Richmond, J.E., and Bessereau, J.-louis (2004). A transmembrane protein required for acetylcholine receptor clustering in Caenorhabditis elegans. Nature *431*, 578–582.

Gautam, M., Noakes, P., and Moscoso, L. (1996). defective neuromuscular synaptogenesis in agrin-deficient mice. Cell *85*, 525–535.

Gautam, M., Noakes, P.G., Mudd, J., Nichol, M., Chu, G., Sanes, J., and Merlie, J. (1995). Failure of postsynaptic specialization to develop at neuromuscular junctions of rapsyn-deficient mice. Nature *377*, 232–236.

Gendrel, M., Rapti, G., Richmond, J.E., and Bessereau, J.-L. (2009). A secreted complement-control-related protein ensures acetylcholine receptor clustering. Nature *461*, 992–996.

Gesemann, M., Denzer, a J., and Ruegg, M. a (1995). Acetylcholine receptor-aggregating activity of agrin isoforms and mapping of the active site. The Journal of Cell Biology *128*, 625–636.

Ghazanfari, N., Fernandez, K.J., Murata, Y., Morsch, M., Ngo, S.T., Reddel, S.W., Noakes, P.G., and Phillips, W.D. (2011). Muscle specific kinase: organiser of synaptic membrane domains. The International Journal of Biochemistry & Cell Biology *43*, 295–298.

Glass, D.J., Bowen, D.C., Stitt, T.N., Radziejewski, C., Bruno, J., Ryan, T.E., Gies, D.R., Shah, S., Mattsson, K., Burden, S.J., et al. (1996). Agrin acts via a MuSK receptor complex. Cell *85*, 513–523.

Gotti, C., and Clementi, F. (2004). Neuronal nicotinic receptors: from structure to pathology. Progress in Neurobiology *74*, 363–396.

Gotti, C., Zoli, M., and Clementi, F. (2006). Brain nicotinic acetylcholine receptors: native subtypes and their relevance. Trends in Pharmacological Sciences *27*, 482–491.

Green, J.L., Kuntz, S.G., and Sternberg, P.W. (2008). Ror receptor tyrosine kinases: orphans no more. Trends in Cell Biology *18*, 536–544.

Gu, Z., and Yakel, J.L. (2011). Timing-dependent septal cholinergic induction of dynamic hippocampal synaptic plasticity. Neuron *71*, 155–165.

Hardin, J., and King, R.S. (2008). The long and the short of Wnt signaling in C. elegans. Current Opinion in Genetics & Development *18*, 362–367.

Henriquez, J.P., Webb, A., Bence, M., Bildsoe, H., Sahores, M., Hughes, S.M., and Salinas, P.C. (2008). Wnt signaling promotes AChR aggregation at the

neuromuscular synapse in collaboration with agrin. Proceedings of the National Academy of Sciences of the United States of America *105*, 18812–18817.
III, K.C., and Burden, S. (1995). Neuregulins and their receptors. Current Opinion in Neurobiology 606–612.

Jensen, A., Frølund, B., Liljefors, T., and Krogsgaard-Larsen, P. (2005). Neuronal nicotinic acetylcholine receptors: structural revelations, target identifications, and therapeutic inspirations. Journal of Medicinal Chemistry *48*, 4705–4745.

Jensen, M., Hoerndli, F.J., Brockie, P.J., Wang, R., Johnson, E., Maxfield, D., Francis, M.M., Madsen, D.M., and Maricq, A.V. (2012). Wnt signaling regulates acetylcholine receptor translocation and synaptic plasticity in the adult nervous system. Cell *149*, 173–187.

Jing, L., Lefebvre, J.L., Gordon, L.R., and Granato, M. (2009). Wnt signals organize synaptic prepattern and axon guidance through the zebrafish unplugged/MuSK receptor. Neuron *61*, 721–733.

Jorgensen, E.M., and Mango, S.E. (2002a). The art and design of genetic screens: caenorhabditis elegans. Nature Reviews. Genetics *3*, 356–369.

Jorgensen, E.M., and Mango, S.E. (2002b). The art and design of genetic screens: caenorhabditis elegans. Nature Reviews. Genetics *3*, 356–369.

Kamath, R.S., Martinez-Campos, M., Zipperlen, P., Fraser, A.G., and Ahringer, J. (2001). Effectiveness of specific RNA-mediated interference through ingested double-stranded RNA in Caenorhabditis elegans. Genome Biology *2*, 002.1-002.10.

Kew, J.N.C., and Kemp, J. a (2005). Ionotropic and metabotropic glutamate receptor structure and pharmacology. Psychopharmacology *179*, 4–29.

Kim, C.-H., Xiong, W.C., and Mei, L. (2003). Regulation of MuSK expression by a novel signaling pathway. The Journal of Biological Chemistry *278*, 38522–38527.

Korkut, C., Ataman, B., Ramachandran, P., Ashley, J., Barria, R., Gherbesi, N., and Budnik, V. (2009). Trans-synaptic transmission of vesicular Wnt signals through Evi/Wntless. Cell *139*, 393–404.

Korkut, C., and Budnik, V. (2009). WNTs tune up the neuromuscular junction. Nature Reviews. Neuroscience *10*, 627–634.

Luo, Z.G., Wang, Q., Zhou, J.Z., Wang, J., Luo, Z., Liu, M., He, X., Wynshaw-Boris, A., Xiong, W.C., Lu, B., et al. (2002). Regulation of AChR clustering by Dishevelled interacting with MuSK and PAK1. Neuron *35*, 489–505.

Marina R. Picciotto, Michele Zoli, Roberto Rimondini§, Cle´ment Le´na, Lisa M. Marubio, Emilio Merlo Pichk, K.F.& J.-P.C. (1998). Acetylcholine receptors containing the b2 subunit are involved in the reinforcing properties of nicotine. Nature *391*, 173–177.

Mathew, D., Ataman, B., Chen, J., Zhang, Y., Cumberledge, S., and Budnik, V. (2005). Wingless signaling at synapses is through cleavage and nuclear import of receptor DFrizzled2. Science (New York, N.Y.) *310*, 1344–1347.

McIntire, S., Jorgensen, E., and Horvitz, H.R. (1993). Genes required for GABA function in Caenorhabditis elegans. Nature *364*, 334–337.

Meissner, B., Rogalski, T., Viveiros, R., Warner, A., Plastino, L., Lorch, A., Granger, L., Segalat, L., and Moerman, D.G. (2011). Determining the sub-cellular localization of proteins within Caenorhabditis elegans body wall muscle. PloS One *6*, e19937.

Mello, C.C., and Conte, D. (2004). Revealing the world of RNA interference. Nature *431*, 338–342.

Minami, Y., Oishi, I., Endo, M., and Nishita, M. (2010). Ror-family receptor tyrosine kinases in noncanonical Wnt signaling: their implications in developmental morphogenesis and human diseases. Developmental Dynamics: An Official Publication of the American Association of Anatomists *239*, 1–15.

Mittaud, P., Camilleri, A.A., Willmann, R., Erb-Vögtli, S., Burden, S.J., and Fuhrer, C. (2004). A single pulse of agrin triggers a pathway that acts to cluster acetylcholine receptors. Molecular and Cellular Biology *24*, 7841–7854.

Mosca, T.J., and Schwarz, T.L. (2010). The nuclear import of Frizzled2-C by Importins-beta11 and alpha2 promotes postsynaptic development. Nature Neuroscience *13*, 935–943.

Moscoso, L.M., Chu, G.C., Gautam, M., Noakes, P.G., Merlie, J.P., and Sanes, J.R. (1995). Synapse-associated expression of an acetylcholine receptor-inducing protein, ARIA/heregulin, and its putative receptors, ErbB2 and ErbB3, in developing mammalian muscle. Developmental Biology *172*, 158–169.

Nishita, M., Yoo, S.K., Nomachi, A., Kani, S., Sougawa, N., Ohta, Y., Takada, S., Kikuchi, A., and Minami, Y. (2006). Filopodia formation mediated by receptor tyrosine kinase Ror2 is required for Wnt5a-induced cell migration. The Journal of Cell Biology *175*, 555–562.

Oishi, I., Suzuki, H., Onishi, N., Takada, R., Kani, S., Ohkawara, B., Koshida, I., Suzuki, K., Yamada, G., Schwabe, G.C., et al. (2003). The receptor tyrosine

kinase Ror2 is involved in non-canonical Wnt5a/JNK signalling pathway. Genes to Cells : Devoted to Molecular & Cellular Mechanisms *8*, 645–654.

Packard, M., Koo, E.S., Gorczyca, M., Sharpe, J., Cumberledge, S., and Budnik, V. (2002). The Drosophila Wnt, wingless, provides an essential signal for pre- and postsynaptic differentiation. Cell *111*, 319–330.

Paganoni, S., Bernstein, J., and Ferreira, a (2010). Ror1-Ror2 complexes modulate synapse formation in hippocampal neurons. Neuroscience *165*, 1261–1274.

Park, M., and Shen, K. (2012). WNTs in synapse formation and neuronal circuitry. The EMBO Journal *31*, 2697–2704.

Richmond, J.E., and Jorgensen, E.M. (1999). NIH Public Access. Nature Neuroscience *2*, 791–797.

Risselada, H.J., and Grubmüller, H. (2012). How SNARE molecules mediate membrane fusion: recent insights from molecular simulations. Current Opinion in Structural Biology *22*, 187–196.

Ruff, R. (2003). Neurophysiology of the neuromuscular junction: overview. Annals of the New York Academy of Sciences *998*, 1–10.

Sahores, M., Gibb, A., and Salinas, P.C. (2010). Frizzled-5, a receptor for the synaptic organizer Wnt7a, regulates activity-mediated synaptogenesis. Development (Cambridge, England) *137*, 2215–2225.

Schambony, A., and Wedlich, D. (2007). Wnt-5A/Ror2 regulate expression of XPAPC through an alternative noncanonical signaling pathway. Developmental Cell *12*, 779–792.

Song, I., and Huganir, R.L. (2002). Regulation of AMPA receptors during synaptic plasticity. Trends in Neurosciences *25*, 578–588.

Speese, S.D., Ashley, J., Jokhi, V., Nunnari, J., Barria, R., Li, Y., Ataman, B., Koon, A., Chang, Y.-T., Li, Q., et al. (2012). Nuclear envelope budding enables large ribonucleoprotein particle export during synaptic Wnt signaling. Cell *149*, 832–846.

Speese, S.D., and Budnik, V. (2007). Wnts: up-and-coming at the synapse. Trends in Neurosciences *30*, 268–275.

Sudhof, T.C. (2004). The synaptic vesicle cycle. Annual Review of Neuroscience *27*, 509–547.

Söllner, T., Bennett, M.K., Whiteheart, S.W., Scheller, R.H., and Rothman, J.E. (1993). A protein assembly-disassembly pathway in vitro that may correspond to sequential steps of synaptic vesicle docking, activation, and fusion. Cell *75*, 409–418.

Touroutine, D., Fox, R.M., Von Stetina, S.E., Burdina, A., Miller, D.M., and Richmond, J.E. (2005). acr-16 encodes an essential subunit of the levamisole-resistant nicotinic receptor at the Caenorhabditis elegans neuromuscular junction. The Journal of Biological Chemistry *280*, 27013–27021.

Wang, J., Jing, Z., Zhang, L., Zhou, G., Braun, J., Yao, Y., and Wang, Z.-Z. (2003). Regulation of acetylcholine receptor clustering by the tumor suppressor APC. Nature Neuroscience *6*, 1017–1018.

Weston, C., Yee, B., Hod, E., and Prives, J. (2000). Agrin-induced acetylcholine receptor clustering is mediated by the small guanosine triphosphatases Rac and Cdc42. The Journal of Cell Biology *150*, 205–212.

White, J., Southgate, E., Thomson, J., and Brenner, S. (1986). The Structure of the Nervous System of the Nematode Caenorhabditis elegans. Philosophical Transactions of the Royal Scociety of London B Biological Sciences *314*, 1–340.

Zhang, B., Luo, S., Dong, X.-P., Zhang, X., Liu, C., Luo, Z., Xiong, W.-C., and Mei, L. (2007). Beta-catenin regulates acetylcholine receptor clustering in muscle cells through interaction with rapsyn. The Journal of Neuroscience : The Official Journal of the Society for Neuroscience *27*, 3968–3973.

Zhang, B., Luo, S., Wang, Q., Suzuki, T., Xiong, W.C., and Mei, L. (2008). LRP4 serves as a coreceptor of agrin. Neuron *60*, 285–297.
Zhang, B., Xiong, W.C., and Mei, L. (2009). Get ready to Wnt: prepatterning in neuromuscular junction formation. Developmental Cell *16*, 325–327.

CHAPTER 2

WNT SIGNALING REGULATES ACETYLCHOLINE RECEPTOR TRANSLOCATION AND SYNAPTIC PLASTICITY IN THE ADULT NERVOUS SYSTEM[1]

Michael Jensen, Frédéric J. Hoerndli, Penelope J. Brockie,

Rui Wang, Erica Johnson, Dane Maxfield, Michael M. Francis[†],

David M. Madsen, and Andres V. Maricq*

[1] Manuscript used with permission from Elsevier Limited; Michael Jensen, Frederic J. Hoerndli, Penelope J. Brockie, Rui Wang, Erica Johnson, Dane Maxfield, Michael M Francis, David M. Madsen and Andres V. Maricq (2012) Wnt signaling regulates acetylcholine receptor translocation and synaptic plasticity in the adult nervous system. *Cell* 149:173-87.

Summary

The adult nervous system is plastic allowing us to learn, remember and forget. Experience-dependent plasticity occurs at synapses – the specialized points of contact between neurons where signaling occurs. However, the mechanisms that regulate the strength of synaptic signaling are not well understood. Here, we define a Wnt signaling pathway that modifies synaptic strength in the adult nervous system by regulating the translocation of one class of acetylcholine receptors (AChRs) to synapses. In *C. elegans*, we show that mutations in CWN-2 (Wnt ligand), LIN-17 (Frizzled), CAM-1 (Ror receptor tyrosine kinase), or the downstream effector DSH-1 (disheveled) result in similar subsynaptic accumulations of ACR-16/α7 AChRs, a consequent reduction in synaptic current, and predictable behavioral defects. Photoconversion experiments revealed defective translocation of ACR-16/α7 to synapses in Wnt signaling mutants. Using optogenetic nerve stimulation, we demonstrate activity-dependent synaptic plasticity and its dependence on ACR-16/α7 translocation mediated by Wnt signaling via LIN-17/CAM-1 heteromeric receptors.

Introduction

Central to information processing by neural networks is neurotransmitter-mediated communication between neurons at specialized points of contact called synapses. Here, neurotransmitter is released at the presynaptic membrane and binds to neurotransmitter receptors specifically localized in the postsynaptic membrane apposed to presynaptic release sites (Jin and Garner, 2008).

Synapses are dynamic structures in the adult nervous system and individual synapses undergo activity-dependent plasticity that is believed to underlie learning and memory (Kessels and Malinow, 2009).

In part, synaptic plasticity depends on the insertion and removal of specific neurotransmitter receptors, thus strengthening or weakening the synapse. A common strategy for changing the number of membrane proteins is to shuttle proteins between intracellular pools and the cell surface (Kennedy and Ehlers, 2011). This strategy is used for diverse homeostatic processes, including synaptic plasticity (Turrigiano, 2008), aquaporin-mediated fluid homeostasis (Brown et al., 2009), and insulin-induced translocation of glucose transporters (Watson and Pessin, 2007). Yet for all of these receptor pathways, we still have only a limited understanding of how trafficking from cytoplasmic compartments to the membrane is regulated. To gain a comprehensive mechanistic understanding of this process at synapses, we used a genetic approach in *C. elegans* to identify and study the signaling molecules that regulate neurotransmission at a model synapse.

The *C. elegans* neuromuscular junction (NMJ) has features usually associated with neuronal synapses, such as multiple classes of neurotransmitter receptors and excitatory cholinergic (ACh) and inhibitory GABAergic synaptic inputs. Synaptic release from cholinergic neurons depolarizes the postsynaptic membrane by activating two independent classes of AChRs that are defined by both pharmacological and genetic criteria. We previously found that CAM-1, a Ror-family receptor tyrosine kinase (RTK), is selectively required for signaling

mediated by one of these receptor classes, ACR-16, which is the *C. elegans* homolog of the vertebrate α7 AChR (Francis et al., 2005). In *cam-1* mutants, the decreased ACh-gated current appears to be secondary to reduced surface delivery of ACR-16/α7. We found that ACR-16/α7 localization and ACR-16/α7-mediated currents were rescued in transgenic *cam-1* mutants that expressed a CAM-1 variant that included the extracellular and transmembrane domains, but lacked the intracellular kinase domain (Francis et al., 2005). These results suggested that CAM-1 might contribute to a cell-surface receptor that regulates the synaptic delivery of ACR-16/α7. Interestingly, the extracellular domain of CAM-1 contains a cysteine-rich (CR) domain predicted to bind to small, secreted glycoproteins called Wnts.

Receptor tyrosine kinases (RTKs), Wnts and Frizzled proteins (Wnt receptors) have diverse roles in the development of the nervous system, including cell migration, cell polarity and axon outgrowth (Budnik and Salinas, 2011; Green et al., 2008; Kennerdell et al., 2009; van Amerongen and Nusse, 2009). Furthermore, Wnts have conserved roles at developing synapses in flies, worms and vertebrates (Budnik and Salinas, 2011; Farias et al., 2010; Korkut and Budnik, 2009). For example, elegant genetic studies in *Drosophila* larva have demonstrated that Wnt signaling can modify the structure and function of developing glutamatergic synapses (Ataman et al., 2008; Korkut et al., 2009).

In mammals, Wnts interact with the muscle specific kinase (MuSK) at the NMJ to coordinate AChR aggregation and motor neuron growth cone targeting (Henriquez et al., 2008; Wu et al., 2010). At neuronal synapses, Wnt7a induces

presynaptic clustering of α7 AChRs with adenomatous polyposis coli (APC) in rat hippocampal neurons, directs synapse formation in the mouse brain (Farias et al., 2007; Hall et al., 2000; Sahores et al., 2010), and regulates the number and strength of hippocampal synapses (Ciani et al., 2011). Application of exogenous Wnts has diverse effects on neuronal structure and synaptic communication, including pre- and post-synaptic differentiation, spine density, receptor endocytosis and recycling (Cuitino et al., 2010; Inestrosa and Arenas, 2010).

Despite our detailed knowledge of Wnt signaling during development, we know far less about Wnt regulation of synaptic signaling, and whether this regulation continues in the mature nervous system. To address these questions, we have taken advantage of the strengths of *C. elegans* for the study of synaptic signaling. The *C. elegans* genome is predicted to encode conserved members of the Wnt signaling pathway, and there are available mutants for the five Wnt ligands, four Fzd receptors, three Dvl proteins, one Ryk/*derailed* receptor, and one Ror RTK (www.wormbase.org).

In this study, we present evidence that Wnt signaling, mediated through a heteromeric Ror/Fzd receptor complex, has an ongoing and important role in shaping transmission at mature synapses in adult animals. We found that mutations in LIN-17 (Fzd), CWN-2 (Wnt), or DSH-1 (Dvl) phenocopied the movement, electrophysiological, and ACR-16/α7 localization defects observed in *cam-1* mutants (Francis et al., 2005). Importantly, expression of LIN-17/Fzd driven by a heat shock promoter at the adult stage rescued the ACR-16/α7-dependent behavior of *lin-17* mutants, indicating that Wnt signaling has a

persistent role in synaptic transmission. Using a new paradigm for plasticity, we also found that optogenetic stimulation of motor neurons induced activity dependent changes in ACR-16/α7 localization and current, and that these changes were abolished in Wnt-signaling mutants. CWN-2 signaling by motor neurons was both necessary and sufficient for rescue of these activity-dependent changes in *cwn-2* mutants. In confirmation of this model, we found that application of recombinant CWN-2 rapidly increased ACR-16/α7-mediated current. In summary, our studies have identified a Wnt signaling pathway that controls the translocation of ACR-16/α7 receptors to synapses, and has a critical role in modulating the strength of established synapses in the adult nervous system.

Results

Wnt signaling contributes to ACR-16/α7-mediated current and behavior

In *C. elegans,* two classes of acetylcholine-gated ion channels – levamisole sensitive (L-AChR) and nicotine sensitive (N-AChR) – and one class of GABA-gated ion channels are expressed in muscle cells (Figure 2.1A) and are necessary for normal worm movement (de Bono and Maricq, 2005; Francis et al., 2005). L-AChRs are ionotropic transmembrane proteins composed of various pentameric combinations of the AChR subunits UNC-38, UNC-63, LEV-1, LEV-8 and UNC-29 (Boulin et al., 2008). In contrast, N-AChRs are homopentamers of the ACR-16 subunit, which is similar to the neuronal type α7 nicotinic AChR in

vertebrates (Francis et al., 2005; Touroutine et al., 2005). The CAM-1/Ror RTK is also expressed in muscle cells (Francis et al., 2005), and in *cam-1* mutants the ACh-gated currents mediated by ACR-16/α7 are reduced compared to those measured in wild-type muscle cells (Figure 2.1B and C). Additionally, in *cam-1* mutants ACR-16/α7 receptors abnormally accumulate in postsynaptic muscle arms – projections that extend from muscles to neurons in the ventral nerve cord. However, ACh-gated currents mediated by L-AChRs and GABA-gated currents are not appreciably affected in *cam-1* mutants (Francis et al., 2005).

The majority of ACh-gated current at the NMJ is dependent on ACR-16/α7; but surprisingly, *acr-16* mutants do not have a discernible defect in locomotion when on standard assay plates (Francis et al., 2005; Touroutine et al., 2005). However, when we challenged *acr-16* mutants with a more rigid substrate (see Experimental Procedures), we found that their movement was diminished compared to wild-type controls, and this defect could be rescued by muscle specific expression of ACR-16/α7 (Figure 2.S1A).

The reduced ACh-gated current in *cam-1* mutants can be rescued by expressing a truncated variant of CAM-1 lacking the intracellular tyrosine kinase domain, CAM-1(ΔTKD), under control of the native *cam-1* promoter (Francis et al., 2005). To further delimit the site of action, we found that muscle-specific expression of GFP tagged CAM-1(ΔTKD), but not neuronal expression, was sufficient to rescue ACR-16/α7-mediated currents (Figure 2.1B and C). These results suggest that changes in ACR-16/α7-mediated signaling might depend on interactions between the extracellular domain of CAM-1 and other signaling

molecules at the muscle membrane. We tested this hypothesis by expressing a muscle-specific GFP-tagged variant of CAM-1 that lacked the extracellular domain, CAM-1(DECD)::GFP, and found that it was not sufficient to rescue ACh-gated current in *cam-1* mutants (Figure 2.1B and C).

The dependence of CAM-1 function on the ECD, but not the TKD, led us to search for gene products that might interact with CAM-1 and contribute to the regulation of synaptic ACR-16/α7 receptors. In heterologous cells, Ror RTKs have been shown to bind frizzled (Fzd) receptors, which are seven-pass transmembrane proteins required for Wnt-mediated signaling (Oishi et al., 2003). Because the intracellular kinase domain of CAM-1 is not required for ACR-16/α7-mediated current, CAM-1 might function via a kinase-independent mechanism – possibly by interacting with a Fzd receptor (Francis et al., 2005; Zinovyeva et al., 2008).

We took advantage of our earlier observation that *unc-29; acr-16* double mutants have a synthetic, near-paralyzed phenotype (Francis et al., 2005), and reasoned that if Wnt-signaling was required for ACR-16/α7-mediated currents then mutations in genes predicted to contribute to Wnt-signaling should also have a synthetic phenotype with the *unc-29* mutation (gene alleles described in Table 2.S, Molecular description of alleles). We therefore made double mutants with *unc-29* and candidate Wnt-signaling mutants and tested these in a movement assay (thrashing in liquid). We found that mutations in a Wnt ligand (CWN-2), a Frizzled receptor (LIN-17), and an intracellular signaling molecule Dishevelled (DSH-1) all had synthetic movement defects similar to those

observed in *unc-29; acr-16* and *unc-29; cam-1* double mutants (Figure 2.1D); but the single mutants were not nearly as impaired (Figure 2.S1B). We also found that locomotion on agar plates was disrupted in *unc-29; lin-17* double mutants and that this defect was rescued by muscle-specific expression of LIN-17 (Figure 2.S1C). We did not observe comparable defects in the Frizzled mutants *mig-1* and *cfz-2*, the Wnt mutants *cwn-1* and *egl-20*, or the Ryk/Derailed mutant *lin-18* (Figure 2.1D and data not shown). This indicates that only a subset of known Wnt-signaling proteins function in this synaptic signaling pathway.

We next asked whether the Wnt signaling pathway was dependent on CWN-2, or if other Wnt ligands could substitute for CWN-2. However, we found no evidence that thrashing behavior was rescued in transgenic *unc-29*; *cwn-2* mutants that expressed the Wnts EGL-20 or LIN-44 driven by the *cwn-2* promoter (Figure 2.S1D).

ACR-16/α7-mediated currents are selectively diminished in Wnt signaling mutants

To directly test whether Wnt signaling is required for normal synaptic function, we used standard electrophysiological techniques to record *in vivo* currents in muscle evoked by pressure application of ACh. We found that the magnitude of the ACh-gated current was significantly diminished for each of the Wnt-signaling mutants (Figure 2.1E and F). The reduced current appeared to be secondary to a selective decrease in the fast, ACR-16/α7-mediated component of the ACh-gated current, similar to what was observed for *cam-1* and *acr-16*

mutants. This was confirmed by the observed reduction in nicotine-gated currents in *cwn-2* and *lin-17* mutants (Figure 2.S2A). Furthermore, ACh-gated currents in *lin-17; cam-1* double mutants were indistinguishable from either single mutant alone, suggesting that CAM-1 and LIN-17 function in the same signaling pathway (Figure 2.1E and F).

The slow component of the current is mediated by UNC-29-containing ionotropic receptors that are selectively activated by levamisole (Francis et al., 2005; Richmond and Jorgensen, 1999). We therefore measured levamisole-gated currents in Wnt-signaling mutants to determine whether these mutations disrupt the UNC-29-mediated component of the ACh-gated current. We found that levamisole-gated currents in these mutants were indistinguishable from wild type (Figure 2.S2B), suggesting that Wnt-signaling is specifically required for ACR-16/α7-mediated current. As an additional control, we found that GABA-activated currents were normal in *cwn-2* mutants (Figure 2.S3A). ACh-gated currents were not disrupted in *cwn-1*, *lin-44* or *egl-20* mutants, providing further evidence for specificity of CWN-2 signaling (Figure 2.S3B). Together, our results indicate that Wnt signaling is required for ACR-16/α7-mediated whole-cell currents.

Presynaptic release is not appreciably disrupted
in Wnt signaling mutants

To further evaluate synaptic transmission, we measured endogenous cholinergic synaptic activity. We found a similar decrease in the average

amplitude of the miniature excitatory postsynaptic current (mEPSC) for each of the Wnt signaling mutants (Figure 2.S3C). In contrast, we did not observe a significant change in mEPSC frequency (wild type, 25 ± 4/s; *cam-1*, 20 ± 7/s; *cwn-2,* 20 ± 5/s; *lin-17,* 23 ± 12/s; and *dsh-1,* 14 ± 8/s, $p>0.05$), indicating that endogenous presynaptic release was not obviously disrupted in the Wnt signaling mutants.

We also asked whether Wnt signaling contributed to nerve-evoked current. To measure these currents, we expressed the light-gated ion channel channelrhodopsin-2 (ChR2) in cholinergic motor neurons and used light to depolarize these motor neurons (Liewald et al., 2008; Liu et al., 2009). We found that light stimulation elicited reproducible nerve-evoked postsynaptic currents in both wild type and *cwn-2* mutants (Figure 2.S2C). However, the peak amplitude of nerve-evoked current was significantly reduced in *cwn-2* mutants while the steady state current, which reflects the contribution of levamisole receptors, was not significantly altered. These results are consistent with the decreased amplitude of mEPSCs (Figure 2.S3C) and the reduction in ACh-gated current (Figure 2.1E and F).

Neuronal Wnt acts through muscle expressed Fzd/Ror/Dvl to regulate ACR-16/α7-mediated behavior and current

The Wnt signaling proteins identified in our screen are expressed in muscles and neurons (Gleason et al., 2006) raising the question of whether these proteins are required in a specific tissue for ACR-16/α7-mediated behavior

and current. To address this question, we first examined whether the *cwn-2* mutants could be rescued by selective expression of the wild-type protein in either muscles or neurons. To isolate the ACR-16/α7-mediated behavior and current, we measured thrashing behavior and recorded ACh-evoked currents in the *unc-29* mutant background. Interestingly, we found that thrashing in *cwn-2* mutants was rescued by expressing wild-type CWN-2, a secreted protein, in neurons or muscles (Figure 2.2A).

Although this finding for sufficiency is consistent with CWN-2's role as a secreted signaling molecule in other tissues (Kennerdell et al., 2009), we sought to address the question of necessity by using RNAi to selectively knock down expression of *cwn-2* in muscles or neurons. Successful knock down was indicated by an RNAi-mediated decrease in secreted CWN-2::mCherry fluorescence (Figure 2.S3D). We found that knock down in neurons, but not in muscles, phenocopied both the synthetic thrashing and current defects observed in *unc-29; cwn-2* mutants (Figure 2.2B–D).

We next asked whether DSH-1 and LIN-17 are required in muscles or neurons. We found that both thrashing and current defects of *lin-17* and *dsh-1* mutants were rescued by selectively expressing wild-type transgenes in muscles. In contrast, we did not observe rescue with neuron-specific expression (Figure 2.2E–J). These results are also consistent with our finding that CAM-1(ΔTKD)::GFP expression in muscle cells rescued current defects in the muscles of *cam-1* mutants (Figure 2.1B and C).

CAM-1 and LIN-17 function in the same pathway

to regulate ACR-16/α7 at synapses

Our analysis of single mutants revealed that the behavioral and electrophysiological phenotypes of Wnt-signaling mutants were similar to those of *cam-1* mutants. Additional genetic analysis revealed that ACh-gated currents recorded from *lin-17; cam-1* double mutants were of similar magnitude and kinetics to those recorded from *cam-1* and *lin-17* single mutants (Figure 2.1E and F). These data suggested that the LIN-17 frizzled receptor and the CAM-1 RTK function in the same pathway. Because the extracellular domain (ECD) of CAM-1 is required for its function at synapses, we speculated that CAM-1 and LIN-17 might interact directly via the ECDs of each protein, possibly forming a heteromeric receptor. To further test this possibility, we examined the subcellular localization of LIN-17 and CAM-1. We found that these functional, fluorescently labeled proteins were expressed in muscle arms of transgenic worms and partially co-localized (Figure 2.3A) suggesting that LIN-17 and CAM-1 might associate in muscle arms.

To address this possibility, we tested bimolecular fluorescence complementation (BiFC) between LIN-17 and CAM-1 (Shyu et al., 2008). We used a split variant of the Venus Yellow Fluorescent Protein (YFP) and fused the N- and C-terminal fragments of Venus YFP to the intracellular regions of CAM-1 (CAM-1::N-YFP) and LIN-17 (LIN-17::C-YFP), respectively. We observed distinct YFP puncta in the muscle arms abutting the ventral cord in transgenic worms that co-expressed the LIN-17::C-YFP and CAM-1::N-YFP fusion proteins (Figure

2.3B). Transgenic worms that expressed either the N- or C-terminal YFP fragment alone exhibited no fluorescence, but we observed a punctate YFP signal in cross progeny that expressed both transgenes (Figure 2.S4A).

The CAM-1 ECD is predicted to be important for Wnt binding and perhaps for interactions between the receptor components (Green et al., 2007; Kim and Forrester, 2003). To determine whether the ECD was required for the interaction between CAM-1 and LIN-17, we generated a split-YFP-tagged CAM-1 variant that lacked the ECD (CAM-1(ΔECD)::N-YFP) and as a control a tagged variant that lacked the intracellular kinase domain (CAM-1(ΔTKD)::N-YFP). We found YFP puncta in transgenic worms that co-expressed CAM-1(ΔTKD)::N-YFP and LIN-17::C-YFP in muscles (Figure 2.3C), but no appreciable fluorescent signal in worms that co-expressed CAM-1(ΔECD)::N-YFP and LIN-17::C-YFP (Figure 2.3D). These data suggest that the CAM-1 ECD is required for the association of LIN-17 with CAM-1, and that the fluorescent signal is not simply due to overexpression of the tagged proteins. Although the ECD was required for BiFC fluorescence, examination of GFP-labeled CAM-1(ΔECD) indicated that this domain was not essential for CAM-1 expression at the NMJ (Figure 2.3E).

Our finding that the CAM-1 ECD mediates its interaction with LIN-17 is consistent with our earlier finding that CAM-1(ΔTKD) rescues current when expressed in transgenic *cam-1* mutants (Francis et al., 2005) (Figure 2.1B and C). Together, these results provide evidence for a mechanistic model in which CAM-1 and LIN-17 form a functional heteromeric receptor in muscle cells. This model is also consistent with our analysis of *lin-17; cam-1* double mutants

(Figure 2.1E and F), which showed that LIN-17 and CAM-1 function in the same signaling pathway to regulate ACR-16/α7-mediated current.

Postsynaptic ACR-16/α7 receptors are mislocalized in Wnt signaling mutants

ACR-16::GFP fluorescence is found at the tips of muscle arms apposed to presynaptic release sites in the cholinergic motor neurons traveling in the ventral cord (Figure 2.3F and G). In *cam-1* mutants, we previously observed subsynaptic accumulations of ACR-16::GFP in muscle arms, but no change in the distribution of UNC-49::GFP GABA receptors or UNC-29::GFP L-AChRs (Francis et al., 2005). We found that ACR-16::GFP was similarly mislocalized in other Wnt signaling mutants (Figure 2.3H). Whereas the distribution of ACR-16 was markedly altered in *cwn-2* mutants, the distribution of the SYD-2 presynaptic protein did not appear appreciably altered (Figure 2.3G). Furthermore, we did not detect obvious changes with respect to the morphology of body wall muscles or the number of muscle arms (Figure 2.S4B).

For each Wnt signaling mutant, the average intensity of ACR-16::GFP was dramatically increased in the muscle arms (Figure 2.3I). The defects were rescued in *lin-17* and *dsh-1* mutants using a muscle specific promoter to express wild type LIN-17 and DSH-1, respectively (Figure 2.3J and K). No rescue was observed when using a neural specific promoter (Figure 2.S4C). In addition, receptor defects appeared specific to ACR-16::GFP, as we found no apparent

change in the subcellular distribution of UNC-49::GFP or UNC-29::GFP in *cwn-2* mutants (Figure 2.S4D).

To determine the tissue from which CWN-2 is secreted in order to mediate ACR-16/a7 localization, we used RNAi to selectively knock down expression of *cwn-2* in muscles or neurons. We found that knock down in neurons, but not in muscles, phenocopied the aberrant localization of ACR-16::GFP in *cwn-2* mutants (Figure 2.3L and M). Taken together, these results demonstrate the necessity of CWN-2 function in neurons, and LIN-17, CAM-1 and DSH-1 in muscles for localization of ACR-16 to the NMJ.

Wnt-signaling is required for surface expression and mobility of ACR-16/α7 at the NMJ

We hypothesized that the subsynaptic accumulation of ACR-16/α7 receptors in Wnt signaling mutants might reflect a decrease in the number of surface receptors. To test this possibility, we labeled surface ACR-16/α7 receptors by injecting fluorescently-labeled alpha-bungarotoxin (α-BgTx) into the pseudocoelomic space of transgenic wild-type and mutant worms that expressed soluble mCherry in muscle cells (Gottschalk et al., 2005; Zheng et al., 2004). In wild-type worms and Wnt signaling mutants, we observed fluorescence in muscle arms at the points of contact with the ventral cord following clearance of excess toxin by coelomocytes. This localization is consistent with a postsynaptic distribution of ACR-16/a7 receptors (Figure 2.4A). Because of the delay in clearing excess a-BgTx, a fraction of the fluorescence signal might also reflect

internalized receptors. However, the signal was decreased in *cwn-2* and *cam-1* mutants compared to wild type suggesting that Wnt signaling promotes surface expression of ACR-16/a7 (Figure 2.4B). Importantly, the fluorescence signal in muscle arms was dependent on ACR-16/a7 since we did not measure appreciable a-BgTx fluorescence at muscle arms of *acr-16* mutants (Figure 2.4A and B). We also observed fluorescence in unidentified processes that lacked muscle mCherry expression in all of the worm strains (Figure 2.4A), suggesting that a-BgTx binds to additional AChRs that are expressed in neurons. This binding was unrelated to Wnt signaling or ACR-16 and served as a useful control for a-BgTx labeling.

Our results suggest that the subsynaptic accumulation of ACR-16::GFP in Wnt-signaling mutants is secondary to reduced surface expression. The percentage reduction in surface expression was roughly equivalent to the percentage reduction in ACh- and nicotine-gated currents (Figure 2.1E and F; Figure 2.S2A) and provides a mechanistic explanation for the selective decrease in the fast component of ACh-gated current found in Wnt-signaling mutants.

Loss of Wnt-signaling results in decreased surface expression of ACR-16/a7 and its intracellular accumulation in muscle arms. Thus, we reasoned that Wnt-signaling might be required for delivery of ACR-16/a7 receptors from subsynaptic pools to the cell surface of the NMJ. We tested this hypothesis by using ACR-16/a7 fused to the photoconvertible fluorophore EosFP (ACR-16::EosFP) and performed optical pulse labeling experiments (Wiedenmann et al., 2004). The fluorescent signal at the distal tips of muscle arms was converted

from green to red with a 405 nm laser (Figure 2.4C and D). We found that the red fluorescence decayed such that little signal remained in wild-type worms one hour after photoconversion (Figure 2.4D and E). In contrast, the decay was significantly slower in *lin-17* mutants. We also attempted to photoconvert the "neck" of the muscle arm and track the movement into the synaptic region. These experiments were technically difficult; however in the few instances that we were successful, we found reduced mobility in *lin-17* mutants (Figures 2.S5A). These results suggest that the turnover of the subsynaptic pool of ACR-16 is decreased in *lin-17* mutants. In addition, the longer lifetime of converted EosFP also argues against a model in which the decreased level of staining by a-BgTx in *cwn-2* and *cam-1* mutants is due to endocytosis of ACR-16/a7 followed by its rapid degradation. Together, these experiments indicate that Wnt signaling is required for the translocation of ACR-16/a7 receptors from subsynaptic pools to the NMJ and that reduced Wnt signaling leads to a large immobile pool of subsynaptic ACR-16/a7.

ACR-16/a7 is required in the adult nervous system

AChRs are critically important for synaptic function; but do they also have essential developmental roles? It is possible that the synaptic defects observed in adult *acr-16* mutants are secondary to developmental defects. For example, the molecular machinery required for postsynaptic function might not be properly assembled or stabilized in *acr-16* mutants causing irreversible changes in synaptic communication. To test whether ACR-16/a7 has an obligate

developmental role, we generated *unc-29; acr-16* transgenic mutants that expressed ACR-16/α7 under an inducible heat-shock promoter (*Phsp*::*acr-16*). We heat shocked young adult transgenic worms and assayed behavior approximately 10 hours later. We found that the defective locomotion and thrashing that is characteristic of *unc-29; acr-16* double mutants were rescued in heat shocked adult transgenic mutants (Figure 2.S5B). Furthermore, we found that heat shock rescued nicotine-gated currents (Figure 2.S5C and D). Thus, synaptic function and behavior mediated by ACR-16/α7 could be restored in adult *unc-29; acr-16* mutants, indicating that ACR-16/α7 does not have an obligate developmental role.

Wnt signaling has an ongoing role in regulating ACR-16/α7-mediated behavior and synaptic plasticity

The Wnt signaling pathway is best known for its many developmental roles (van Amerongen and Nusse, 2009). To determine whether Wnt regulation of ACR-16/α7 at the NMJ is primarily developmental, we used a heat shock-inducible promoter to drive the expression of LIN-17 (*Phsp*::*lin-17*) in transgenic *lin-17; unc-29* double mutants. We found that normal motor behavior was restored approximately 10 hours following heat shock, but not in mutants lacking the transgene (Figure 2.5A). However, the rescue did not persist and thrashing rates returned to approximately pre-heat-shock levels within 24 hours, suggesting that ongoing expression of LIN-17 in adult worms is required for Wnt signaling and ACR-16/α7 dependent behavior. In addition, we observed that

ACR-16::GFP fluorescence intensity in muscle arms could be rescued as early as 2 hours after heat shock driven expression of LIN-17 in adult *lin-17* mutants (Figure 2.5B and C). As we found for locomotion, the rescue was transient with ACR-16::GFP intensity increasing to mutant levels within 24 hours post heat shock. Together, our results suggest that Wnt signaling has an ongoing role in the maintenance of synaptic transmission in the adult nervous system.

An ongoing role for Wnt signaling suggests that ACR-16 translocation might be dynamically regulated in an experience dependent fashion. To address whether Wnt signaling contributes to experience-dependent plasticity, we expressed ChR2 in cholinergic motor neurons. We stimulated worms with light pulses to depolarize the motor neurons and measured ACR-16::GFP fluorescence in muscle arms. We found that 30 or 60 minutes of light stimulation reduced ACR-16::GFP fluorescence in wild-type worms, but not in control worms or in *cwn-2* mutants (Figure 2.6A and B).

We next asked whether optogenetic stimulation altered ACh-gated current at the NMJ. We found that the ACR-16-mediated current, but not the UNC-29-dependent component, was increased in worms after one hour of light stimulation; however, no stimulation-dependent increase was observed in control worms (Figure 2.6C and D). The decreased fluorescent signal following stimulation suggests that ACR-16::GFP is more diffuse following translocation to the cell surface. Significantly, we did not observe a stimulation-induced augmentation of current in *cwn-2* mutants. The changes were specific to ACh-gated currents since we did not observe activity-dependent changes in GABA-

activated current (Figure 2.S6A). We also found that prolonged light stimulation increased the amplitude of both endogenous synaptic events (Figure 2.S6B) and nerve evoked currents (Figure 2.S6C) in wild-type worms. These activity dependent changes were dependent on neuronal expression of CWN-2. Thus, activity dependent changes were rescued in transgenic *cwn-2* mutants that expressed neuronal, but not muscle, *cwn-2* (Figure 2.6E and F). Furthermore, activity dependent changes were blocked by RNAi knock down of *cwn-2* in neurons, but not by knock down in muscles (Figure 2.6G and H). In agreement with the requirement for *cwn-2* signaling, we found that activity dependent changes were blocked in *lin-17* mutants and could be rescued in transgenic *lin-17* mutants with muscle-specific expression of a wild-type *lin-17* transgene (Figure 2.S6D).

Wnt-mediated changes in ACR-16/α7 surface expression
are independent of protein synthesis

Wnts can signal through multiple pathways, including the well-characterized canonical Wnt-signaling pathway, which depends on TCF/LEF transcription factors and new protein synthesis, and through non-canonical pathways (Korkut and Budnik, 2009; van Amerongen and Nusse, 2009). In *C. elegans*, *pop-1* encodes the only known TCF/LEF homologue, and we did not observe altered ACR-16::GFP following knock down of *pop-1* using RNAi (data not shown). To rigorously test the requirement for new protein synthesis in CWN-2 signaling, we adapted an existing protocol to block protein synthesis using the

drug cycloheximide (CHX) (Kourtis and Tavernarakis, 2009). We found that CHX blocked new protein synthesis (Figure 2.S7A and B), but did not have significant effects on activity-dependent changes in ACR-16::GFP (Figure 2.7A and B).

The neuronal requirement for Wnt-mediated changes in ACR-16/α7 translocation predicts that prolonged light-stimulation should be associated with neuronal release of CWN-2. To test this prediction, we co-expressed CWN-2::GFP and ChR2 in cholinergic motor neurons and used our light stimulation protocol to depolarize the motor neurons. We found that CWN-2::GFP fluorescence was decreased in motor neurons following light stimulation, but unchanged in control worms (Figure 2.7C and D). This result is consistent with activity-dependent secretion of CWN-2, but could also represent activity-dependent degradation of CWN-2. To distinguish between these possibilities, we evaluated changes in CWN-2 in the *mig-14* mutant background. The secretion of all Wnts is believed to be dependent on the Wntless transmembrane protein (Port and Basler, 2010), which is encoded by *mig-14* in *C. elegans*. We found that the activity-dependent decrease in CWN-2::GFP fluorescence was blocked in *mig-14* mutants (Figure 2.7C and D). This result indicates that the decrease in CWN-2::GFP in light-stimulated motor neurons is a consequence of activity-dependent secretion of CWN-2. Moreover, we selectively knocked down expression of MIG-14 in muscles or neurons and found that MIG-14 is required in neurons for ACR-16::GFP localization (Figure 2.S7C).

Our data strongly suggest a model where neuronal activity leads to secretion of CWN-2, which then rapidly, and independently of new protein

synthesis, increases ACh-gated current by mediating the translocation of additional ACR-16/α7 receptors to the muscle surface. To directly test this model, we produced recombinant CWN-2 by expressing *cwn-2* in cultured mammalian HEK cells using a previously published protocol (Cuitino et al., 2010). We found that application of recombinant CWN-2 to our dissected neuromuscular preparation rapidly (within approximately 15 minutes) caused an increase in ACh-gated current (Figure 2.7E and F). This result clearly shows that there is no developmental requirement for CWN-2 with respect to ACR-16/α7 translocation and that CWN-2 alone is capable of triggering a rapid increase in the number of functional ACR-16/α7 receptors at the NMJ. Thus, we have found that the cholinergic synapse is plastic and responds by modifying surface ACR-16/α7 receptors in response to prolonged stimulation of motor neurons. These plastic changes are dependent on activity-mediated and Wntless/MIG-14-dependent secretion of CWN-2 from neurons, heteromeric CAM-1/LIN-17 postsynaptic receptors in muscle cells and the critical downstream signaling protein Dishevelled/DSH-1.

Discussion

Neuronal signaling is shaped by the time-dependent sum of the excitatory and inhibitory synaptic inputs. In *C. elegans*, the same mechanisms can be found at the NMJ, an experimentally accessible synapse ideal for mechanistic studies of synaptic function. We found that in *C. elegans*, the N-AChR ACR-16/α7-mediated currents are selectively diminished in mutants with disrupted Wnt

signaling. In Wnt mutants the neuromuscular architecture is grossly normal and synaptic functions mediated by both GABAergic inputs and postsynaptic L-AChRs are indistinguishable from those in wild type. The ACR-16/α7-mediated current shares a similar dependence on the CWN-2 Wnt ligand, the CAM-1/RTK and LIN-17/Frizzled membrane proteins, and the DSH-1/dishevelled downstream effector protein. These results suggest that CAM-1 and LIN-17 contribute to a heteromeric receptor for the CWN-2 ligand; a hypothesis supported by our studies using bifluorescence complementation to map LIN-17 and CAM-1 proximity (Figure 2.3). Furthermore, CAM-1 and other Ror RTKs contain extracellular cysteine-rich domains that are also found in Frizzled proteins. In mammalian Ror RTKs, these domains bind Wnt5, the mammalian homologue of CWN-2 (Mikels and Nusse, 2006; Oishi et al., 2003).

In a recent study, CAM-1 appeared to associate with the Frizzled protein MIG-1 and bind to CWN-2 (Kennerdell et al., 2009). We found that a truncated variant of CAM-1 that lacks the cytoplasmic kinase domain restores ACR-16/a7-mediated current in transgenic *cam-1* mutants. This result, together with the interaction between LIN-17 and CAM-1, indicates that CAM-1/RTK contributes to CWN-2/Wnt signaling, but that the intracellular signaling is mediated primarily by LIN-17 (and DSH-1/Dvl). Thus, CAM-1 might have a direct role in regulating CWN-2 binding, or an indirect role by localizing or stabilizing LIN-17. In contrast to previously described developmental roles for CAM-1 and Wnt signaling (Green et al., 2008; van Amerongen and Nusse, 2009), we show that this signaling

pathway has an ongoing functional role in regulating the strength of synaptic transmission in adult worms.

The possible contributions of Wnt signaling to the function of the adult nervous system are difficult to study and are not well understood. We found that heat-shock promoter driven expression of LIN-17 in adult *lin-17* transgenic mutants rescued ACR-16/α7-mediated behavior and ACR-16/α7 localization (Figure 2.5). The rescue of behavior and localization was transient, indicating rapid turnover of LIN-17 and ongoing dependence on this signaling pathway.

In support of our model that a heteromeric CAM-1/LIN-17 receptor mediates the surface expression of ACR-16/α7 in postsynaptic muscle, we found that CAM-1 and LIN-17 co-localize at the NMJ and that muscle-specific expression of CAM-1 and LIN-17 in transgenic mutants rescues ACR-16/α7-mediated current and behavior, whereas CWN-2 and MIG-14 are required in neurons. CWN-2 signaling rapidly causes translocation of ACR-16/α7 from subsynaptic pools to the cell surface, as evidenced by our finding of increased ACh-gated currents following application of recombinant CWN-2. Our data favor a model in which the levels of CWN-2 are limiting for receptor translocation and are controlled in part by neural activity. In support of this model, we found that neuronal CWN-2 levels are altered by optogenetic stimulation of the neurons, suggesting that CWN-2 secretion responds to neuronal activity. Less clear is whether LIN-17 and CAM-1 function as constitutive heteromers; whether CWN-2 induces dimerization; or whether dimerization itself might be altered by synaptic

activity. A dimerization model was proposed for CWN-2 regulation of axonal guidance (Kennerdell et al., 2009).

Heteromeric RTK/Frizzled complexes have been described for Wnt signaling during development (Lu et al., 2004; Minami et al., 2010). However, to our knowledge, a heteromeric CAM-1/LIN-17 receptor complex participating in Wnt-mediated signaling at adult synapses has not been previously described, and contrasts with the known signaling roles for CAM-1 and LIN-17. Presumably, the heteromeric complex provides additional signaling specificity, e.g., shunting signaling from the canonical pathway to an alternate pathway, such as the PCP pathway, to cause rapid changes in receptor translocation and synaptic transmission.

Dynamic translocation of receptors from subcellular pools to the surface membrane is an essential and conserved feature found in diverse signaling pathways. Yet we still lack a comprehensive understanding of how extracellular signals lead to precise translocation of receptors. Our data suggest that Wnt signaling regulates the translocation of subsynaptic ACR-16/α7 receptors to muscle arm synapses in *C. elegans*. Thus, in Wnt-signaling mutants ACR-16/α7 receptors accumulate in subsynaptic pools and surface expression is reduced. Associated with decreased surface expression of ACR-16/α7 is a marked reduction in receptor mobility as defined by photoconversion experiments (Figure 2.4). Interestingly, CWN-2/Wnt signaling does not appear to have an effect on GABARs, L-AChRs or the currents mediated by these receptors. Thus, we were

able to cleanly dissect and distinguish the signaling pathway that contributes to ACR-16/α7 synaptic signaling from other developmental or regulatory pathways.

We also found that cholinergic synapses at the NMJ are plastic and their strength is modified by prolonged activity. Under our conditions of optogenetic stimulation, ACR-16/α7 puncta diminished in size and ACh-gated current was increased. These effects were not observed in *cwn-2* mutants. Perhaps different environmental challenges, e.g., increased load or resistance, are associated with increased nervous system activity, which then leads to a Wnt-mediated recruitment of additional receptors. We envision a model where synaptic strength is dynamically modulated by translocation of receptors regulated by a Wnt signaling pathway. This mode of regulation might be evolutionarily conserved and could contribute to fundamental processes of synaptic plasticity and homeostasis in other organisms and for other classes of synaptic receptors.

Experimental procedures

Strains, genetics, and germline transformation

All *C. elegans* strains were raised under standard conditions on the *E. coli* strain OP50 at 20° C unless otherwise noted. Wild-type worms were the Bristol N2 strain. Mutant alleles used were *cam-1(ak37)*, *cwn-2(ok895)*, *lin-17(n671)*, *dsh-1(ok1445)*, *acr-16(ok789)*, *unc-29(x29), cwn-1(ok546)*, *cfz-2(ok1201)*, *egl-20(n585ts)*, *lin-44(n1792), mig-1(e1787), mig-14(mu71),* and *lin-18(e620).* Plasmids, transgenic arrays and strains are described in Supplemental

Experimental Procedures. All fluorescently labeled proteins were found to be functional in transgenic rescue experiments of the respective mutant phenotype.

Behavioral analysis

Thrashing assays were performed as described previously (Francis et al., 2005). All thrashing assays were done blind. For heat-shock rescue experiments, worms were kept at 30° C for 30 minutes. For movement on agarose, worms were mounted on 5% agarose pads with 1 ml of Polybead Microspheres 0.625% (w/v) in M9 solution and covered with a glass cover slip (Fang-Yen, et al., Worm Breeders Gazette, Vol. 18, 2010). Time-lapse images were acquired for 30 seconds with a Hamamatsu CCD camera using a 10X 0.5 NA Zeiss objective mounted on an inverted Zeiss compound microscope. Images were acquired with Metamorph software and analyzed with ImageJ software. Statistical significance was determined using Student's T-test.

Electrophysiological analysis

Ligand-gated currents were recorded from voltage-clamped muscle cells using patch-clamp technology as previously described (Francis et al., 2005). Drugs were applied for 250 ms using pressure application. All drugs were used at a concentration of 100 mM. Light-evoked currents were elicited from worms expressing ChR2 under the *unc-17* promoter following a recently described protocol (Liu et al., 2009).

Microscopy and labeling

For confocal fluorescence microscopy, worms were mounted on agarose pads and imaged as previously described (Francis et al., 2005). For ACR-16::GFP intensity analysis in muscle arms, image stacks were imported into ImageJ software for maximum projection analysis. A region of interest (ROI) was drawn around individual muscle arms along the ventral nerve cord in one-day old adult worms and the average intensity was calculated with correction for background fluorescence. There was no significant difference in the ROI area (pixels) for all genotypes. For CWN-2::GFP quantification, a ROI was drawn around each motor neuron cell body and the average intensity was calculated for light (+) retinal (-) after correcting for background fluorescence. This value was then used to normalize activity-dependent changes in GFP. Surface expression of ACR-16/α7 was assessed with α-bungarotoxin conjugated to Alexa Fluor 488 (Molecular Probes). All analyses were done blind to genotype. Additional details about confocal microscopy and labeling are found in Supplemental Experimental Procedures.

EosFP photoconversion

Worms were immobilized on agarose pads (Fang-Yen, et al., Worm Breeders Gazette, Vol. 18, 2010) and single ACR-16::EosFP puncta at the tips of distinct muscle arms were converted using a single 3 seconds pulse of a 405 nm laser set to a total output of 35 mW applied to a Mosaic II digital mirror device (Photonics) controlled by Metamorph software. Confocal stack images were

acquired before, immediately after, and at various time points after conversion as described above. The time-dependent photoconverted signal was expressed as a percentage of the signal immediately following photoconversion. For pulse-chase experiments, statistical significance was determined using a 2-way ANOVA test.

Synaptic plasticity

Transgenic worms expressed ChR2 under control of the *unc-17* promoter, which drives expression in the cholinergic motor neurons. Worms were stimulated with 470 nm light delivered by a Lambda DG4 light source (Sutter). Light intensity at the surface of the NGM (nematode growth media) was approximately 240 $\mu W/mm^2$ and worms were stimulated at 3 Hz with 100 ms pulses of light for specified durations (Liu et al., 2009).

Recombinant CWN-2

We expressed *cwn-2* in mammalian HEK cells as previously described (Cuitino et al., 2010). Briefly, HEK cells were stably transfected with Lipofectamine (Invitrogen) with either empty vector pcDNA or pcDNA encoding *cwn-2* cDNA coupled to a hemagglutinin (HA) tag. HEK cell supernatant was then collected and concentrated using a Centrifugal Filter Device (Millipore; 30 kDa), and diluted 1 to 50 in ECF (1 mM Ca^{2+}). Secreted CWN-2 was detected by western blot using a HA-specific antibody.

Acknowledgments

We thank members of the Maricq laboratory for comments on the manuscript, Kang Shen and Erik Jorgensen for plasmids and transgenic strains, and the *Caenorhabditis* Genetics Center [funded by the National Institutes of Health (NIH)] for providing worm strains. This research was made possible by support from NIH Grant R01 NS070280 and American Heart Association Predoctoral Grant 09PRE2060730 (MJ).

Figure 2.1. Wnt and CAM-1/Ror signaling proteins contribute to synaptic signaling.
(A) Schematic of the NMJ showing the three classes of ligand-gated receptors and deletion variants of the CAM-1/Ror RTK. The orange oblong represents the serine/threonine rich domain. (B) Currents recorded in muscle cells in response to pressure application of 100 uM ACh in wild-type worms, *cam-1(ak37)* mutants, and transgenic mutants that expressed either CAM-1(DECD)::GFP or CAM-1(ΔTKD)::GFP in muscles or neurons, respectively. (C) Normalized peak ACh-gated current, $n \geq 4$ for all genotypes. (D) Thrashing behavior of Wnt-signaling mutants in the *unc-29(x29)* mutant background. For all genotypes, $n \geq 10$. (E) ACh-gated currents in the muscle cells of wild-type (WT) and mutant worms. (F) Peak ACh-gated current normalized to wild-type values. For all genotypes, $n \geq 5$. *, $p<0.05$; **, $p<0.01$. Error bars indicate SEM. See also Figure 2.S1, 2.S2 and 2.S3.

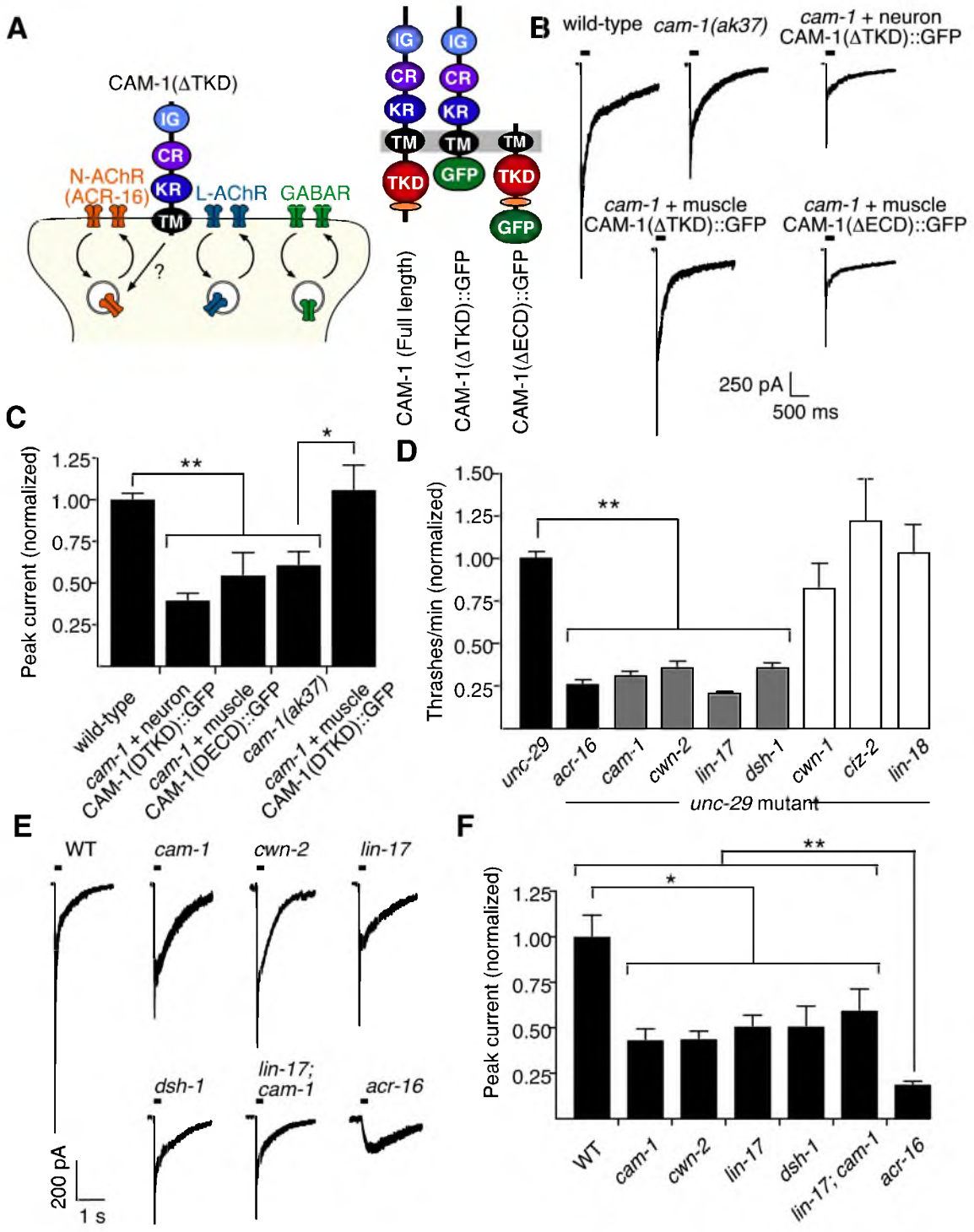
A
CAM-1(ΔTKD)
IG
CR
KR
TM
N-AChR
(ACR-16)
L-AChR
GABAR
?
CAM-1 (Full length)
CAM-1(ΔTKD)::GFP
CAM-1(ΔECD)::GFP
TKD
GFP
B
wild-type
cam-1(ak37)
cam-1 + neuron
CAM-1(ΔTKD)::GFP
cam-1 + muscle
CAM-1(ΔTKD)::GFP
cam-1 + muscle
CAM-1(ΔECD)::GFP
250 pA
500 ms
C
Peak current (normalized)
1.25
1.00
0.75
0.50
0.25
**
*
wild-type
cam-1 + neuron
CAM-1(DTKD)::GFP
cam-1 + muscle
CAM-1(DECD)::GFP
cam-1(ak37)
cam-1 + muscle
CAM-1(DTKD)::GFP
D
Thrashes/min (normalized)
1.50
1.25
1.00
0.75
0.50
0.25
**
unc-29
acr-16
cam-1
cwn-2
lin-17
dsh-1
cwn-1
ciz-2
lin-18
unc-29 mutant
E
WT
cam-1
cwn-2
lin-17
dsh-1
lin-17;
cam-1
acr-16
200 pA
1 s
F
Peak current (normalized)
1.25
1.00
0.75
0.50
0.25
**
*
WT
cam-1
cwn-2
lin-17
dsh-1
lin-17; cam-1
acr-16

Figure 2.2. ACR-16/a7-dependent behavior requires neuronal CWN-2 and Fzd/Ror/Dvl in muscles.
(A) Thrashing behavior normalized to *unc-29* single mutants. For all genotypes, n≥7. (B) Thrashing behavior normalized to wild-type (WT) worms (left) or *unc-29* mutants (right) in transgenic worms in which *cwn-2* was knocked down [*cwn-2(RNAi)*] in either neurons or muscles. For WT background, n≥5; and *unc-29* mutant background, n≥10. Gray bars indicate *unc-29* mutant background. (C) ACh-gated currents in *unc-29* mutants with or without *cwn-2* knock down. (D) Peak ACh-gated current normalized to *unc-29* mutants. For all genotypes, n≥4. (E and F) Thrashing behavior showing muscle specific rescue of *lin-17* (E) and *dsh-1* (F) mutants. For all genotypes, n≥9. (G and I) Currents evoked in muscle cells by pressure application of 100 mM ACh. (H and J) Average peak current amplitude of ACh-gated currents. For all genotypes, n≥4. *, $p<0.05$; **, $p<0.01$. Error bars indicate SEM. See also Figure 2.S3.

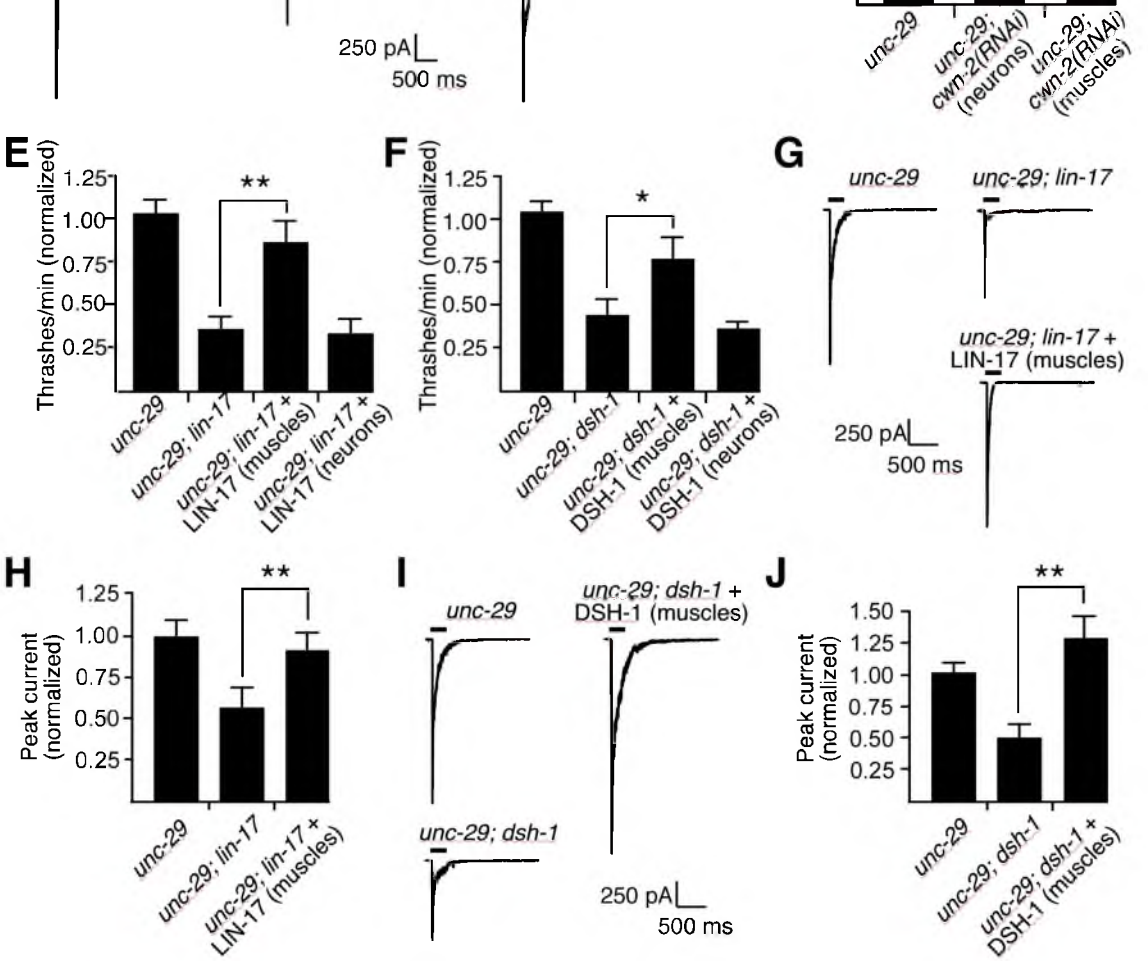
250 pA
500 ms
unc-29
unc-29; cwn-2(RNAi) (neurons)
unc-29; cwn-2(RNAi) (muscles)
E
Thrashes/min (normalized)
1.25
1.00
0.75
0.50
0.25
**
unc-29
unc-29; lin-17
unc-29; lin-17 + LIN-17 (muscles)
unc-29; lin-17 + LIN-17 (neurons)
F
Thrashes/min (normalized)
*
unc-29
unc-29; dsh-1
unc-29; dsh-1 + DSH-1 (muscles)
unc-29; dsh-1 + DSH-1 (neurons)
G
unc-29
unc-29; lin-17
unc-29; lin-17 + LIN-17 (muscles)
250 pA
500 ms
H
Peak current (normalized)
1.25
1.00
0.75
0.50
0.25
**
unc-29
unc-29; lin-17
unc-29; lin-17 + LIN-17 (muscles)
I
unc-29
unc-29; dsh-1
unc-29; dsh-1 + DSH-1 (muscles)
250 pA
500 ms
J
Peak current (normalized)
1.50
1.25
1.00
0.75
0.50
0.25
**
unc-29
unc-29; dsh-1
unc-29; dsh-1 + DSH-1 (muscles)

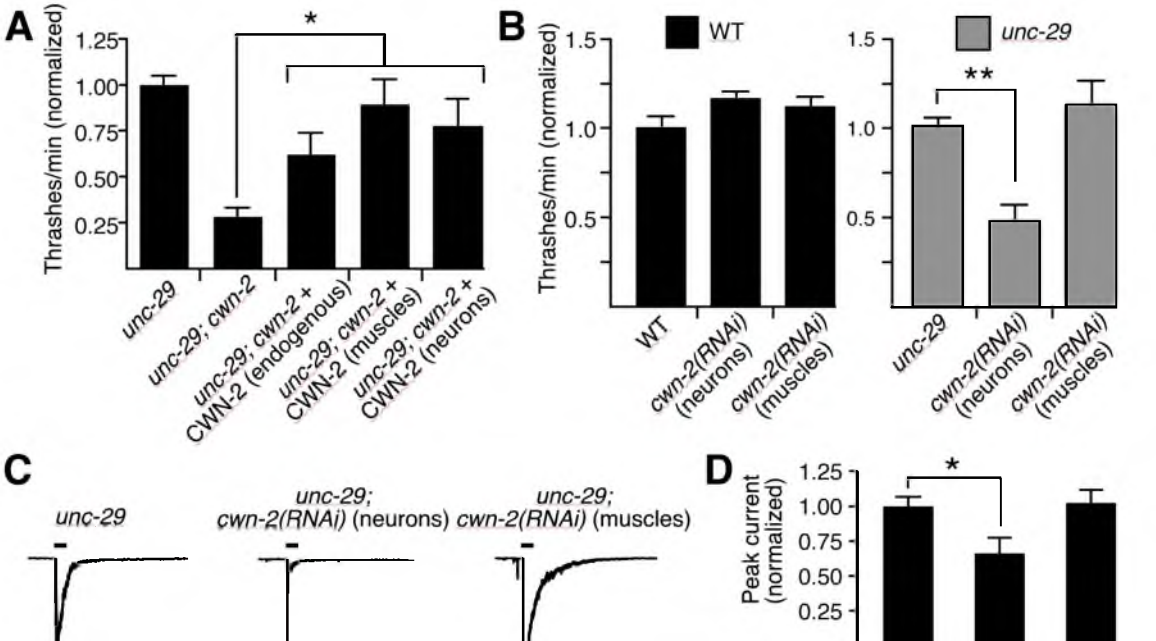
A
Thrashes/min (normalized)
1.25
1.00
0.75
0.50
0.25
*
unc-29
unc-29; cwn-2
unc-29; cwn-2 + CWN-2 (endogenous)
unc-29; cwn-2 + CWN-2 (muscles)
unc-29; cwn-2 + CWN-2 (neurons)
B
Thrashes/min (normalized)
1.5
1.0
0.5
WT
WT
cwn-2(RNAi) (neurons)
cwn-2(RNAi) (muscles)
unc-29
**
unc-29
cwn-2(RNAi) (neurons)
cwn-2(RNAi) (muscles)
C
unc-29
unc-29; cwn-2(RNAi) (neurons)
unc-29; cwn-2(RNAi) (muscles)
D
Peak current (normalized)
1.25
1.00
0.75
0.50
0.25
*

Figure 2.3. Muscle LIN-17/CAM-1 heteromeric receptors regulate ACR-16 localization.
(A) Single plane confocal images showing expression of CAM-1::GFP and LIN-17::mCherry in the tips of muscle arms. Box indicates the region shown in the images on the right. Scale bars, 2 mm. (B-E) Images of the tips of muscle arms in transgenic worms that expressed split-YFP fused to LIN-17 and either full-length CAM-1 (B), one of two CAM-1 deletion variants (C and D), or CAM-1(DECD)::GFP (E). Scale bars, 1 mm. (F) Image of the ventral nerve cord in a transgenic worm that expressed ACR-16::GFP in muscle cells and ChR2::mCherry in motor neurons. Scale bar, 5 mm. (G) ACR-16::GFP and SYD-R::RFP expression in the muscle arm of a transgenic wild-type (WT) worm or *cwn-2* mutant. Scale bar, 2 mm. (H) Images of muscle arms in transgenic wild-type and mutant worms that expressed ACR-16::GFP. The red, dashed lines outline the muscle arms. Scale bar, 1 mm. (I) Intensity of ACR-16::GFP fluorescence in muscle arms normalized to wild type. For all genotypes, $n \geq 8$. (J) Images of ACR-16::GFP expression in muscle arms. Scale bar, 1 mm. (K) Intensity of ACR-16::GFP fluorescence in muscle arms relative to wild-type. For all genotypes, $n \geq 11$. (L) ACR-16::GFP expression in muscle arms of wild-type worms with or without *cwn-2* knock down. Scale bar, 2 mm. (M) ACR-16::GFP fluorescence intensity in muscle arms relative to wild type, $n \geq 11$. *, $p<0.05$; **, $p<0.01$. Error bars indicate SEM. See also Figure 2.S4.

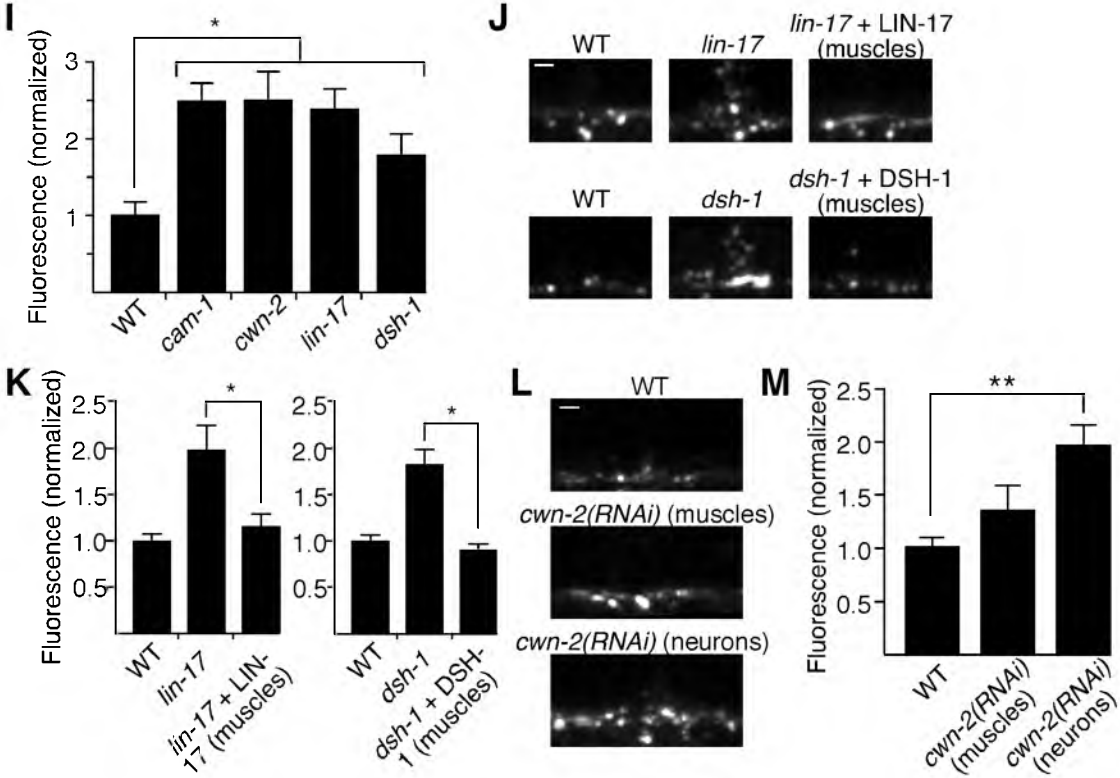
I
Fluorescence (normalized)
3
2
1
*
WT
cam-1
cwn-2
lin-17
dsh-1
J
WT
lin-17
lin-17 + LIN-17 (muscles)
WT
dsh-1
dsh-1 + DSH-1 (muscles)
K
Fluorescence (normalized)
2.5
2.0
1.5
1.0
0.5
*
WT
lin-17
lin-17 + LIN-17 (muscles)
*
WT
dsh-1
dsh-1 + DSH-1 (muscles)
L
WT
cwn-2(RNAi) (muscles)
cwn-2(RNAi) (neurons)
M
Fluorescence (normalized)
2.5
2.0
1.5
1.0
0.5
**
WT
cwn-2(RNAi) (muscles)
cwn-2(RNAi) (neurons)

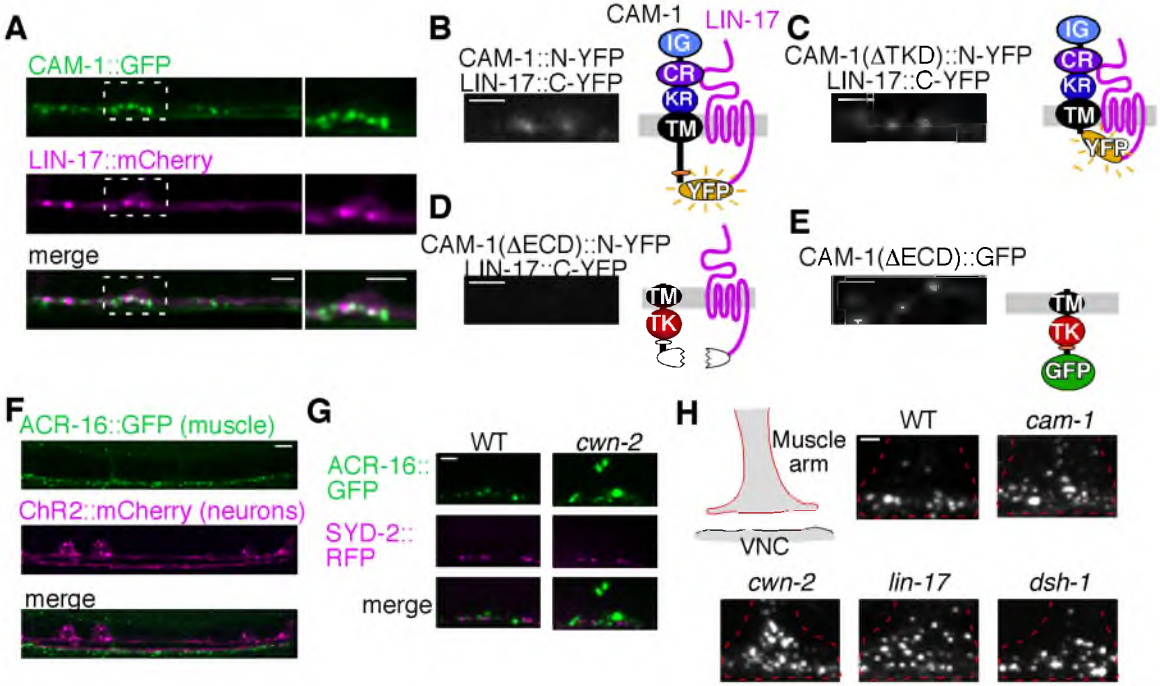
A
CAM-1::GFP
LIN-17::mCherry
merge
B
CAM-1
LIN-17
CAM-1::N-YFP
LIN-17::C-YFP
IG
CR
KR
TM
YFP
C
CAM-1(ΔTKD)::N-YFP
LIN-17::C-YFP
D
CAM-1(ΔECD)::N-YFP
LIN-17::C-YFP
TM
TK
E
CAM-1(ΔECD)::GFP
GFP
F
ACR-16::GFP (muscle)
ChR2::mCherry (neurons)
merge
G
WT
cwn-2
ACR-16::GFP
SYD-2::RFP
merge
H
Muscle arm
VNC
WT
cam-1
cwn-2
lin-17
dsh-1

Figure 2.4. ACR-16::GFP is mislocalized and its mobility reduced in Wnt-signaling mutants.
(A) Images of the tips of muscle arms in transgenic wild-type (WT) and mutant worms injected with fluorescently labeled a-BgTx. These worms also expressed soluble mCherry in muscle cells to identify muscle arms. Scale bar, 1 mm. (B) Quantification of a-BgTx fluorescence. *, $p<0.05$; **, $p<0.01$. For all genotypes, $n \geq 12$. (C) Images of muscle arms in a wild-type transgenic worm that expressed ACR-16::EosFP both before and after photoconversion from green to red. The white, dashed lines outline individual muscle arms. The circles show the converted EosFP puncta. Scale bar, 5 mm. (D) Loss of fluorescence observed with photoconversion-chase strategy. Shown are examples of the loss of ACR-16::EosFP fluorescence in muscle arms following photoconversion from green to red. Scale bar, 1 mm. (E) Quantification of EosFP after photoconversion in wild-type worms and *lin-17* mutants ($n \geq 11$). *lin-17* mutants are significantly different from WT, $p<0.001$. Error bars represent SEM. See also Figure 2.S5.

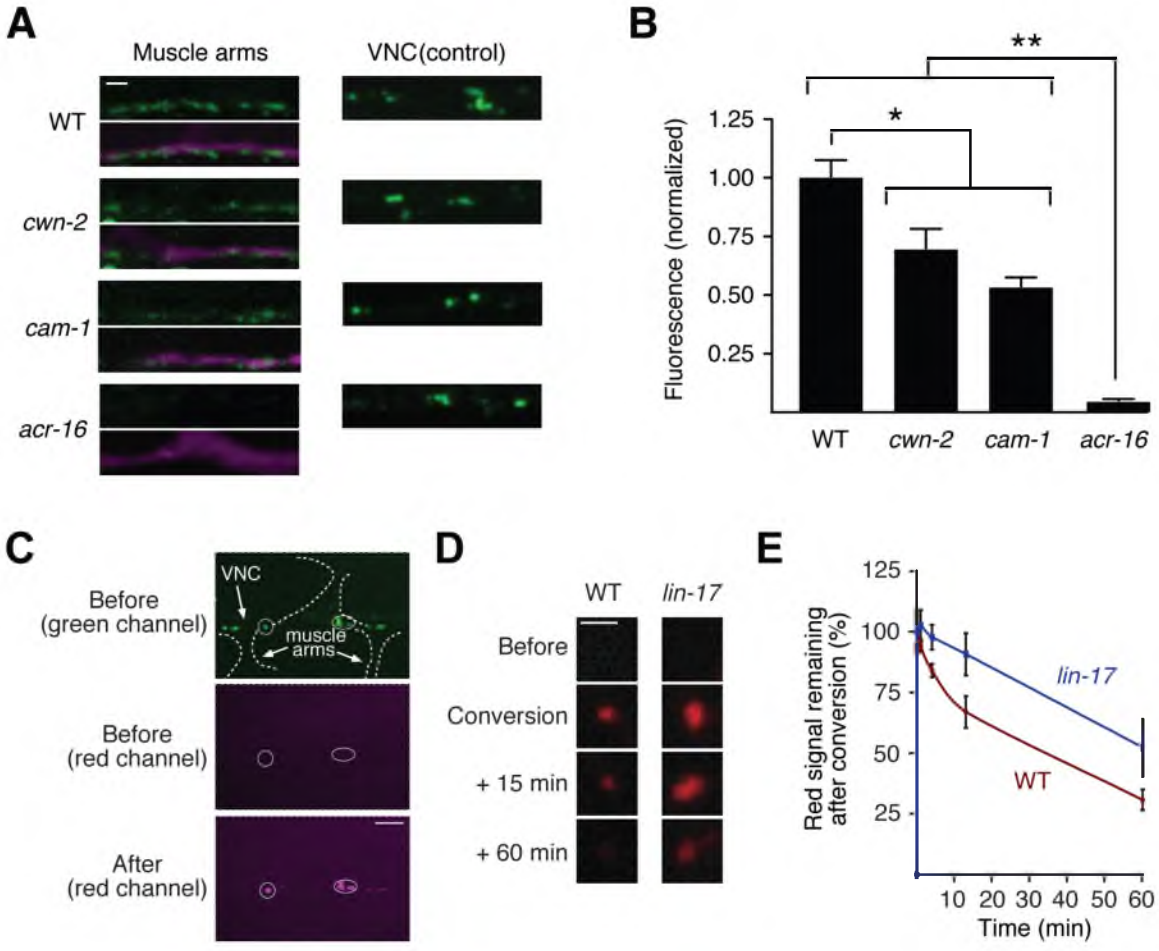
A
Muscle arms
VNC(control)
WT
cwn-2
cam-1
acr-16
B
**
*
Fluorescence (normalized)
1.25
1.00
0.75
0.50
0.25
WT
cwn-2
cam-1
acr-16
C
Before
(green channel)
VNC
muscle
arms
Before
(red channel)
After
(red channel)
D
WT
lin-17
Before
Conversion
+ 15 min
+ 60 min
E
Red signal remaining
after conversion (%)
125
100
75
50
25
lin-17
WT
10 20 30 40 50 60
Time (min)

Figure 2.5. LIN-17 expression in adult mutants rescues ACR-16-mediated behavior and receptor localization.
(A) Thrashing behavior in *unc-29* single mutants, *lin-17; unc-29* double mutants and transgenic double mutants that expressed *Phsp::lin-17*. n≥10 for each strain and condition. Shown is behavior 10 and 24 hrs following heat shock. (B) Images of ACR-16::GFP expression in the muscle arms of wild-type (WT) worms, *lin-17* mutants and transgenic mutants following heat shock (HS). Scale bar, 1 mm. (C) Intensity of ACR-16::GFP fluorescence relative to wild-type worms. n≥9 for each strain and condition. *, significantly different from *lin-17*, heat shock (–), $p<0.05$. Error bars indicate SEM. See also Figure 2.S5.

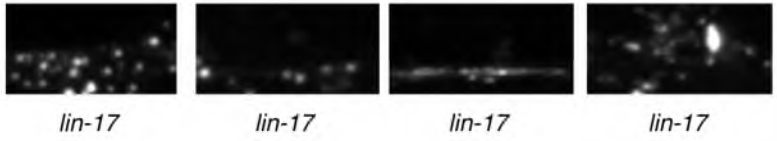

	lin-17	*lin-17*	*lin-17*	*lin-17*
Heat shock	+	+	+	+
Phsp::lin-17	+	+	+	+
Time after HS	30 min	2 hr	10 hr	24 hr

C

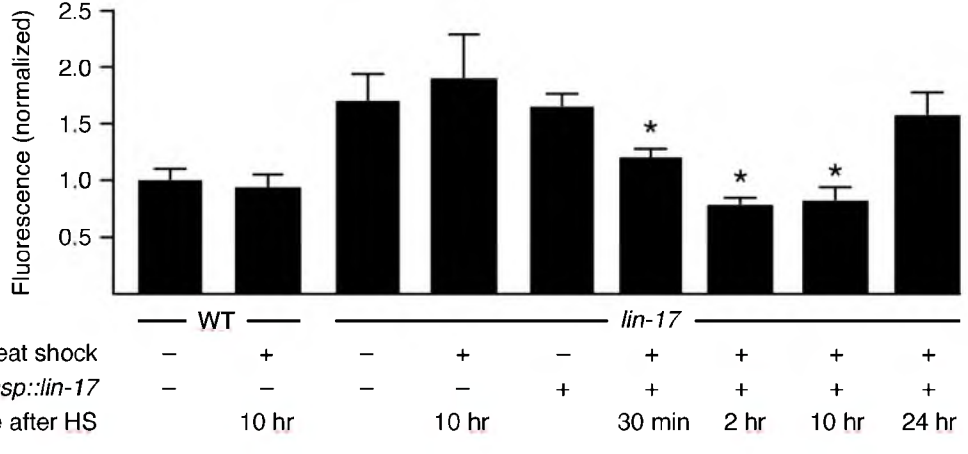

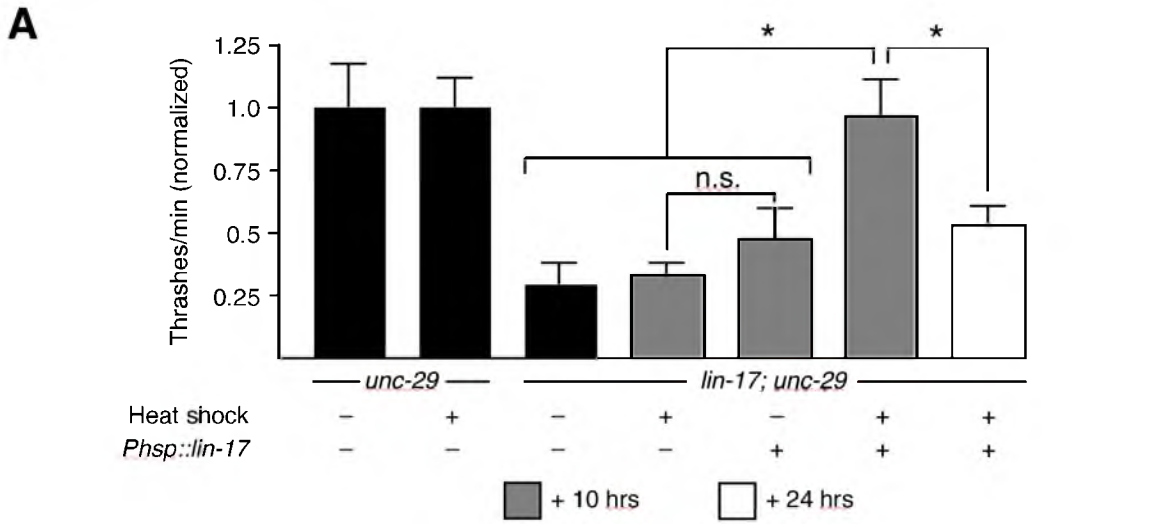
A
Thrashes/min (normalized)
1.25
1.0
0.75
0.5
0.25
*
*
n.s.
unc-29
lin-17; unc-29
Heat shock
Phsp::lin-17
+ 10 hrs
+ 24 hrs
B
WT
WT
lin-17
lin-17
lin-17
Heat shock
Phsp::lin-17
Time after HS
10 hr
10 hr

Figure 2.6. Chronic stimulation of the NMJ modifies ACR-16 localization and ACh-gated current.
(A) ACR-16::GFP in muscle arms of transgenic wild type (WT) and *cwn-2* mutant worms that expressed ChR2 with or without light stimulation and in the presence or absence of retinal. Scale bar, 1 mm. (B) Quantification of GFP fluorescence in the worms shown in (A). Normalized to WT, retinal (–) (black bars) or *cwn-2*, retinal (–) (gray bars). For all strains and conditions, $n \geq 12$. (C) ACh-gated currents in the muscle cells of light stimulated, transgenic worms that expressed ChR2 in motor neurons. (D) Peak ACh-gated current amplitude normalized to WT, retinal (–) (black bars) or *cwn-2*, retinal (–) (gray bars). For each genotype and condition, $n \geq 6$. *, $p<0.05$. (E) ACR-16::GFP expression in muscle arms of *cwn-2* mutants with or without a wild-type *cwn-2* transgene expressed in muscles or neurons. Scale bar, 2 mm. (F) Quantification of ACR-16::GFP fluorescence normalized to transgene (–) controls. For all genotypes and conditions, $n \geq 18$. (G) ACR-16::GFP fluorescence in muscle arms of light-stimulated, transgenic wild-type worms with *cwn-2* knock down in either muscles or neurons. Scale bar, 1 mm. (H) Quantification of ACR-16::GFP fluorescence in muscle arms. For all genotypes and conditions, $n \geq 15$. *, $p<0.05$. Error bars indicate SEM. See also Figure 2.S6.

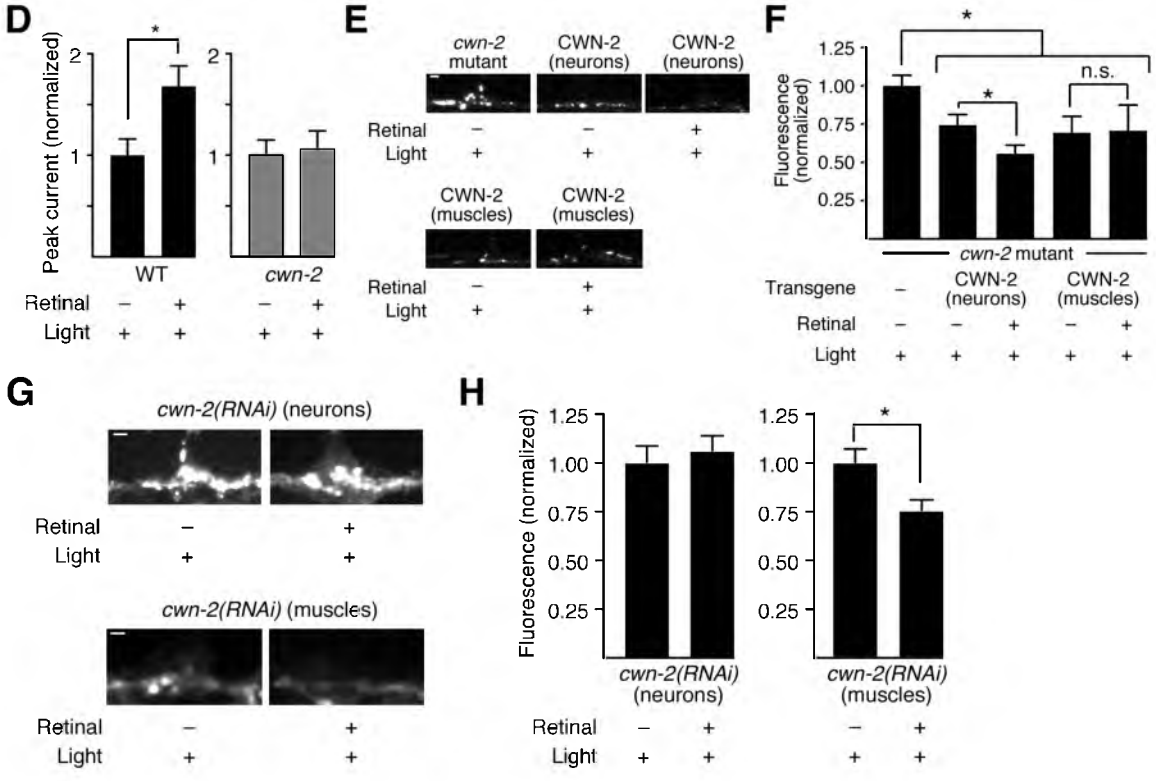
D
Peak current (normalized)
2
1
*
WT
cwn-2
Retinal – + – +
Light + + + +
E
cwn-2 mutant
CWN-2 (neurons)
CWN-2 (neurons)
Retinal – – +
Light + + +
CWN-2 (muscles)
CWN-2 (muscles)
Retinal – +
Light + +
F
Fluorescence (normalized)
1.25
1.00
0.75
0.50
0.25
*
*
n.s.
cwn-2 mutant
Transgene – CWN-2 (neurons) CWN-2 (muscles)
Retinal – – + – +
Light + + + + +
G
cwn-2(RNAi) (neurons)
Retinal – +
Light + +
cwn-2(RNAi) (muscles)
Retinal – +
Light + +
H
Fluorescence (normalized)
1.25
1.00
0.75
0.50
0.25
cwn-2(RNAi) (neurons)
cwn-2(RNAi) (muscles)
*
Retinal – + – +
Light + + + +

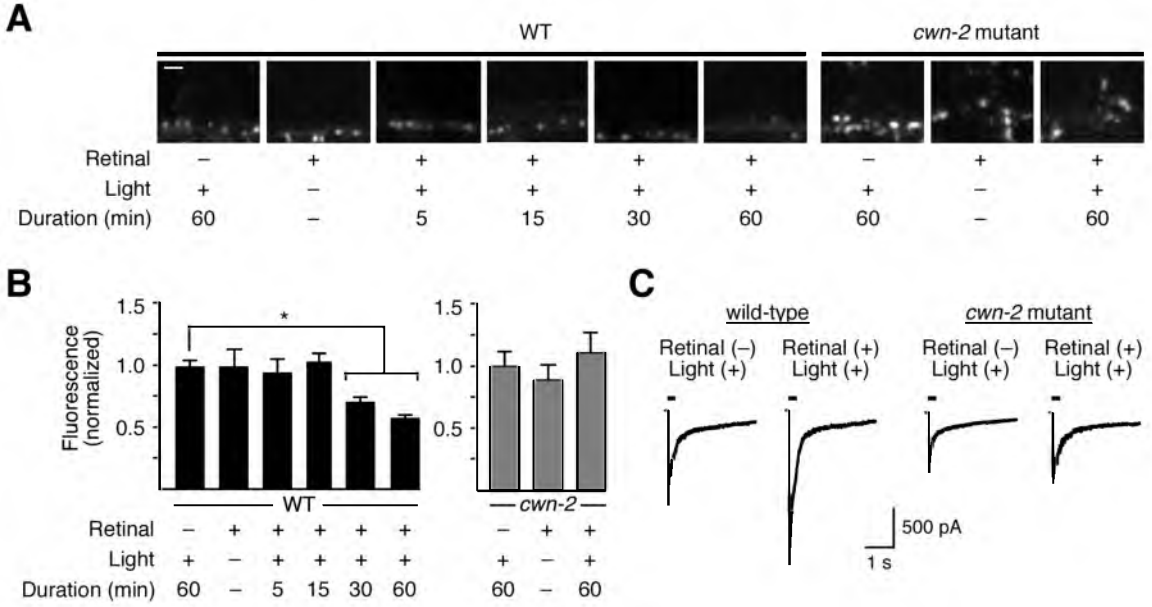
A
WT
cwn-2 mutant
Retinal
Light
Duration (min)
B
Fluorescence (normalized)
1.5
1.0
0.5
*
WT
cwn-2
C
wild-type
cwn-2 mutant
Retinal (–) Light (+)
Retinal (+) Light (+)
500 pA
1 s

Figure 2.7. Translocation of ACR-16/a7 is independent of protein synthesis and rapidly induced by recombinant CWN-2.
(A) ACR-16::GFP expression in muscle arms of transgenic wild-type worms that expressed ChR2 in motor neurons. Scale bar, 2 mm. (B) Quantification of ACR-16::GFP fluorescence intensity normalized to retinal (–), light (–), CHX (–) control. For all conditions, n≥9. (C) CWN-2::GFP expression in motor neuron cell bodies in transgenic wild-type (WT) and *mig-14* mutant worms. Scale bars, 4 mm. (D) Quantification of CWN-2::GFP fluorescence intensity normalized to either WT, retinal (–) (black bars) or *mig-14*, retinal (–) (gray bars). For all genotypes and conditions, n≥16. (E) ACh-gated currents in *cwn-2* mutants with or without the application of recombinant CWN-2. (F) Quantification of peak ACh-gated current normalized to *cwn-2* control. For all conditions, n≥4. *,$p<0.05$, **$p<0.01$. Error bars indicate SEM. See also Figure 2.S7.

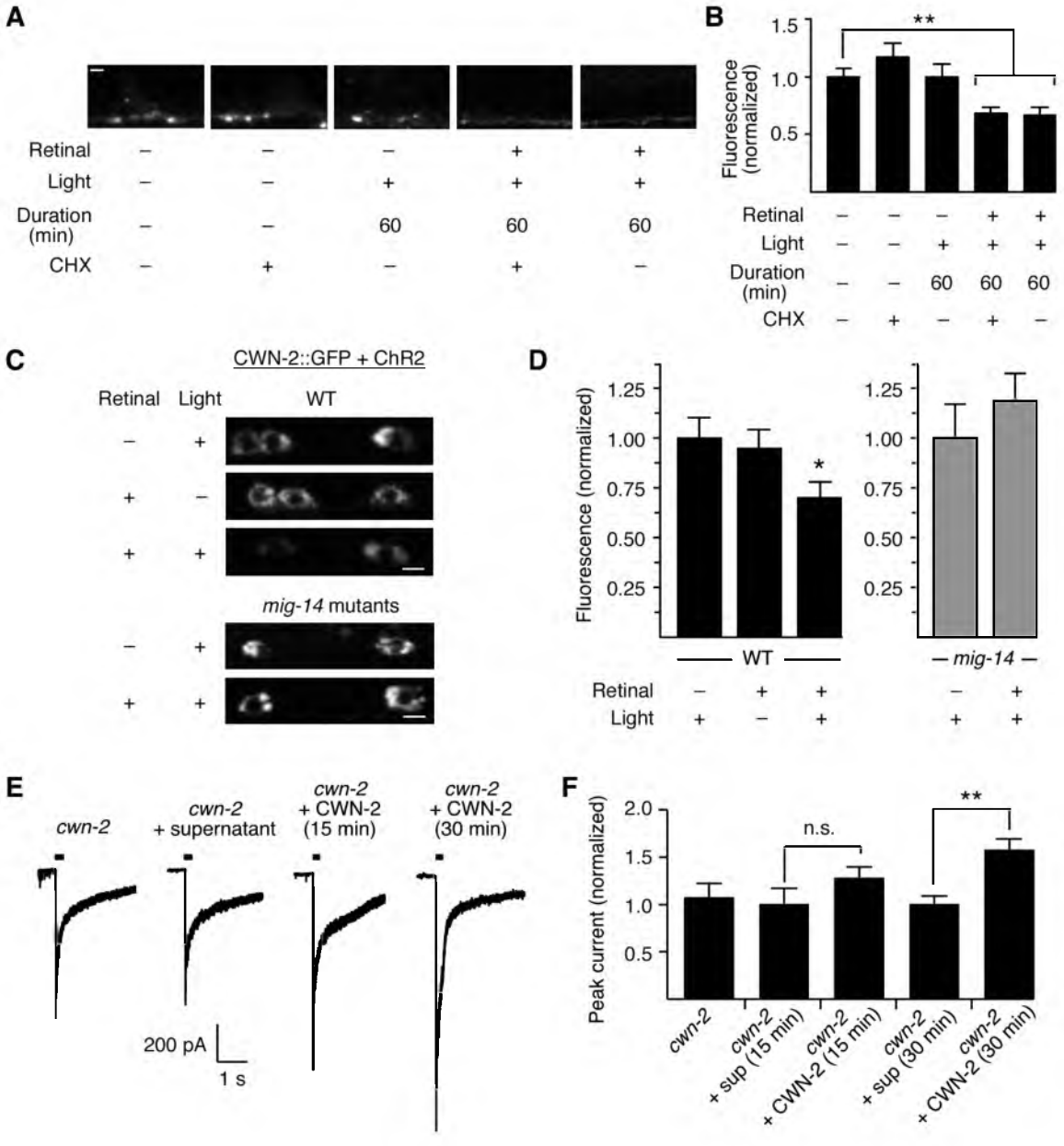
A
Retinal – – – + +
Light – – + + +
Duration (min) – – 60 60 60
CHX – + – + –
B
Fluorescence (normalized)
1.5
1.0
0.5
**
Retinal – – – + +
Light – – + + +
Duration (min) – – 60 60 60
CHX – + – + –
C
CWN-2::GFP + ChR2
Retinal Light
WT
mig-14 mutants
D
Fluorescence (normalized)
1.25
1.00
0.75
0.50
0.25
*
WT
mig-14
Retinal – + + – +
Light + – + + +
E
cwn-2
cwn-2 + supernatant
cwn-2 + CWN-2 (15 min)
cwn-2 + CWN-2 (30 min)
200 pA
1 s
F
Peak current (normalized)
2.0
1.5
1.0
0.5
n.s.
**
cwn-2
cwn-2 + sup (15 min)
cwn-2 + CWN-2 (15 min)
cwn-2 + sup (30 min)
cwn-2 + CWN-2 (30 min)

Figure 2.S1. Wnt-signaling mutants have a synthetic locomotory defect with *unc29* mutants. Supplemental data associated with Figure 2.1.

(A) Superimposed time lapse images from wild-type worms, *acr-16(ok789)*, transgenic *acr-16(ok789)* + *Pmyo-3::acr-16::gfp*, and *cwn-2(ok895)* mutants. Worms were mounted on 5% agarose pads with 1 ml of Polybead Microspheres 0.625% (w/v) in M9 buffer. (B) Thrashing behavior in single mutant worms. For all genotypes, $n \geq 10$. *, $p<0.05$ (significantly different from *unc-29*); **, $p<0.01$. (C) Images of *unc-29* single mutants, *lin-17; unc-29* double mutants, and *lin-17; unc29* transgenic double mutants that expressed LIN-17 under the *myo-3* muscle specific promoter. Images taken immediately and 25 s after the worms were placed on a lawn of bacteria on an agarose plate. (D) Thrashing behavior in *unc29* single and double mutants, and transgenic double mutants that expressed either LIN-44 or EGL-20 under the regulation of the *cwn-2* promoter. For all genotypes, $n \geq 10$. *, $p<0.05$ (significantly different from *unc-29*). Error bars indicate SEM.

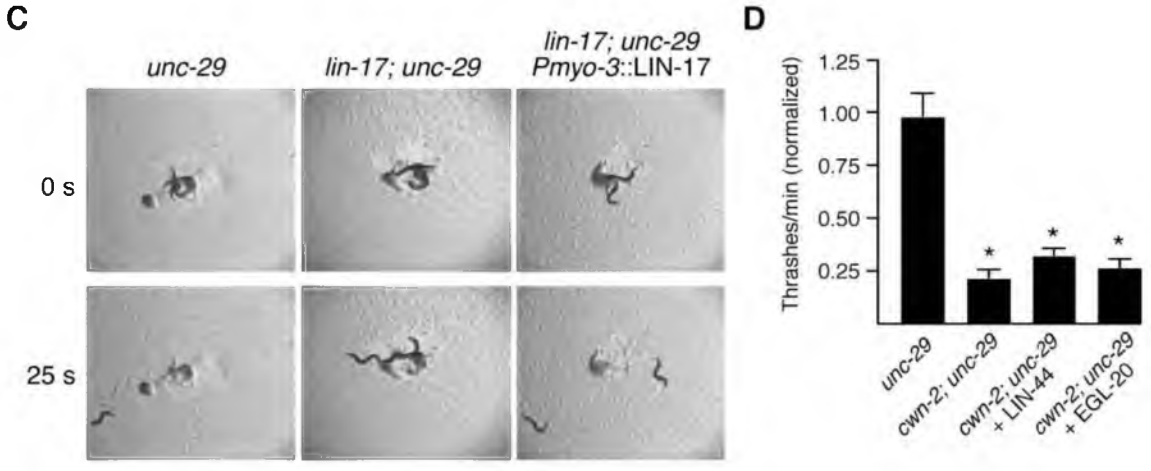
C
unc-29
lin-17; unc-29
lin-17; unc-29
Pmyo-3::LIN-17
0 s
25 s
D
Thrashes/min (normalized)
1.25
1.00
0.75
0.50
0.25
*
*
*
unc-29
cwn-2; unc-29
cwn-2; unc-29 + LIN-44
cwn-2; unc-29 + EGL-20

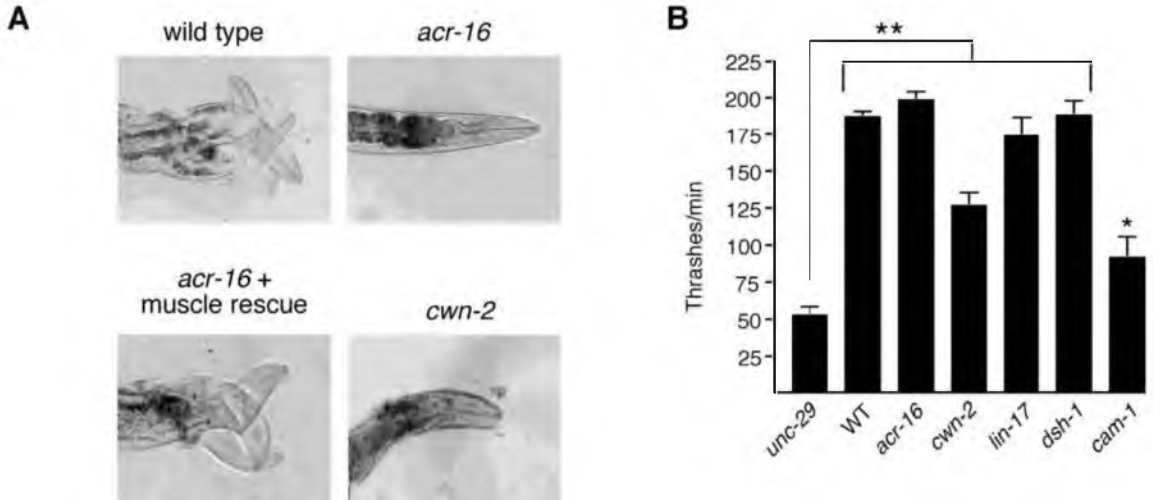
A
wild type
acr-16
acr-16 +
muscle rescue
cwn-2
B
**
*
Thrashes/min
225
200
175
150
125
100
75
50
25
unc-29
WT
acr-16
cwn-2
lin-17
dsh-1
cam-1

Figure 2.S2. Mutating Wnt-signaling molecules specifically disrupts the nicotine component of the ACh-gated current. Supplemental data associated with Figure 2.1. (A) Nicotine-gated currents in muscle cells of wild-type worms, and *cwn-2* and *lin-17* mutants (left), and the average peak nicotine-gated current normalized to wild-type values (right). $n \geq 5$ for all genotypes. (B) Levamisole-gated currents in muscle cells of wild-type and mutant worms (left), and the average peak levamisole-gated current normalized to wild-type values (right). $n \geq 3$ for all genotypes. (C) Light evoked currents in muscle cells of wild-type and *cwn-2* mutant worms (left), and the average light-evoked current normalized to wild-type values (right). $n \geq 5$ for both genotypes. *, $p<0.05$. **, $p<0.01$. Error bars indicate SEM.

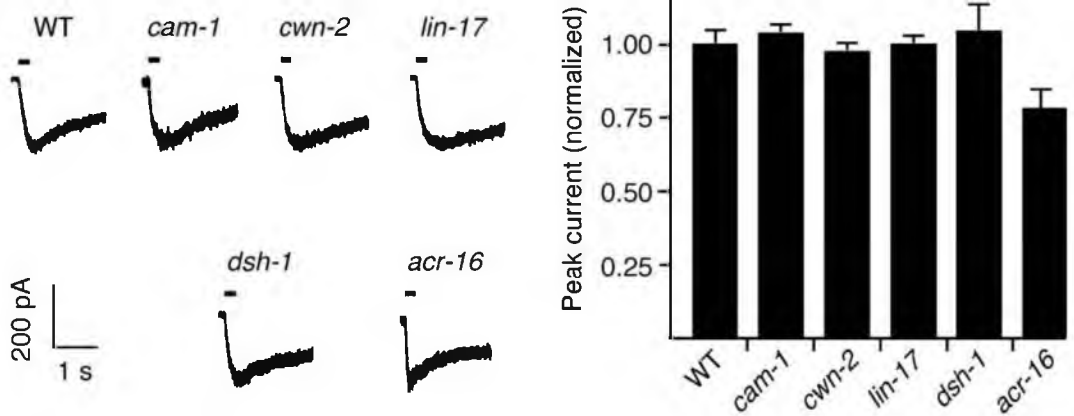
WT
cam-1
cwn-2
lin-17
dsh-1
acr-16
200 pA
1 s
Peak current (normalized)
1.00
0.75
0.50
0.25
WT
cam-1
cwn-2
lin-17
dsh-1
acr-16

C

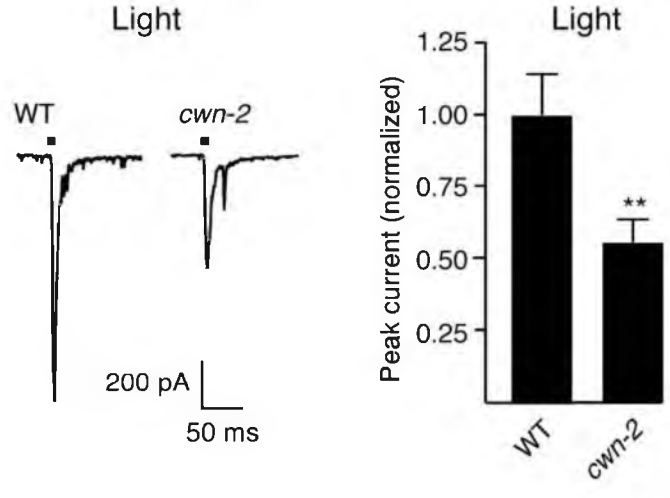
Light
WT
cwn-2
200 pA
50 ms
Light
Peak current (normalized)
1.25
1.00
0.75
0.50
0.25
**
WT
cwn-2

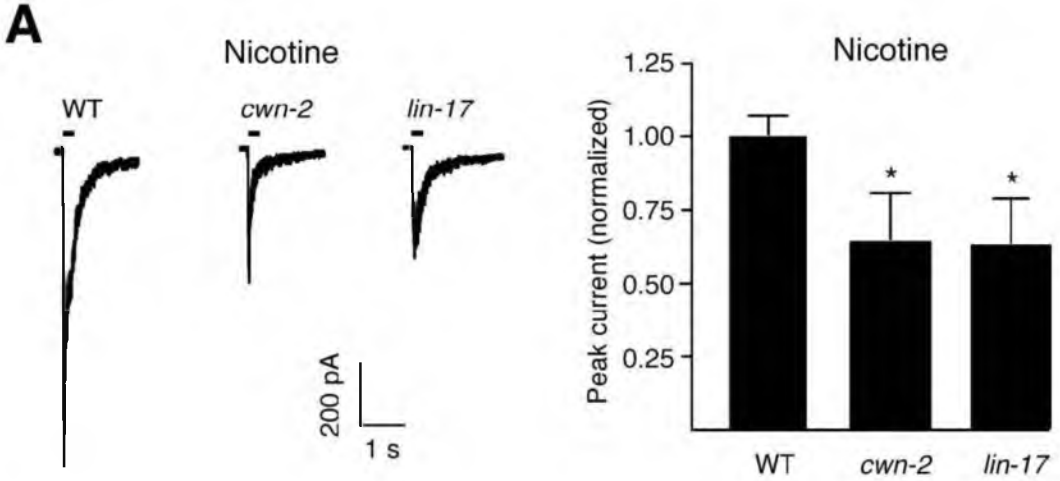
A
Nicotine
WT
cwn-2
lin-17
200 pA
1 s
Nicotine
Peak current (normalized)
1.25
1.00
0.75
0.50
0.25
*
*
WT
cwn-2
lin-17
B
Levamisole
Levamisole
1.25

Figure 2.S3. Selective disruption of ACR-16-mediated current and cell specific knock down of CWN-2. Supplemental data associated with Figures 2.1 and 2.2.

(A) GABA-gated current in muscle cells of wild-type (WT) and *cwn-2* mutants (left). Horizontal bar represents the application of 100 mM GABA. Average peak GABA-gated current (right). WT, *cwn-2(ok895)*, n³4. Error bars indicate SEM. (B) ACh-gated current in muscle cells of wild-type (WT) and *cwn-1, lin-44* and *egl-20* mutants (left). Average peak ACh-gated current (right). For all genotypes, n³4. (C) Miniature excitatory postsynaptic current (mEPSC) in *unc-29* single and double mutants (left). Average peak mEPSC amplitude (right). For all genotypes, (*unc-29(x29)*, 11,471 events, n=10; *unc-29(x29); cam-1(ak37)*, 2,861 events, n=7; *unc-29(x29); cwn-2(ok895)*, 4,756 events, n=9; *unc-29(x29); lin-17(n671)*, 1, 271 events, n=5; *unc-29(x29); dsh-1(ok1445)*, 1,167 events, n=6). *, $p<0.05$. Error bars represent SEM. (D) CWN-2::mCherry expression in coelomocytes in transgenic worms with or without *cwn-2* knock down in muscles or neurons. Scale bars, 1 mm

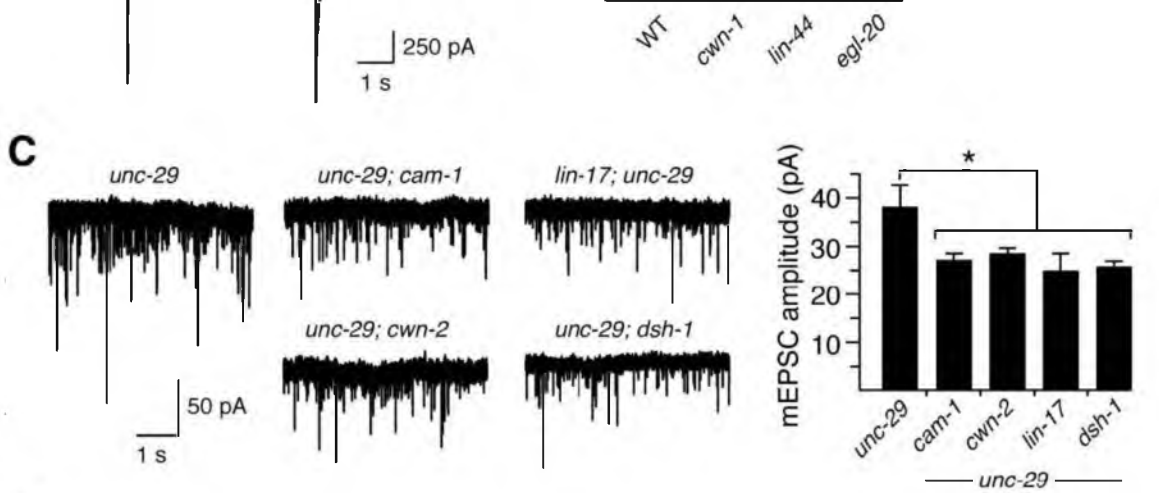
250 pA
1 s
WT
cwn-1
lin-44
egl-20
C
unc-29
unc-29; cam-1
lin-17; unc-29
unc-29; cwn-2
unc-29; dsh-1
50 pA
1 s
mEPSC amplitude (pA)
40
30
20
10
*
unc-29
cam-1
cwn-2
lin-17
dsh-1
unc-29
D
CWN-2::mCherry (from neurons)
CWN-2::mCherry (from muscle)
CWN-2::mCherry (neurons) cwn-2(RNAi) (neurons)
CWN-2::mCherry (muscle) cwn-2(RNAi) (muscle)

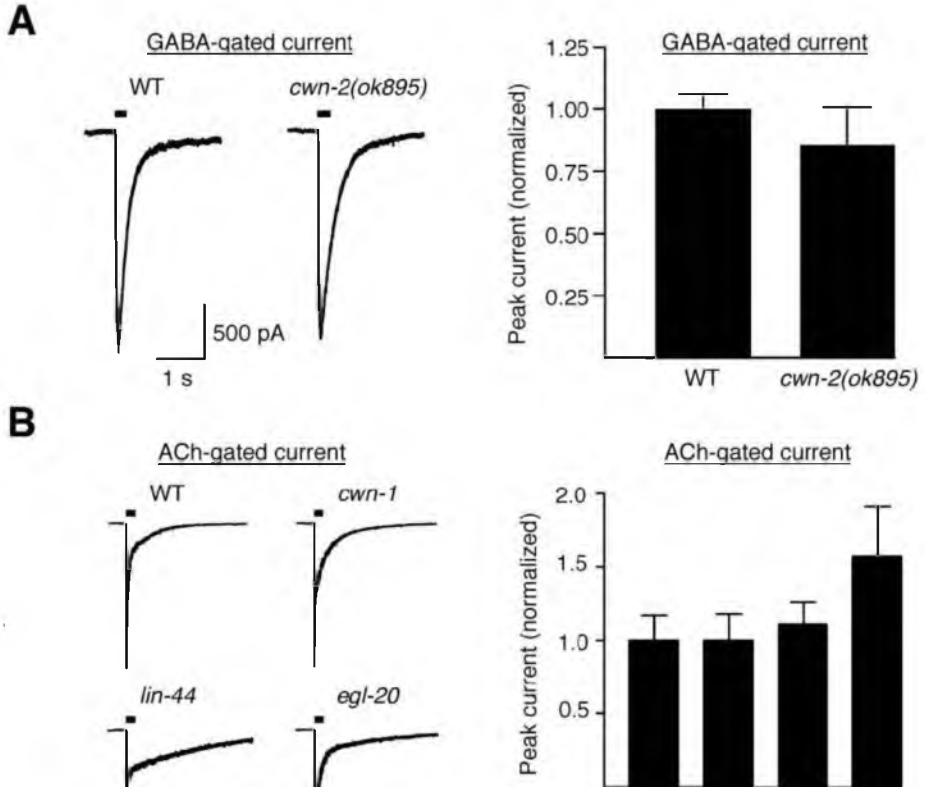
A
GABA-gated current
WT
cwn-2(ok895)
500 pA
1 s
GABA-gated current
Peak current (normalized)
1.25
1.00
0.75
0.50
0.25
WT
cwn-2(ok895)
B
ACh-gated current
WT
cwn-1
lin-44
egl-20
ACh-gated current
Peak current (normalized)
2.0
1.5
1.0
0.5

Figure 2.S4. LIN-17/CAM-1 heteromers expressed in muscle arms. Supplemental data associated with Figure 2.3.
(A) Images of YFP expression in the tips of muscle arms in transgenic worms that carried either the *Pmyo-3::cam-1(*D*TKD)::n-yfp* transgene (left), the *Pmyo-3::lin-17::c-yfp* transgene (middle), or both transgenes (right). Worms that carried both transgenes were cross progeny of worms that carried only one of the two transgenes. Scale bar, 1 mm. (B) Top and lower left panels show images of either single (top) or multiple (lower left) muscle arms in transgenic wild-type (WT) and mutant worms that expressed soluble mCherry under control of the *myo-3* muscle specific promoter. Scale bars, 1 mm (top); 2 mm (lower left). Quantification of muscle arm density (lower right panel). (C) ACR-16::GFP expression in muscle arms of wild type, *lin-17(n671),* and *lin-17(n671)* transgenic mutants that expressed a wild-type *lin-17* transgene in neurons. Scale bars, 1 mm. Quantification of ACR-16::GFP fluorescence intensity relative to WT ($n \geq 10$ for all genotypes. *, $p<0.05$). (D) UNC-29::GFP and UNC-49::GFP expression in muscle arms of transgenic wild type (WT) and *cwn-2* mutants. Scale bars, 1 mm. Error bars represent SEM.

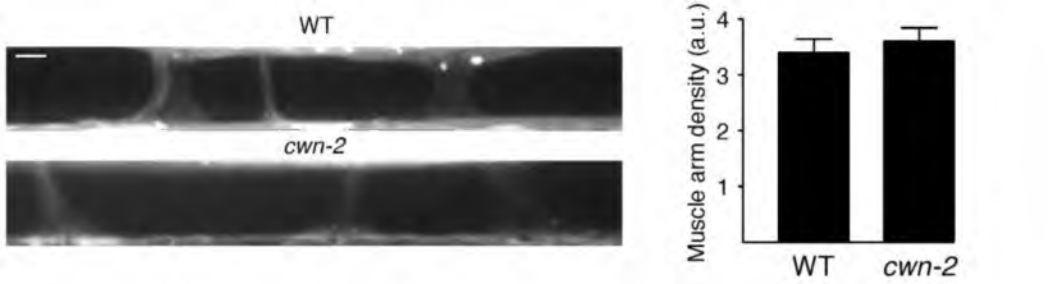
WT
cwn-2
Muscle arm density (a.u.)
4
3
2
1
WT
cwn-2

C

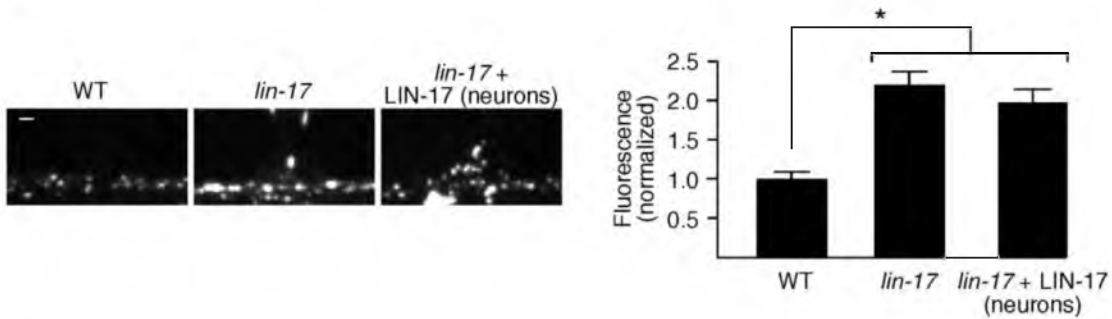
WT
lin-17
lin-17 +
LIN-17 (neurons)
*
Fluorescence
(normalized)
2.5
2.0
1.5
1.0
0.5
WT
lin-17
lin-17 + LIN-17
(neurons)

D

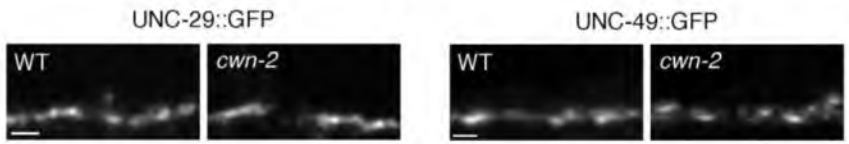
UNC-29::GFP
WT
cwn-2
UNC-49::GFP
WT
cwn-2

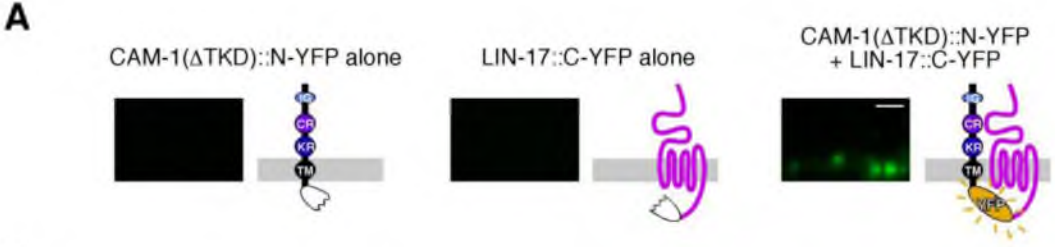
A
CAM-1(ΔTKD)::N-YFP alone
LIN-17::C-YFP alone
CAM-1(ΔTKD)::N-YFP
+ LIN-17::C-YFP
SP
CR
KR
TM
YFP
B
WT
cwn-2
cam-1
lin-17
dsh-1

Figure 2.S5 ACR-16 mobility is decreased in *lin-17* mutants; and ACR-16 expression in adult mutants rescues behavior and current defects. Supplemental data associated with Figures 2.4 and 2.5.

(A) Images of ACR-16::EosFP before and at various time points after photoconversion from green to red (red signal shown) in wild type (left) and *lin-17* mutants (right). Scale bars, 5 mm. (B) Thrashing behavior in *unc-29* single mutants, *unc-29; acr-16* double mutants and transgenic *unc-29; acr-16* mutants that express *Phsp*::*acr-16*. $n \geq 10$ for each strain and condition. **, $p<0.01$. (C) Nicotine-gated currents in muscle cells of *unc-29* single mutants, *unc-29; acr-16* double mutants and transgenic *unc-29; acr-16* mutants that expressed *Phsp::acr 16*. (D) Average peak nicotine-gated currents from heat-shocked worms and controls. For all genotypes, $n \geq 3$. **, $p<0.01$. Error bars indicate SEM.

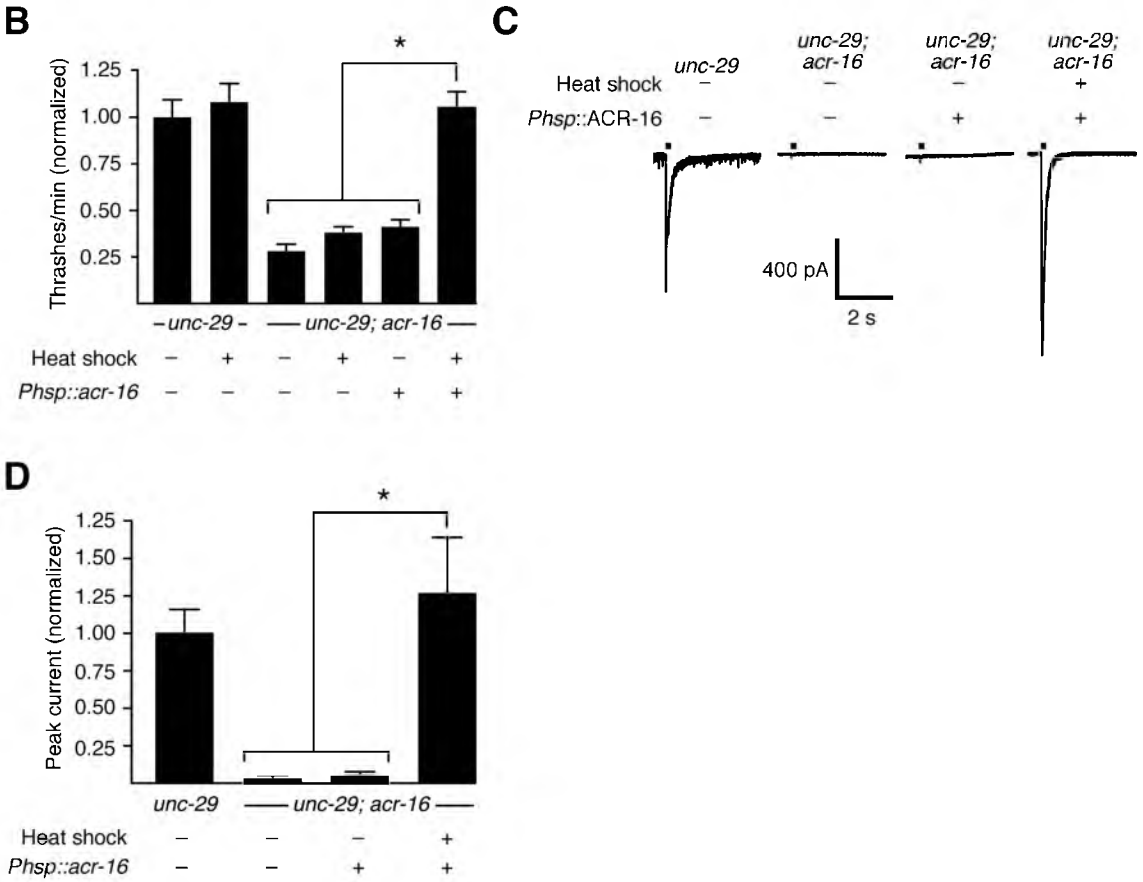
B
Thrashes/min (normalized)
1.25
1.00
0.75
0.50
0.25
*
unc-29
unc-29; acr-16
Heat shock
Phsp::acr-16
C
unc-29
unc-29; acr-16
unc-29; acr-16
unc-29; acr-16
Heat shock
Phsp::ACR-16
400 pA
2 s
D
Peak current (normalized)
1.25
1.50
1.25
1.00
0.75
0.50
0.25
*
unc-29
unc-29; acr-16
Heat shock
Phsp::acr-16

A

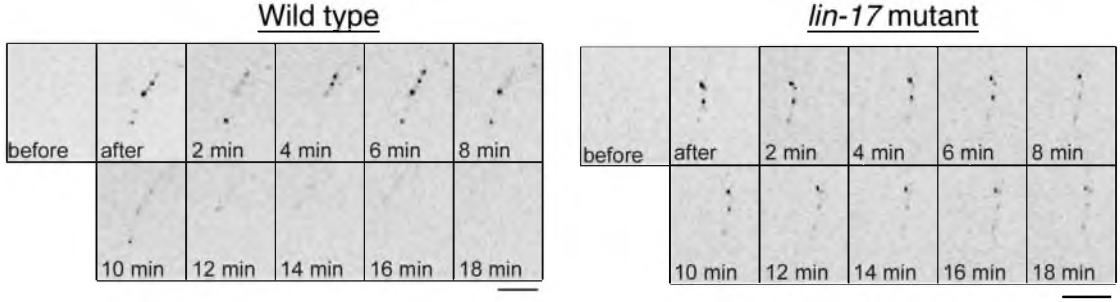
Wild type
before
after
2 min
4 min
6 min
8 min
10 min
12 min
14 min
16 min
18 min
lin-17 mutant
before
after
2 min
4 min
6 min
8 min
10 min
12 min
14 min
16 min
18 min

Figure 2.S6. Motor neuron activity requires muscle LIN-17 to selectively increase ACR-16-mediated currents. Supplemental data associated with Figure 2.6 .
(A) GABA-gated currents in transgenic wild-type worms that expressed ChR2 in motor neurons after light stimulation (left). Quantification of peak GABA-gated current normalized to retinal (–) controls (right). For all conditions, $n \geq 4$. (B) Miniature excitatory postsynaptic currents (mEPSC) in transgenic wild-type worms that expressed ChR2 in motor neurons after light stimulation (left). Quantification of peak mEPSC normalized to retinal (–) controls (right). For all conditions, $n \geq 5$. (C) Following prolonged ChR2 activity, nerve-evoked current is increased (left), $n \geq 7$. Average peak current normalized to light stim (–) control (right). (D) ACR-16::GFP expression in muscle arms of transgenic *lin-17* mutants that expressed ChR2 in motor neurons with or without wild-type *lin-17(+)* transgene expression in muscle cells (left). Scale bar, 1 mm. Quantification of ACR-16::GFP fluorescence intensity in muscle arms normalized to retinal (–), *lin17(+)* transgene (–) control (right). For all genotypes and conditions, $n \geq 19$. *, $p<0.05$; **, $p<0.01$. Error bars represent SEM

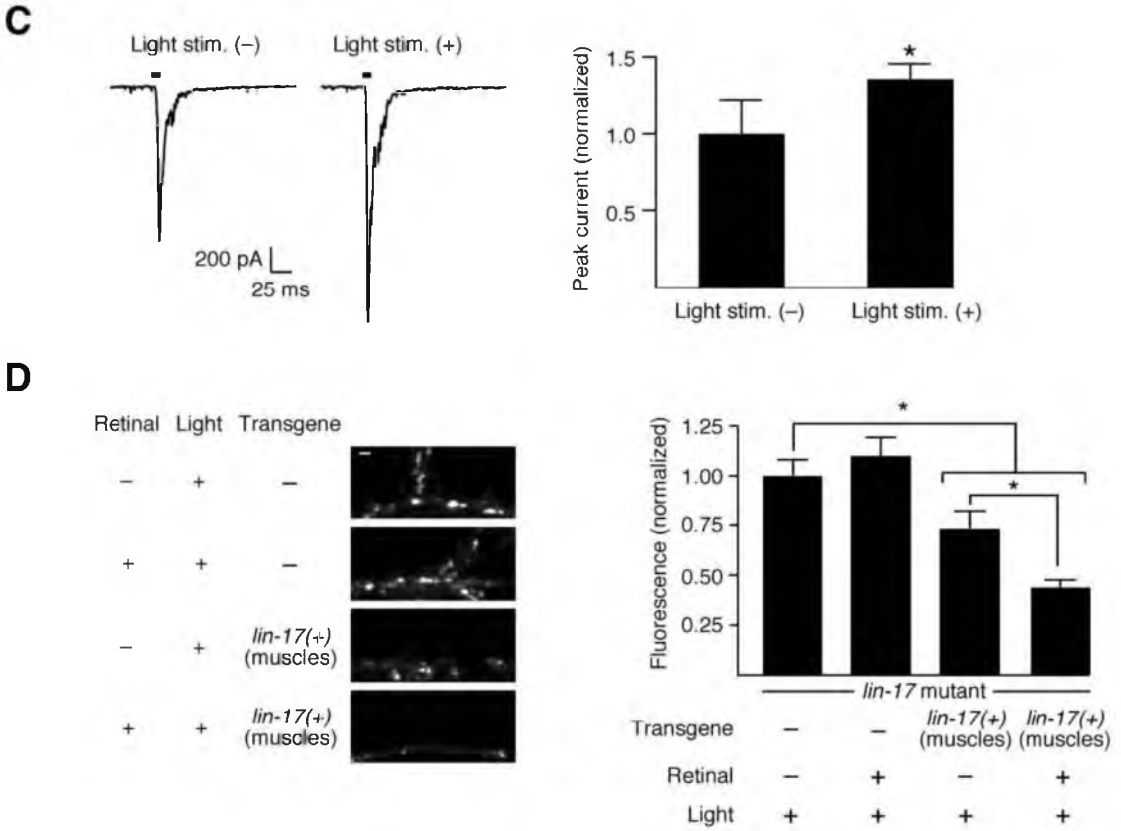
C
Light stim. (–)
Light stim. (+)
200 pA
25 ms
Peak current (normalized)
1.5
1.0
0.5
*
Light stim. (–)
Light stim. (+)
D
Retinal
Light
Transgene
–
+
–
+
+
–
–
+
lin-17(+)
(muscles)
+
+
lin-17(+)
(muscles)
Fluorescence (normalized)
1.25
1.00
0.75
0.50
0.25
*
*
lin-17 mutant
Transgene
–
–
lin-17(+)
(muscles)
lin-17(+)
(muscles)
Retinal
–
+
–
+
Light
+
+
+
+

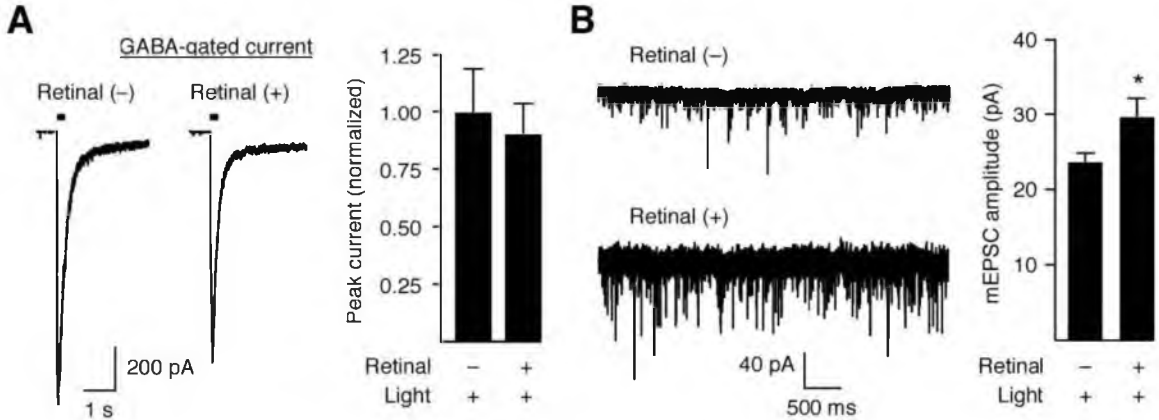
A
GABA-gated current
Retinal (–)
Retinal (+)
200 pA
1 s
Peak current (normalized)
1.25
1.00
0.75
0.50
0.25
Retinal – +
Light + +
B
Retinal (–)
Retinal (+)
40 pA
500 ms
mEPSC amplitude (pA)
40
30
20
10
*
Retinal – +
Light + +

Figure 2.S7. CWN-2-mediated translocation of ACR-16 requires neuronal MIG-14 and is independent of new protein synthesis. Supplemental data associated with Figure 2.7.
(A and B) CWN-2::mCherry expression in either a motor neuron cell body (A) or coelomocyte (B) in transgenic worms with or without heat shock or treatment with cycloheximide (CHX). Scale bars, 1 mm (A); 2 mm (B). (C) ACR-16::GFP expression in a muscle arm of transgenic wild-type worms without (top) or with Wnt signaling regulates translocation of synaptic receptors *mig-14(RNAi)* knock down in muscles (middle) or neurons (bottom). Scale bar, 1 mm.

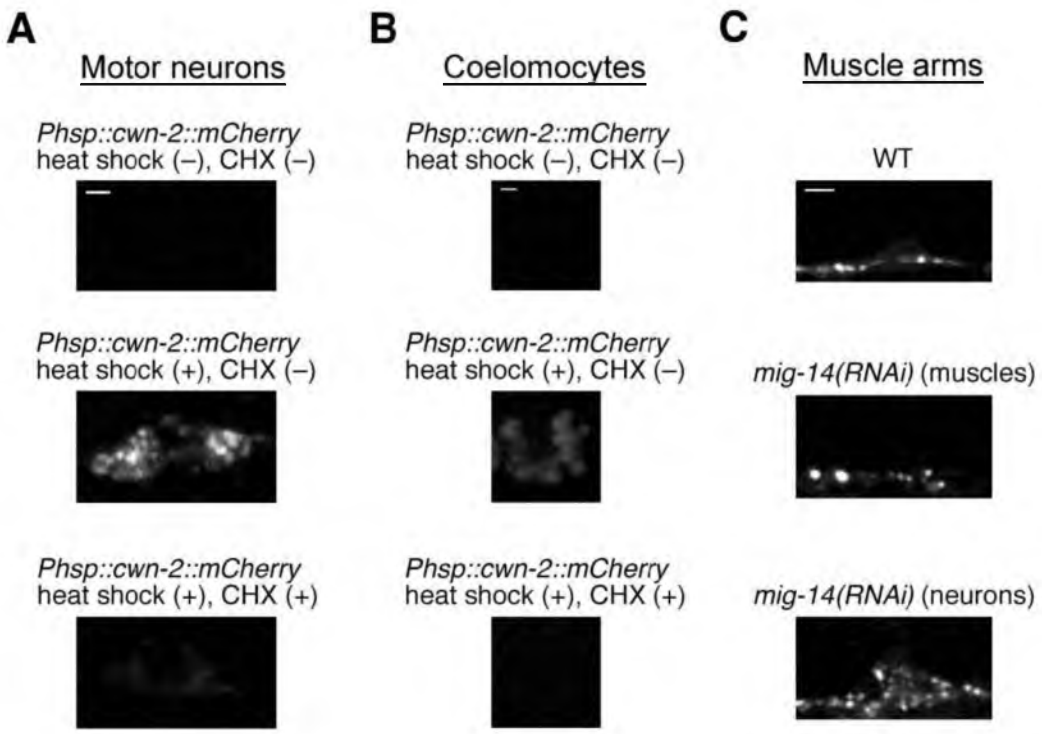
A
Motor neurons
Phsp::cwn-2::mCherry
heat shock (–), CHX (–)
Phsp::cwn-2::mCherry
heat shock (+), CHX (–)
Phsp::cwn-2::mCherry
heat shock (+), CHX (+)
B
Coelomocytes
Phsp::cwn-2::mCherry
heat shock (–), CHX (–)
Phsp::cwn-2::mCherry
heat shock (+), CHX (–)
Phsp::cwn-2::mCherry
heat shock (+), CHX (+)
C
Muscle arms
WT
mig-14(RNAi) (muscles)
mig-14(RNAi) (neurons)

Table 2.S Molecular description of alleles

Alleles	Mutations	References
AChR & GABAR		
unc-29(x29)	Y to ochre stop (449	(Fleming, 1997)
acr-16(ok789)	1082bp deletion	(Francis, 2005)
Wnt		
cwn-1(ok546)	785bp deletion	(Zinovyeva, 2005)
cwn-2(ok895)	905bp deletion	(Zinovyeva, 2005)
egl-20(n585)	G295A (C99S)	(Maloof, 1999)
lin-44(n1792)	W100 amber stop	(Herman, 1994)
Frizzled		
lin-17(n671)	Q499 ochre stop	(Sawa, 1996)
mig-1(e1787)	Q281 ochre stop	(Harris, 1996)
cfz-2(ok1201)	1174bp deletions	(Zinovyeva, 2005)
Ryk		
lin-18(e620)	Q105 amber stop	(Inoue, 2004)
ROR RTK		
cam-1(ak37)	1885bp deletion	(Francis, 2005)
Dishevelled		
dsh-1(ok1445)	1132bp deletion	(Klassen, 2007)

References

Ataman, B., Ashley, J., Gorczyca, M., Ramachandran, P., Fouquet, W., Sigrist, S.J., and Budnik, V. (2008). Rapid activity-dependent modifications in synaptic structure and function require bidirectional Wnt signaling. Neuron *57*, 705-718.

Boulin, T., Gielen, M., Richmond, J.E., Williams, D.C., Paoletti, P., and Bessereau, J.L. (2008). Eight genes are required for functional reconstitution of the Caenorhabditis elegans levamisole-sensitive acetylcholine receptor. Proc Natl Acad Sci U S A *105*, 18590-18595.

Brown, D., Breton, S., Ausiello, D.A., and Marshansky, V. (2009). Sensing, signaling and sorting events in kidney epithelial cell physiology. Traffic *10*, 275-284.

Budnik, V., and Salinas, P.C. (2011). Wnt signaling during synaptic development and plasticity. Curr Opin Neurobiol *21*, 151-159.

Ciani, L., Boyle, K.A., Dickins, E., Sahores, M., Anane, D., Lopes, D.M., Gibb, A.J., and Salinas, P.C. (2011). Wnt7a signaling promotes dendritic spine growth and synaptic strength through Ca(2)/Calmodulin-dependent protein kinase II. Proc Natl Acad Sci U S A *108*, 10732-10737.

Cuitino, L., Godoy, J.A., Farias, G.G., Couve, A., Bonansco, C., Fuenzalida, M., and Inestrosa, N.C. (2010). Wnt-5a modulates recycling of functional GABAA receptors on hippocampal neurons. J Neurosci *30*, 8411-8420.

de Bono, M., and Maricq, A.V. (2005). Neuronal substrates of complex behaviors in C. elegans. Annu Rev Neurosci *28*, 451-501.

Farias, G.G., Godoy, J.A., Cerpa, W., Varela-Nallar, L., and Inestrosa, N.C. (2010). Wnt signaling modulates pre- and postsynaptic maturation: therapeutic considerations. Dev Dyn *239*, 94-101.

Farias, G.G., Valles, A.S., Colombres, M., Godoy, J.A., Toledo, E.M., Lukas, R.J., Barrantes, F.J., and Inestrosa, N.C. (2007). Wnt-7a induces presynaptic colocalization of alpha 7-nicotinic acetylcholine receptors and adenomatous polyposis coli in hippocampal neurons. J Neurosci *27*, 5313-5325.

Francis, M.M., Evans, S.P., Jensen, M., Madsen, D.M., Mancuso, J., Norman, K.R., and Maricq, A.V. (2005). The Ror receptor tyrosine kinase CAM-1 is required for ACR-16-mediated synaptic transmission at the C. elegans neuromuscular junction. Neuron *46*, 581-594.

Gleason, J.E., Szyleyko, E.A., and Eisenmann, D.M. (2006). Multiple redundant Wnt signaling components function in two processes during C. elegans vulval development. Dev Biol *298*, 442-457.

Gottschalk, A., Almedom, R.B., Schedletzky, T., Anderson, S.D., Yates, J.R., 3rd, and Schafer, W.R. (2005). Identification and characterization of novel nicotinic receptor-associated proteins in Caenorhabditis elegans. Embo J *24*, 2566-2578.

Green, J.L., Inoue, T., and Sternberg, P.W. (2007). The C. elegans ROR receptor tyrosine kinase, CAM-1, non-autonomously inhibits the Wnt pathway. Development *134*, 4053-4062.

Green, J.L., Kuntz, S.G., and Sternberg, P.W. (2008). Ror receptor tyrosine kinases: orphans no more. Trends Cell Biol *18*, 536-544.

Hall, A.C., Lucas, F.R., and Salinas, P.C. (2000). Axonal remodeling and synaptic differentiation in the cerebellum is regulated by WNT-7a signaling. Cell *100*, 525-535.

Henriquez, J.P., Webb, A., Bence, M., Bildsoe, H., Sahores, M., Hughes, S.M., and Salinas, P.C. (2008). Wnt signaling promotes AChR aggregation at the neuromuscular synapse in collaboration with agrin. Proc Natl Acad Sci U S A *105*, 18812-18817.

Inestrosa, N.C., and Arenas, E. (2010). Emerging roles of Wnts in the adult nervous system. Nat Rev Neurosci *11*, 77-86.

Jin, Y., and Garner, C.C. (2008). Molecular mechanisms of presynaptic differentiation. Annu Rev Cell Dev Biol *24*, 237-262.

Kennedy, M.J., and Ehlers, M.D. (2011). Mechanisms and function of dendritic exocytosis. Neuron *69*, 856-875.

Kennerdell, J.R., Fetter, R.D., and Bargmann, C.I. (2009). Wnt-Ror signaling to SIA and SIB neurons directs anterior axon guidance and nerve ring placement in C. elegans. Development *136*, 3801-3810.

Kessels, H.W., and Malinow, R. (2009). Synaptic AMPA receptor plasticity and behavior. Neuron *61*, 340-350.

Kim, C., and Forrester, W.C. (2003). Functional analysis of the domains of the C elegans Ror receptor tyrosine kinase CAM-1. Dev Biol *264*, 376-390.

Korkut, C., Ataman, B., Ramachandran, P., Ashley, J., Barria, R., Gherbesi, N., and Budnik, V. (2009). Trans-synaptic transmission of vesicular Wnt signals through Evi/Wntless. Cell *139*, 393-404.

Korkut, C., and Budnik, V. (2009). WNTs tune up the neuromuscular junction. Nat Rev Neurosci *10*, 627-634.

Kourtis, N., and Tavernarakis, N. (2009). Cell-specific monitoring of protein synthesis in vivo. PLoS One *4*, e4547.

Liewald, J.F., Brauner, M., Stephens, G.J., Bouhours, M., Schultheis, C., Zhen, M., and Gottschalk, A. (2008). Optogenetic analysis of synaptic function. Nat Methods *5*, 895-902.

Liu, Q., Hollopeter, G., and Jorgensen, E.M. (2009). Graded synaptic transmission at the Caenorhabditis elegans neuromuscular junction. Proc Natl Acad Sci U S A *106*, 10823-10828.

Lu, W., Yamamoto, V., Ortega, B., and Baltimore, D. (2004). Mammalian Ryk is a Wnt coreceptor required for stimulation of neurite outgrowth. Cell *119*, 97-108.

Mikels, A.J., and Nusse, R. (2006). Purified Wnt5a protein activates or inhibits beta-catenin-TCF signaling depending on receptor context. PLoS Biol *4*, e115.

Minami, Y., Oishi, I., Endo, M., and Nishita, M. (2010). Ror-family receptor tyrosine kinases in noncanonical Wnt signaling: their implications in developmental morphogenesis and human diseases. Dev Dyn *239*, 1-15.

Oishi, I., Suzuki, H., Onishi, N., Takada, R., Kani, S., Ohkawara, B., Koshida, I., Suzuki, K., Yamada, G., Schwabe, G.C.*, et al.* (2003). The receptor tyrosine kinase Ror2 is involved in non-canonical Wnt5a/JNK signalling pathway. Genes Cells *8*, 645-654.

Port, F., and Basler, K. (2010). Wnt trafficking: new insights into Wnt maturation, secretion and spreading. Traffic *11*, 1265-1271.

Richmond, J.E., and Jorgensen, E.M. (1999). One GABA and two acetylcholine receptors function at the C. elegans neuromuscular junction. Nat Neurosci *2*, 791-797.

Sahores, M., Gibb, A., and Salinas, P.C. (2010). Frizzled-5, a receptor for the synaptic organizer Wnt7a, regulates activity-mediated synaptogenesis. Development *137*, 2215-2225.

Shyu, Y.J., Hiatt, S.M., Duren, H.M., Ellis, R.E., Kerppola, T.K., and Hu, C.D. (2008). Visualization of protein interactions in living Caenorhabditis elegans using bimolecular fluorescence complementation analysis. Nat Protoc *3*, 588-596.
Touroutine, D., Fox, R.M., Von Stetina, S.E., Burdina, A., Miller, D.M., 3rd, and Richmond, J.E. (2005). acr-16 encodes an essential subunit of the levamisole-

resistant nicotinic receptor at the Caenorhabditis elegans neuromuscular junction. J Biol Chem *280*, 27013-27021.

Turrigiano, G.G. (2008). The self-tuning neuron: synaptic scaling of excitatory synapses. Cell *135*, 422-435.

van Amerongen, R., and Nusse, R. (2009). Towards an integrated view of Wnt signaling in development. Development *136*, 3205-3214.

Watson, R.T., and Pessin, J.E. (2007). GLUT4 translocation: the last 200 nanometers. Cell Signal *19*, 2209-2217.

Wiedenmann, J., Ivanchenko, S., Oswald, F., Schmitt, F., Rocker, C., Salih, A., Spindler, K.D., and Nienhaus, G.U. (2004). EosFP, a fluorescent marker protein with UV-inducible green-to-red fluorescence conversion. Proc Natl Acad Sci U S A *101*, 15905-15910.

Wu, H., Xiong, W.C., and Mei, L. (2010). To build a synapse: signaling pathways in neuromuscular junction assembly. Development *137*, 1017-1033.

Zheng, Y., Mellem, J.E., Brockie, P.J., Madsen, D.M., and Maricq, A.V. (2004). SOL-1 is a CUB-domain protein required for GLR-1 glutamate receptor function in C. elegans. Nature *427*, 451-457.

Zinovyeva, A.Y., Yamamoto, Y., Sawa, H., and Forrester, W.C. (2008). Complex network of Wnt signaling regulates neuronal migrations during Caenorhabditis elegans development. Genetics *179*, 1357-1371.

CHAPTER 3

DISCUSSION

The spatial regulation and restriction of synaptic α7 receptors is essential for neural transmission in brain. Indeed, deficiencies in synaptic α7 receptor levels are observed in several neuronal diseases and disorders, suggesting that the proper regulation of receptor levels at synapses is critical for neuronal function (Gotti et al., 2006). Therefore, explicating the cellular mechanism(s) that regulate α7 receptors at synapses will provide new insights into the pathophysiology of neuronal disorders associated with deficiencies in cholinergic neurotransmission.

Wnt signaling molecules are required for ACR-16-mediated behavior and current

Our previous studies showed that current mediated by the α7-like ACR-16 nAChR is dependent on the Ror RTK *cam-1* (Francis et al., 2005). We predicted that *cam-1* forms a co-receptor with an unidentified protein based on our observations that expression of CAM-1ΔID rescues ACh-gated currents in *cam-1* mutants. The extracellular domain of CAM-1 contains a CRD, and vertebrate

Rors are known to associate with Wnts and frizzled receptors via their CRD. Because of these observations, we hypothesized that CAM-1 interacts with Wnts to regulate ACR-16 at the NMJ. To identify candidate Wnt signaling molecules, we conducted a candidate genetic screen to observe if genes in the Wnt signaling pathway(s) regulate ACR-16-mediated behavior.

Sinusoidal movement in worms is dependent on cholinergic neurotransmission. When worms are placed in liquid they exhibit a characteristic movement behavior known as thrashing (Francis et al., 2005). Thrashing behavior is quantified by counting the number of body bends made by worms in an arbitrary time period. If a gene is required for movement, we expect to observe a decrease in thrashing when that gene is mutated. As predicted, thrashing is decreased in null *unc-29* mutants – an essential subunit in the L-AChR – when compared to wild type worms. *unc-29; acr-16* double mutants have a severe reduction in thrashing due to the loss of all cholinergic current at the NMJ. As expected, we found that *unc-29; cam-1* double mutants have the same thrashing defects − i.e., phenocopies − as *unc-29; acr-16* mutants, indicating that *cam-1* and *acr-16* are in the same genetic pathway at the NMJ. Using this strategy, we conducted a candidate genetic screen (using mutations in Wnt genes) to identify Wnt mutants that exhibit a synthetic thrashing behavior when crossed into the *unc-29* mutant background. We found that double mutants between *cwn-2*, *lin-17* or *dsh-1,* and *unc-29*, phenocopies *unc-29; cam-1* and *unc-29; acr-16* double mutants. Interestingly, defects in thrashing were not caused by a general loss of Wnt signaling because mutants for both *unc-29* and

other Wnts (*cwn-1/Wnt)* or Fzd receptors (*cfz-2/Fzd)* did not phenocopy *unc-29; acr-16* double mutants.

Our previous studies demonstrated that *cam-1* is required for ACh-gated current at the NMJ (Francis et al., 2005). We reasoned that Wnt signaling mutants identified in the genetic screen would also have defects in ACh-gated current. Indeed, *cwn-2, lin-17,* and *dsh-1* phenocopied the ACh-gated current defects found in *cam-1* mutants. However, Lev-gated currents are unaffected in *cam-1, cwn-2, lin-17,* and *dsh-1,* suggesting that Wnt signaling is specifically required for ACR-16-meditated current at the NMJ. In concurrence with this model, nicotinic current is reduced in *cam-1, cwn-2,* and *lin-17* mutants.

Expression of CAM-1 is required in muscle to rescue ACh-gated current in *cam-1* mutants. We sought to ascertain in which tissues expression of CWN-2, LIN-17, and DSH-1 is required to rescue thrashing and ACh-gated current defects observed in their respective mutant backgrounds. Expression of LIN-17 or DSH-1, driven by a muscle specific promoter, rescued the thrashing defects of *unc-29; lin-17* and *unc-29; dsh-1* respectively. Neural specific expression of LIN-17 or DSH-1 did not rescue thrashing in their respective mutant background, demonstrating that LIN-17 and DSH-1 act specifically in muscle to regulate ACR-16 dependent behavior. Interestingly, expression of CWN-2 from either a neural or muscle specific promoter rescued the thrashing defects of *unc-29; cwn-2* mutants. This result is consistent with CWN-2's role as a secreted molecule, as reported in previous studies showing that the overexpression of CWN-2, in

various tissue types, is sufficient to rescue ganglion orientation defects in *cwn-2* mutants (Kennerdell et al., 2009).

To identify which tissues types expression of CWN-2 is necessary to regulate ACR-16-mediated behavior, we specifically knocked down expression of *cwn-2,* in either neurons or muscle, using a dsRNA technique. Knock down of *cwn-2* expression in neurons, but not muscle, results in decreased thrashing movements in *unc-29* mutant worms. Based on these results, we hypothesized that LIN-17 and DSH-1 are expressed in muscle and CWN-2 is secreted from neurons to regulate ACR-16-mediated behavior in worms.

To test our model, we recorded ACh-gated current in *lin-17* and *dsh-1* worms expressing DSH-1 or LIN-17 in muscle. We found that expression of LIN-17 and DSH-1 in muscle was sufficient to rescue ACh-gated current in their respective mutant backgrounds. To address necessity of *cwn-2,* we recorded ACh-gated current in *unc-29* worms expressing either neuronal or muscle specific *cwn-2* dsRNA. We found that neuronal, but not muscle, CAM-1ΔID expression of *cwn-2* dsRNA decreased ACh-gated current. These results support a model where neural secreted CWN-2 activates LIN-17 and DSH-1 in muscle to regulate ACR-16-mediated current and behavior at the NMJ. The presence of the CRD in CAM-1 and LIN-17 brings forth a hypothesis that CAM-1 and LIN-17 form a co-receptor complex in muscle that binds CWN-2.

CAM-1 and LIN-17 form a co-receptor complex

To test if CAM-1 and LIN-17 form a co-receptor complex at the NMJ, we fused CAM-1 to GFP (CAM-1::GFP) and LIN-17 to the red fluorescent protein mCherry (LIN-17::mCherry), and expressed these proteins in muscle. We found that CAM-1::GFP and LIN-17::mCherry partially co-localize at the NMJ. Next, we sought to address whether CAM-1 and LIN-17 physically interact with one another using bifluorescence complementation (BiFC) (Hiatt et al., 2008). Using a split version of the yellow fluorescent protein Venus, we fused one half to CAM-1 (CAM-1::N-YFP) and the other half to LIN-17 (LIN-17::C-YFP). If CAM-1::N-YFP and LIN-17::C-YFP are within 100 Å of one another, the split YFP fluorophore will reconstitute and fluorescence will be observed. As predicated, we saw YFP fluorescence at the NMJ in worms expressing both CAM-1::N-YFP and LIN-17::C-YFP. Interestingly, fluorescence was observed in worms expressing LIN-17::C-YFP and a truncated version of CAM-1 lacking the intracellular domain (CAM-1ΔTK::N-YFP). We hypothesized that CAM-1 and LIN-17 interacted with one another via the CRD in each proteins extracellular region; therefore, we predict that fluorescence will not be observed in worms expressing LIN-17::C-YFP and a truncated version of CAM-1 lacking the extracellular domain (CAM-1ΔECD). Indeed, fluorescence was not observed at the NMJ in worms expressing CAM-1ΔECD::N-YFP and LIN-17::C-YFP. Interestingly, CAM-1ΔECD tagged to GFP was present at the NMJ, indicating that the absence of signal, at the NMJ, in worms expressing CAM-1ΔECD::N-YFP and LIN-17::C-YFP is not due to degradation or transport defects of CAM-1ΔECD::N-YFP.

Based on our results we hypothesize that CAM-1 and LIN-17 form a co-receptor complex at the NMJ that is dependent on the presence of the CRD in each protein.

Wnt signaling regulates ACR-16 receptor localization at the NMJ

Our previous studies found that *cam-1* is required for ACh-gated current and ACR-16 receptor localization at the NMJ. In *cam-1* mutants, ACR-16 receptors are mislocalized and accumulate in MAs. Based on our observations that *lin-17, dsh-1,* and *cwn-2* are required for ACR-16-mediated behavior and current, we hypothesized that ACR-16 receptor localization in Wnt signaling mutants will phenocopy *cam-1*. We expressed ACR-16::GFP in muscle of *cwn-2, lin-17,* and *dsh-1* mutants and found that ACR-16::GFP accumulates in MAs similar to the phenotype observed in *cam-1* mutants. Also, in *lin-17* and *dsh-1* mutants, ACR-16::GFP localization defects were rescued by expressing LIN-17 or DSH-1 in muscle. Expressing LIN-17 in neurons did not rescue ACR-16::GFP localization in *lin-17* mutants. Interestingly, dsRNA knock down of *cwn-2* in neurons, but not muscle, resulted in ACR-16::GFP localization defects, further supporting our model that neural secreted CWN-2 signals through CAM-1/LIN-17/DSH-1 in muscle to regulate ACR-16.

ACR-16 surface expression and mobility is dependent on Wnt signaling

The increase in ACR-16::GFP appears contradictory to the decrease in ACh-gated current in Wnt signaling mutants. We hypothesized that the increase in ACR-16::GFP, observed in Wnt signaling mutants, was due to nonfunctional receptors accumulating at synapses or ACR-16::GFP was immobilized in intracellular pools below the surface of the synapse (subsynaptic). To test this model we used α-bungarotoxin (α-Btx) – that specifically binds to a domain in the extracellular region of α7 subunits – conjugated to a fluorescent dye to label surface-expressed ACR-16 receptors. If perturbations in Wnt signaling leads to an accumulation of nonfunctional ACR-16 receptors at synapses, we would expect augmented α-Btx staining at the NMJ in Wnt signaling mutants. However, if loss of Wnt signaling results in ACR-16 receptors agglomerating in subsynaptic pools, then we predict that α-Btx staining will be abated at the NMJ.

We injected α-Btx into the pseudocelomic space of wild type worms and imaged the region where the MA came in contact with the VNC (NMJ). Following removal of excess α-Btx by coelomocytes, we found that injected wild type worms had bright α-Btx staining at the distal tip of MAs and in unidentified nerve processes in the VNC. α-Btx staining in muscle is dependent on *acr-16* because no α-Btx staining was observed at the NMJ in *acr-16* mutants. Interestingly, α-Btx staining in *cam-1* and *cwn-2* mutants was decreased when compared to wild type, supporting the hypothesis that ACR-16 accumulates in subsynaptic pools when Wnt signaling is disrupted.

Accruement of ACR-16::GFP in subsynaptic pools suggests that ACR-16 receptor mobility is decreased in Wnt signaling mutants. To test this hypothesis, we tagged ACR-16 to the photoconvertible fluorophore EosFP. Excitation of EosFP with 506 nm light causes the fluorophore to emit photons in the green spectrum (peak emission at 516 nm). EosFP emission is converted to the red spectrum (peak emission at 581 nm) by irradiating EosFP with ultraviolet light (UV, 400 nm) and then exciting with 571 nm light (Wiedenmann et al., 2004). Using a digital micromirror device, UV can be focused onto a individual ACR-16::EosFP puncta, allowing for a single subsynatpic pool of ACR-16::EosFP to be converted in MAs. We converted single ACR-16::EosFP from green to red at the tips of MAs, and tracked dispersion of red ACR-16::EosFP puncta for one hour. We found that ACR-16::EosFP fluorescence intensity steadily declined to approximately 30% after one hour in wild type worms. In contrast, the decrease in ACR-16::EosFP fluorescence was appreciably slower in *lin-17* mutants. This data supports a model where Wnt signaling mobilizes ACR-16 receptors from subsynaptic pools, leading to translocation of ACR-16 to synapses.

ACR-16 is required for synaptic function at adult synapses

We hypothesize that ACR-16's role at the NMJ is to regulate the strength of BWM contraction in a given environment. However, *acr-16* may be required for synaptic formation and development. To test these hypotheses, we drove expression of *acr-16* using a heat-shock inducible promoter (HSP) in adult transgenic worms. Under normal growth conditions the HSP is quiescent;

however, when transgenic worms are exposed to temperatures of 30° C or more, the HSP becomes active and drives expression of a particular gene of interest in many tissue types – including neurons and muscle. We generated transgenic *unc-29; acr-16* mutant worms expressing *acr-16* driven by HSP (HSP::ACR-16). Interestingly, we found that heat shock of adult *unc-29; acr-16* transgenic worms expressing HSP::ACR-16, rescued the thrashing defects characteristic of *unc-29; acr-16* mutants. Heat shock did not increase the thrashing rate of *unc-29; acr-16* mutant controls. We then tested whether heat shock rescued nicotinic current in adult *unc-29; acr-16* mutants. Indeed, we observed large nicotinic currents at the NMJ in heat-shocked *unc-29; acr-16* worms expressing HSP::ACR-16. We did not observe nicotinic current in heat-shocked *unc-29; acr-16* controls. Thus, it is unlikely that *acr-16* is required for synaptic development, but instead is necessary for synaptic function in adult animals.

Wnts regulate ACR-16 receptor localization at adult synapses

We have found that Wnt signaling regulates surface expression of ACR-16 by mobilizing receptors from subsynaptic pools resulting in translocation to synapses. Interestingly, ACR-16 is not required for neuronal development and has an ongoing role in synaptic function in adult animals. We hypothesize that Wnt signaling has an ongoing role in regulating ACR-16 receptor levels at synapses in adult animals. To test this hypothesis, we used HSP::LIN-17 to observe if HS could rescue ACR-16-mediated behavior and localization in *lin-17* mutants.

unc-29; lin-17 mutants have severe defects in thrashing due to diminished ACh-gated current, which is secondary to localization defects of ACR-16::GFP. To observe whether Wnt signaling regulates ACR-16-mediated behavior in adults, we heat shocked *unc-29; lin-17* mutants expressing HSP::LIN-17 and observed thrashing. We found that heat-shock-induced expression of HSP::LIN-17 rescued thrashing in *unc-29; lin-17* mutants. Importantly, heat shock did not rescue *unc-29; lin-17* mutant controls. Next, we observed if Wnt signaling regulates ACR-16::GFP localization at adult synapses. We heat shocked adult *lin-17* mutants expressing ACR-16::GFP and HSP::LIN-17. We found that two hours after heat shock, ACR-16::GFP localization was rescued when compared to *lin-17* mutant controls. Interestingly, heat shock rescue of *lin-17* mutants did not perdure, as ACR-16::GFP localization was indistinguishable between heat-shocked *lin-17* worms expressing HSP::LIN-17 and *lin-17* mutant controls after 24 hrs. Therefore, our data shows that Wnt signaling has an ongoing role in regulating ACR-16-mediated behavior and localization at adult synapses.

Plasticity at the NMJ is dependent on Wnt signaling

Based on our observations that Wnts continually regulate ACR-16 receptors at synapses, we predicted that increased synaptic activity would alter ACR-16 receptor levels in a Wnt-dependent manner. To test this hypothesis, we expressed channelrhodopsin-2 (ChR2) in the cholinergic nervous system of the worm. ChR2 is a light (photon)-gated nonspecific cation channel from the green alga *Chlamydomonas reinhardtii* (Liewald et al., 2008). In the presence of all-

trans retinal, stimulation with 470 nm light induces a cationic current in ChR2-expressing cells. Light can then be used to depolarize and activate specific neurons expressing ChR2. We expressed ChR2 in cholinergic neurons, and observed ACR-16::GFP expression patterns in worms stimulated with light at 3 hertz (Hz) for one hour. Surprisingly, we found that ACR-16::GFP puncta intensity was reduced in worms stimulated with light. We hypothesize that the decrease in puncta intensity is due to increased mobilization, dispersal and translocation of receptors after stimulation with light. To test this hypothesis, we observed whether light stimulation altered ACh-gated current at the NMJ. In support of our hypothesis, we found that light stimulation augmented ACh-gated, but not GABA-gated, current at the NMJ. Thus, increased neural activity leads to plastic changes in ACR-16::GFP and ACh-gated current.

If Wnt signaling regulates mobility of ACR-16 receptors, then plasticity at the NMJ should be abrogated in Wnt signaling mutants. To test this hypothesis, we stimulated *cwn-2* mutants − expressing ChR2 and ACR-16::GFP – with light, and observed ACh-gated current and ACR-16::GFP localization. Surprisingly, we found that light induced plastic changes of ACR-16 were abolished in *cwn-2* mutants. From our previous studies, we found that neural expressed CWN-2 is required for ACR-16 receptor localization. Is expression of CWN-2 from neurons, muscle, or both, required for plastic changes of ACR-16? To address this question, we used light to stimulate *cwn-2* mutants, expressing neural or muscle derived CWN-,2 and observed if changes occurred in ACR-16::GFP. Consistent with our previous behavioral studies, we found that both neural and muscle

expressed CWN-2 rescued the ACR-16::GFP localization defects found in *cwn-2* mutants. However, only neural-derived CWN-2 altered ACR-16::GFP puncta intensity in response to light when compared to nonstimulated controls. To test whether neural-derived CWN-2 is necessary for plastic changes of ACR-16, we expressed *cwn-2* dsRNA in neurons or muscle and observed if light stimulation altered ACR-16::GFP puncta in MAs. Interestingly, we found that only neural expressed *cwn-2* dsRNA prevented plasticity. These data sets support our model that Wnt signaling is required for activity-dependent plastic changes of ACR-16 receptors at synapses.

Wnts regulate ACR-16 receptor translocation to the NMJ

We hypothesize that neural-secreted CWN-2 binds to and activates the CAM-1/LIN-17/DSH-1 signaling pathway, resulting in rapid translocation of ACR-16 from subsynaptic pools to synapses. If this hypothesis is correct then plasticity should be independent of protein translation, i.e., canonical Wnt signaling does not regulate receptor translocation, and application of recombinant CWN-2 onto muscle cells should result in rapid augmentation of ACh-gated current. To observe if plasticity is dependent on protein translation, we stimulated worms expressing ChR2 and ACR-16::GFP with light in the presence of cycloheximide (CHX) – a potent inhibitor of protein translation. To test the efficacy of CHX on inhibition of translation, we generated transgenic strains that expressed HSP::CWN-2::mCherry. Following heat shock, we observed bright CWN-2::mCherry fluorescence in neurons, muscle and coelomocytes. As predicted,

CWN-2::mCherry fluorescence was severely reduced when treated with CHX following heat shock.

We stimulated ACR-16::GFP worms with light in the presence or absence of CHX. Interestingly, ACR-16::GFP intensity in worms treated with CHX was indiscernible from that in control worms, suggesting that protein translation is not required for plasticity at the NMJ. Next, we tested whether recombinant CWN-2 was capable of augmenting ACh-gated current in muscle. We transfected human embryonic kidney-293 (HEK293) cells with *cwn-2* cDNA inserted into a mammalian expression vector to induce expression and secretion of CWN-2. We collected recombinant CWN-2 from the extracellular milieu and then concentrated and exchanged CWN-2 into an extracellular fluid appropriate for worm electrophysiological experiments. We then incubated dissected *cwn-2* mutant worms with recombinant CWN-2 and a control solution. Thirty minutes after incubation with CWN-2, we observed an augmentation in ACh-gated current in muscle. We did not observe any change in current in worms incubated with a control solution. The results of these experiments support the hypothesis that secreted CWN-2 activates CAM-1/LIN-17/DSH-1 noncanonical signaling to rapidly mobilize and translocate ACR-16 receptors from subsynaptic pools to synapses.

We have found a novel noncanonical Wnt signaling pathway that regulates translocation of ACR-16 receptors to synapses (Jensen et al., 2012) (Figure 3.1). In the absence of Wnt signaling, ACh-gated current is diminished and ACR-16 receptors are immobilized in subsynaptic pools. Interestingly, Wnt

signaling is not required for synaptogenesis of the NMJ, and has on ongoing role in regulating receptor levels at adult synapses. Surprisingly, increased neural activity engenders plastic changes of ACR-16 receptor levels that are dependent on Wnt signaling. Finally, augmentation of ACR-16 receptors is independent of protein translation, suggesting noncanonical Wnt signaling regulates plasticity at the NMJ. Despite our advances in elucidating the cellular mechanisms that regulate translocation of ACR-16 to synapses, we still have a limited understanding about the identity of the subsynaptic membrane pools that ACR-16 resides in, the cellular mechanisms that controls mobilization of ACR-16, how ACR-16 is transported to and from its target destination, the cellular machinery that governs ACR-16 exocytosis to synapses, and what DSH-1 regulates to control this process.

Subsynaptic localization and receptor recycling of ACR-16

Increased synaptic activity results in dynamic changes in receptor levels by altering the balance of delivery and removal of receptors from synapses (exocytosis/endocytosis). Much of what we know about this process comes from studies done on α-amino-3-hydroxy-5-methyl-4-isoxazolepropionic acid receptors (AMPAR, a glutamate receptor subclass) recycling at synapses (Kennedy and Ehlers, 2011; Yap and Winckler, 2012). AMPARs are synthesized in the endoplasmic reticulum where they are typically transported to the Golgi apparatus. From the Golgi, AMPARs are trafficked to postsynaptic sites where they are exocytosed at synapses. Once at synapses, AMPARs undergo dynamic

recycling in response to synaptic activity. In LTP models, AMPAR exocytosis is enhanced, whereas endocytosis of AMPAR is increased in LTD. Recycling occurs when AMPARs are endocytosed and targeted to recycling endosomes (RE). Once at REs, receptors are either recycled back to synapses or targeted to late endosomes where they are eventually degraded (Kennedy and Ehlers, 2011; Yap and Winckler, 2012). Proper targeting of membrane cargos in the RE pathway is dependent on several member of the Rab family of small GTPases (Yap and Winckler, 2012). Interestingly, Wnt signaling is known to interact with small GTPases to coordinate a number of cellular processes. Are ACR-16 receptors recycled and stored at the NMJ in endosomal membranes?

In Wnt signaling mutants, mobility of ACR-16 is decreased leading to accumulation of receptors in subsynaptic pools (Francis et al., 2005; Jensen et al., 2012). Does Wnt signaling regulate recycling of ACR-16 receptors to REs? What are the membrane compartment(s) in which ACR-16 receptors accrue when Wnt signaling is perturbed? Elucidating the cellular mechanisms that regulate recycling of ACR-16 receptors will give insight into the cellular processes that Wnts utilize to alter ACR-16 surface expression in response to synaptic activity.

SNAREs mediate synaptic receptor exocytosis and plasticity

SNAREs are the core protein machinery − composed of the syntaxin, SNAP-23/25, and synatobrevin protein families − that facilitate fusion of intracellular vesicles with their target membrane (Jahn and Scheller, 2006;

Martens and McMahon, 2008; Risselada and Grubmüller, 2012). SNARE proteins have well defined roles in mediating exocytosis of neurotransmitter from presynaptic neurons; however, the role that SNAREs have in regulating exocytosis in postsynaptic cells is less understood. Increased synaptic activity augments AMPAR levels in postsynaptic dendrites, presumably from trafficking of AMPARs to synapses from subsynaptic compartments (Kennedy and Ehlers, 2011; Yap and Winckler, 2012). The identity of these compartments remained unknown until recent studies showed that AMPARs resided in dendritic REs. Following synaptic stimulation, subsynaptic REs fused with the plasma membrane of dendrites resulting in augmented levels of AMPARs at synapses (Kennedy et al., 2010). Intriguingly, exocytosis of AMPARs to synapses is attenuated when expression of the plasma membrane syntaxin-4 (Syx-4) is reduced. Also, activity dependent exocytosis of AMPARs to synapses is inhibited when Syx-4 expression is eliminated. Syx-4 localizes to exocytic zones, and marks the site on dendrites where AMPARs are exocytosed to synaptic membranes. Unlike the presynaptic syntaxin-1, Syx-4 associates with actin, suggesting that Syx-4 is part of a large complex at the postsynaptic density that regulates AMPAR exocytosis in response to various levels of synaptic activity (Kennedy et al., 2010).

We have found that Wnts regulate surface expression of α7-like ACR-16 receptors at adult synapses in worms. We hypothesize that Wnts promote translocation of ACR-16 receptors to synapses in response to increased levels of synaptic activity. Are SNARE complexes required in muscle to mediate ACR-16

receptor exocytosis? Do Wnts control SNARE function, or do SNAREs act independent of Wnts to mediate receptor exocytosis? We predict that *C. elegans* is the best-suited organism to elucidate the signaling mechanisms that regulate receptor exocytosis in adult synapses. We are currently assessing the role, if any, that SNAREs have in facilitating receptor exocytosis in response to changes in synaptic activity. Because many of the signaling mechanisms that regulate synaptic function are conserved from invertebrates to vertebrates, we hypothesize that our results will have direct relevance to ongoing studies in the vertebrate nervous system, and will ultimately lead to new therapeutic modalities for neuronal disorders associated with defects in cholinergic neurotransmission.

Figure 3.1. Wnt signaling promotes ACR-16 translocation to synapses. Cartoon schematic of the Wnt signaling pathway at the NMJ. We hypothesize that secreted CWN-2 binds to the CAM-1/LIN-17 co-receptor complex, which activates DSH-1 to promote ACR-16 receptor translocation to synapses.

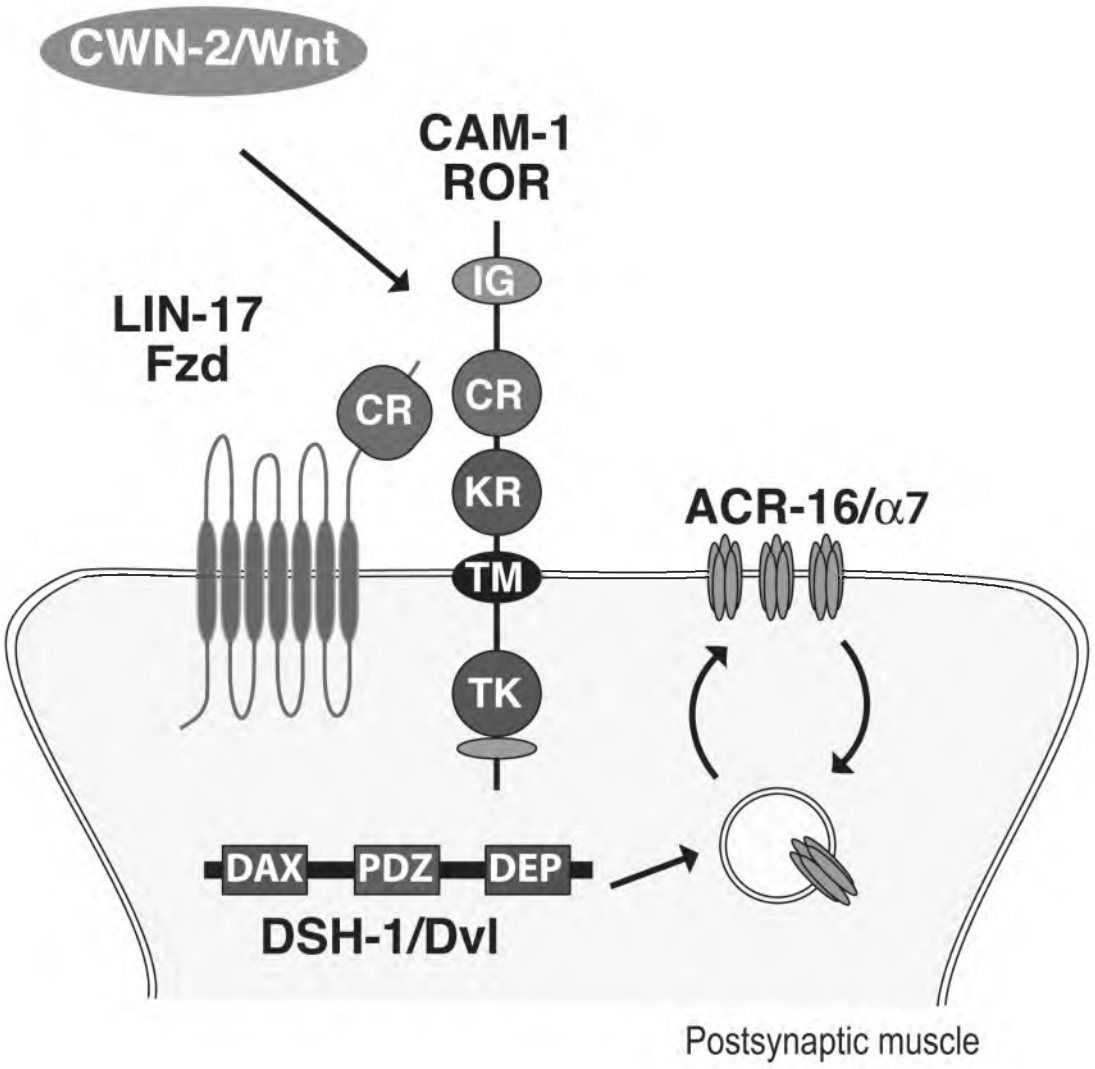
CWN-2/Wnt
CAM-1
ROR
IG
LIN-17
Fzd
CR
CR
KR
ACR-16/α7
TM
TK
DAX
PDZ
DEP
DSH-1/Dvl
Postsynaptic muscle

Figure 3.2. Model of ACR-16 receptor recycling at the NMJ. Cartoon schematic of a hypothetical Wnt signaling pathway that regulates ACR-16 receptor recycling in MAs. We hypothesize that Wnts signaling dynamically regulates ACrR-16 receptor levels at synapses by mobilizing ACR-16 receptors from REs, which leads to receptor exocytosis.

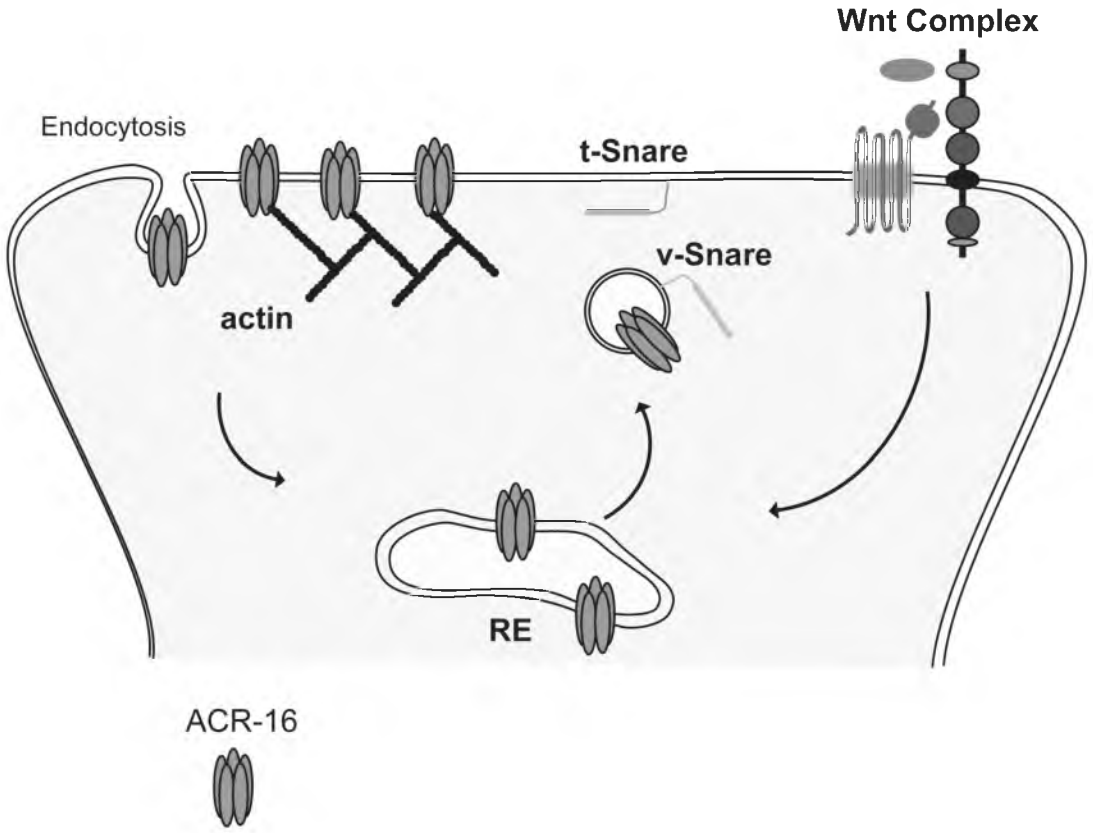
Wnt Complex
Endocytosis
t-Snare
v-Snare
actin
RE
ACR-16

References

Francis, M.M., Evans, S.P., Jensen, M., Madsen, D.M., Mancuso, J., Norman, K.R., and Maricq, A.V. (2005). The Ror receptor tyrosine kinase CAM-1 is required for ACR-16-mediated synaptic transmission at the C. elegans neuromuscular junction. Neuron *46*, 581–594.

Gotti, C., Zoli, M., and Clementi, F. (2006). Brain nicotinic acetylcholine receptors: native subtypes and their relevance. Trends in Pharmacological Sciences *27*, 482–491.

Hiatt, S.M., Shyu, Y.J., Duren, H.M., and Hu, C.-D. (2008). Bimolecular fluorescence complementation (BiFC) analysis of protein interactions in Caenorhabditis elegans. Methods (San Diego, Calif.) *45*, 185–191.

Jahn, R., and Scheller, R.H. (2006). SNAREs--engines for membrane fusion. Nature Reviews. Molecular Cell Biology *7*, 631–643.

Jensen, M., Hoerndli, F.J., Brockie, P.J., Wang, R., Johnson, E., Maxfield, D., Francis, M.M., Madsen, D.M., and Maricq, A.V. (2012). Wnt signaling regulates acetylcholine receptor translocation and synaptic plasticity in the adult nervous system. Cell *149*, 173–187.

Kennedy, M.J., Davison, I.G., Robinson, C.G., and Ehlers, M.D. (2010). Syntaxin-4 defines a domain for activity-dependent exocytosis in dendritic spines. Cell *141*, 524–535.

Kennedy, M.J., and Ehlers, M.D. (2011). Mechanisms and function of dendritic exocytosis. Neuron *69*, 856–875.

Kennerdell, J.R., Fetter, R.D., and Bargmann, C.I. (2009). Wnt-Ror signaling to SIA and SIB neurons directs anterior axon guidance and nerve ring placement in C. elegans. Development (Cambridge, England) *136*, 3801–3810.

Liewald, J.F., Brauner, M., Stephens, G.J., Bouhours, M., Schultheis, C., Zhen, M., and Gottschalk, A. (2008). Optogenetic analysis of synaptic function. *5*, 895–902.

Martens, S., and McMahon, H.T. (2008). Mechanisms of membrane fusion: disparate players and common principles. Nature Reviews. Molecular Cell Biology *9*, 543–556.

Risselada, H.J., and Grubmüller, H. (2012). How SNARE molecules mediate membrane fusion: recent insights from molecular simulations. Current Opinion in Structural Biology *22*, 187–196.

Wiedenmann, J., Ivanchenko, S., Oswald, F., Schmitt, F., Röcker, C., Salih, A., Spindler, K.-D., and Nienhaus, G.U. (2004). EosFP, a fluorescent marker protein with UV-inducible green-to-red fluorescence conversion. Proceedings of the National Academy of Sciences of the United States of America *101*, 15905–15910.

Yap, C.C., and Winckler, B. (2012). Harnessing the power of the endosome to regulate neural development. Neuron *74*, 440–451.